

Chapter 4

Results

4.1. Biochemical composition of mustard (*Brassica nigra*) seeds and garlic (*Allium sativum*)

4.1.1. Moisture content

The moisture content in raw garlic cloves and mustard seeds was found to be 59.75 and 6.38 g/100 g, respectively (Table 10).

4.1.2. Ash content

The ash content in raw garlic cloves and mustard seeds was found to be 1.22 and 4.24 g/100, respectively (Table 10).

4.1.3. Total carbohydrate

After conducting the Anthrone method, the total carbohydrate content in mustard seeds and raw garlic cloves was found to be 25.81 and 32.30 g/100g with respect to the dextrose standard (Table 10).

4.1.4. Crude fibre content

The total crude fibre content in mustard seeds and garlic cloves was found to be 23.20 and 4.09 g/100g, respectively (Table 10).

4.1.5. Crude fat

In 100 grams of mustard seeds and garlic cloves, the crude fat content was found to be 42.39 g and 0.27 g, respectively (Table 10).

4.1.6. Crude protein

The crude protein content in mustard seeds and garlic cloves was observed to be 21.18 and 6.46 g/100 g samples (Table 10).

Table 10: The proximate analysis of mustard (*Brassica nigra* L.) seeds and raw garlic (*Allium sativum* L.)

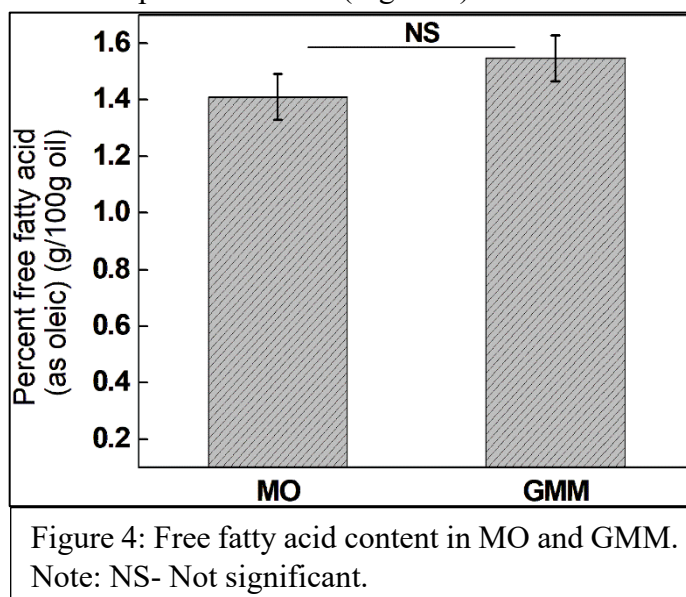
| Analysis | Garlic (<i>Allium sativum</i>) (g/100g) | Mustard seed (<i>Brassica nigra</i>) (g/100g) |
|--------------------|---|---|
| Moisture content | 59.75±1.35 | 6.38±0.84 |
| Crude fat | 0.27±0.05 | 42.39±3.55 |
| Crude protein | 6.46±0.031 | 21.18±1.35 |
| Crude fibre | 4.09±0.21 | 23.20±1.75 |
| Total ash | 1.22±0.05 | 4.24±0.232 |
| Total carbohydrate | 32.30±1.25 | 25.81±1.25 |

4.2. Physicochemical examination and phytochemical analysis of oil from GMM

4.2.1. Chemical properties

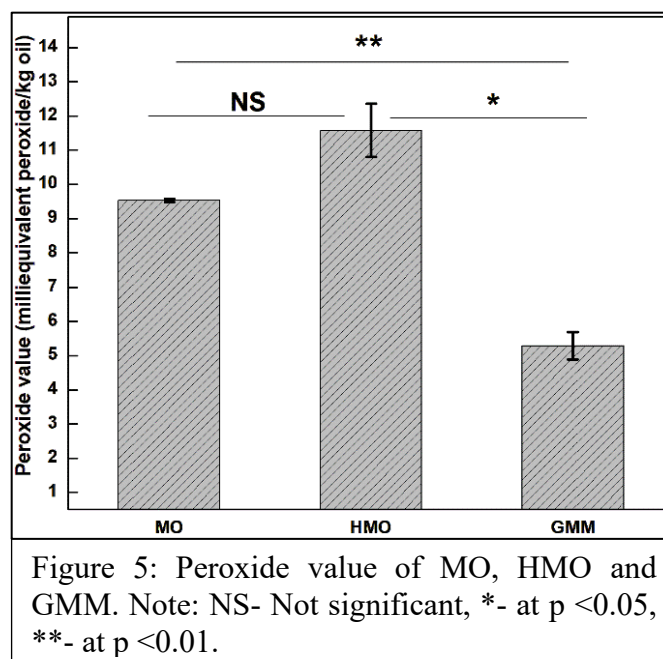
4.2.1.1. Free fatty acid

FFA for GMM was found to be 1.54 ± 0.08 g/100g oil, which was higher than MO, which was found to be 1.41 ± 0.08 g/100g oil. We found no significant difference between the mean FFA values of the GMM and MO with a p-value of 0.29 (Figure 4).



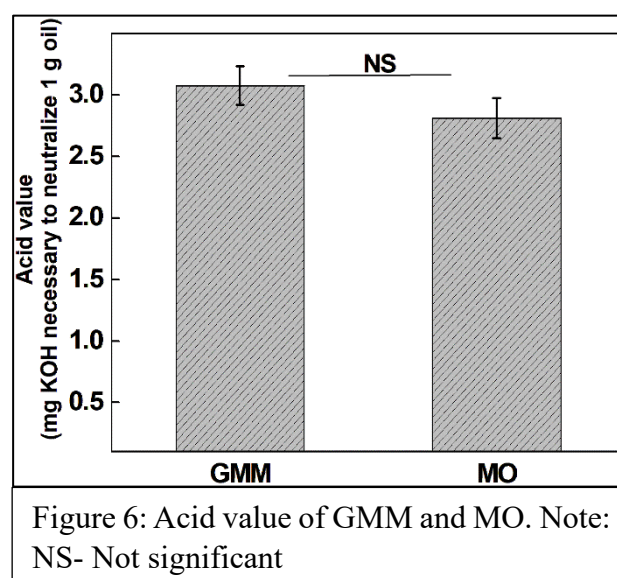
4.2.1.2. Peroxide value

PV of MO, heated (80°C for 8 hours) mustard oil (HMO) and GMM were found to be 9.53 ± 0.04 , 11.57 ± 0.77 and 5.29 ± 0.40 meq O₂/kg, respectively. The PV of MO and GMM were found to be significantly different with a p-value of 0.0092. The PV of HMO and GMM were significantly different with a p-value of 0.018 (Figure 5).



4.2.1.3. Acid value

When compared to MO, which has an AV of 2.81 ± 0.16 , it was found that the acid value for GMM was 3.07 ± 0.15 . The mean AV of the GMM and MO, however, were found to be not significantly different with a p-value of 0.306 (Figure 6).



4.2.1.4. Iodine value

The IV of MO and GMM were found to be 100.82 ± 0.41 and 101.76 ± 0.36 g/100 g of oil (Figure 7). The means were not found to be significantly different from each other at a p-value of 0.05.

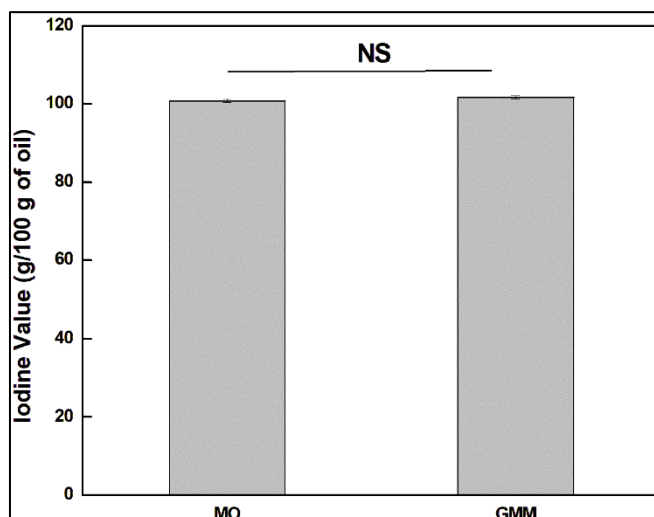


Figure 7: Iodine value of MO and GMM. Note: NS- Not significant.

4.2.1.5. Saponification value

The SV of the Mustard oil (MO), Heated mustard oil (HMO) and Garlic mustard oil macerate (GMM) was found to be 195.19 ± 1.97 ,

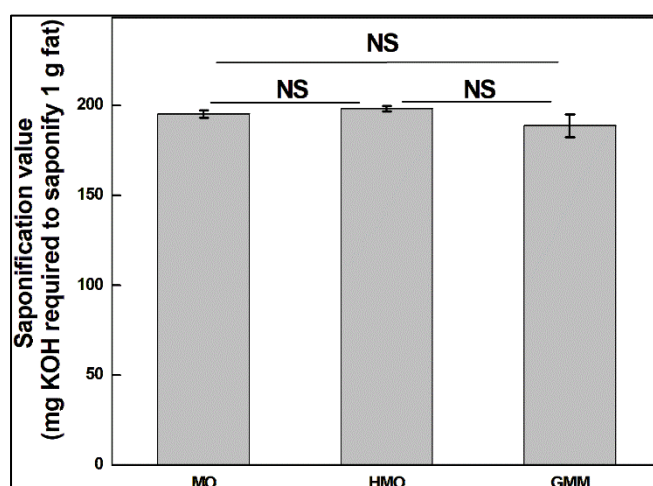


Figure 8: Saponification value of mustard oil and garlic mustard oil macerate. Note: NS- Not significant.

198.20 \pm 1.37 and 188.71 \pm 6.36 respectively (Figure 8). The mean between all the samples was not significantly different at p value< 0.05.

4.2.2. Physical properties

4.2.2.1. Density and specific gravity

The density of MO, HMO and GMM were found to be 0.91, 0.85 and 0.88 g/cm³, respectively. The specific gravity was found to be 0.91, 0.84 and 0.88 for MO and GMM, respectively.

4.2.2.2. Viscosity

The viscosity of HMO and GMM were found to be 116.23 \pm 0.54 and 116.58 \pm 0.22 milipoise, respectively. The means were found to be not significantly different with p-value<0.05.

4.2.2.3. Refractive index

The RI of mustard oil and GMM was found to be 1.474 \pm N.D. and 1.478 \pm N.D. The means were found to be significantly different with a p-value of 0.0015.

4.2.3. Phytochemical analysis

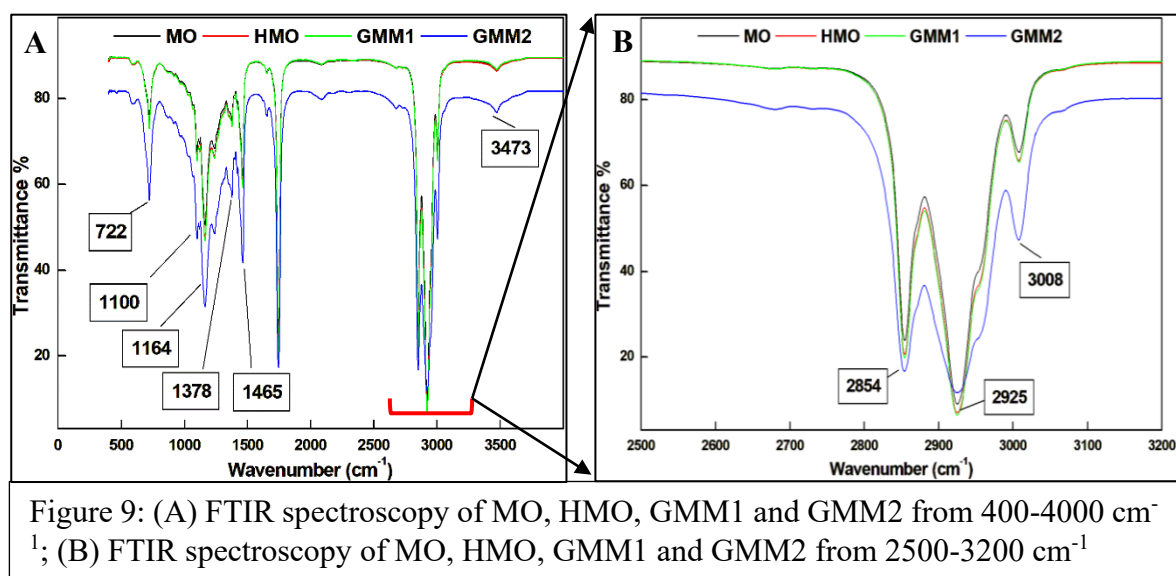
4.2.3.1. FTIR analysis

FTIR analysis of mustard oil (MO) and heated mustard oil (HMO) has shown transmittance at 722, 1100, 1120, 1164, 1239, 1378, 1418, 1465, 1747, 2854, 2925, 3008 cm⁻¹ (Table 11). Although, freshly prepared GMM (GMM4) was prepared and the results showed slight change in the intensity in 3008, 2095, 1465, 1418, 1378, 1239, 1164, 1120, 1100, 722 cm⁻¹ (Figure 9, A and B). Moreover, FTIR analysis of the GMM kept for one month at -20°C shows similar peaks as shown by MO and HMO.

Table 11: Showing the characteristic bonds and type for the observed peak for MO and GMM.

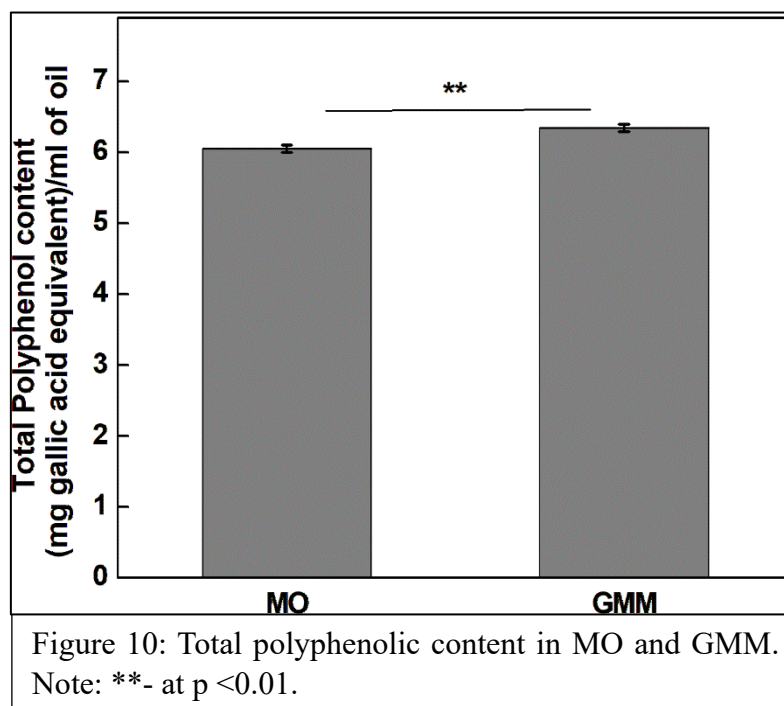
| Wavenumber (cm ⁻¹) | T % MO | T % HMO | T % GMM1 | T % GMM2 | Assignments of functional groups for the observed bands | Reference |
|-----------------------------------|-----------|------------|-------------|-------------|---|-----------|
| 722 | 74.6 | 73.24 | 73.04 | 56.3 | CH ₂ bending rocking vibrations and - HC=CH- out of plane vibrations. | [26] |
| 1100 | 67.7 | 65.8 | 65.48 | 47.39 | C-O stretching vibrations. | [26] |
| 1120 | 69.5 | 67.77 | 67.45 | 49.57 | C-O stretching vibrations. | [26] |

| | | | | | | |
|------|-------|-------|-------|-------|--|----------|
| 1164 | 50.53 | 47.53 | 46.86 | 31.53 | C-O stretching vibrations. | [26] |
| 1239 | 68.33 | 66.59 | 66.15 | 48.48 | Stretching vibrations of -CO groups. | [26] |
| 1378 | 74.84 | 73.65 | 73.39 | 56.99 | C=S stretching (Sulfur compounds), bending vibrations of CH ₂ groups. | [26, 91] |
| 1418 | 78.67 | 77.72 | 77.71 | 62.66 | Rocking vibrations of the CH ₂ and CH ₃ aliphatic groups. | [26] |
| 1465 | 61.84 | 59.56 | 59.09 | 41.74 | Rocking vibrations of the CH ₂ and CH ₃ aliphatic groups. | [26] |
| 1747 | 23.28 | 20.16 | 19.35 | 17.35 | Ester carbonyl functional group of the triglycerides. | [26] |
| 2854 | 23.93 | 20.72 | 19.85 | 16.74 | Symmetrical C-H stretching vibrations of the aliphatic -CH ₃ and -CH ₂ groups in acyl group chains. | [26] |
| 2925 | 9.11 | 7.04 | 6.53 | 11.73 | Symmetrical C-H stretching vibrations of the aliphatic -CH ₃ and -CH ₂ groups in acyl group chains: Lipids | [26] |
| 3008 | 67.73 | 65.79 | 65.4 | 47.26 | =C-H stretching vibrations of cis double bonds. | [26] |



4.2.3.2. Total polyphenol content

The total polyphenolic content in MO and GMM was found to be 7.37 ± 0.04 and 7.60 ± 0.04 respectively. The mean between both the samples was significantly different with a p-value of 0.002 (Figure 10).



4.2.3.3. Antioxidant activity

A significant difference between the mustard oil and GMM was observed in the lipophilic part and the whole oil at p-values of 2.055×10^{-5} and 1.803×10^{-5} , respectively (Table 12). Although the hydrophilic parts of the MO and GMM did not show any significant differences. The descending order of antioxidant activity of the samples is as follows: $GMM > GMLF > MO > MLF > GMHF > MHF$ (Figure 11). The ratio of the lipophilic part to that of the hydrophilic part of MO and GMM was found to be 1.40 and 1.47, respectively.

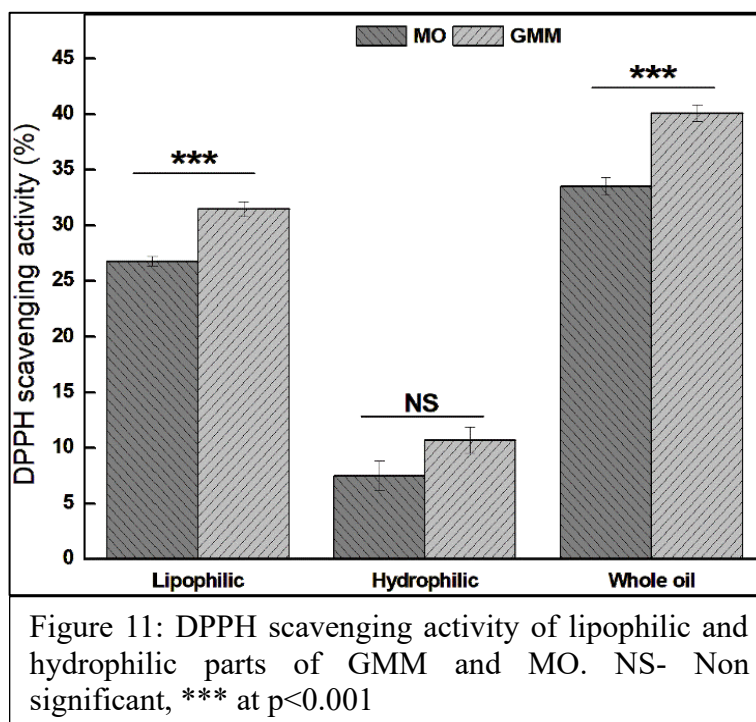
Table 12: Details of antioxidant activity in terms of scavenging percentage and concentration (mM GAEAC) and the ratio of lipophilic and hydrophilic part of the hydrophilic part, lipophilic part and whole oil of mustard oil and garlic mustard oil macerated

| Sample | DPPH | | DPPH scavenging of LF/HF | |
|--------|--------------------------|--------------------------|--------------------------|------|
| | Scavenging % | mM GAEAC | MO | GMM |
| MHF | 7.866±0.44 ^a | 0.055±0.003 ^a | | |
| GMHF | 11.043±0.39 ^b | 0.079±0.002 ^b | | |
| MLF | 16.161±0.87 ^c | 0.117±0.006 ^c | 1.40 | 1.47 |
| GMLF | 23.894±1.78 ^d | 0.175±0.013 ^d | | |
| MO | 21.524±1.14 ^d | 0.157±0.008 ^d | | |
| GMM | 31.424±1.62 ^e | 0.232±0.012 ^e | | |

Results expressed as mean ± S.E. (n=9); 95% confidence interval

^{a,b,c,d,e} Value followed by the same letter within each column were not significantly different according to one-way-ANOVA (p<0.05)

MHF- mustard oil hydrophilic part, GMHF- garlic mustard oil macerate hydrophilic part, MLF- mustard oil lipophilic part, GMLF- garlic mustard oil macerate lipophilic part, MO- whole mustard oil, GMM- whole garlic mustard oil macerate, GAE- gallic acid equivalence.



4.2.3.4. TLC analysis of raw garlic, MO and GMM

For MO, 2 spots were observed at R_f values of 0.687 and 0.875. For GMM, three spots were observed at R_f values of 0.625, 0.712 and 0.875. For raw garlic, we observed two spots at R_f values of 0.9 and 0.95 (Figure 12).

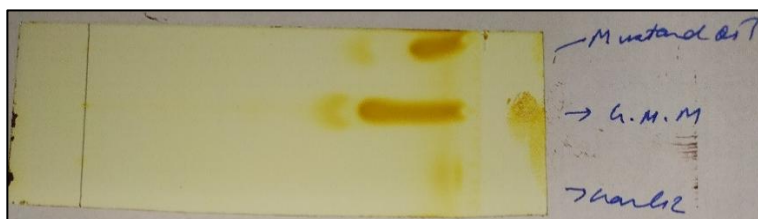


Figure 12: Thin layer chromatography analysis of MO, GMM and raw garlic.

4.2.3.5. High-performance liquid chromatography analysis of GTE, MO and GMM

As mustard oil is non-polar therefore, toluene which is a non-polar solvent was used for the preparation of garlic toluene extract (GTE) and was hypothesized that similar compounds may form when garlic is mixed and heated. In the results, GTE has shown two major peaks at retention times of 3.46 and 4.10 minutes (Figure 13). Similarly, GMM also showed peaks at 3.48 and 4.08 minutes. MO has shown peaks at 3.20 and 4.074 minutes. Thus, LCMS analysis of the sample was done for the identification of the compounds.

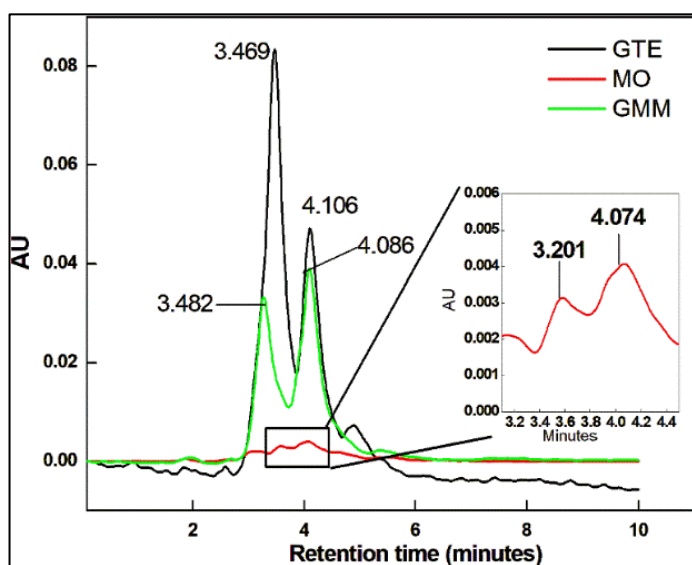


Figure 13: HPLC chromatogram of mustard oil (MO), garlic mustard oil macerate (GMM) and garlic toluene extract (GTE). (Image courtesy: Singha, J., Dutta, N., and Saikia, J.P. A novel method to produce maximum ajoene and vinyl dithiin during garlic mustard oil macerate preparation. *Journal of Sulfur Chemistry*: 1-13, 2025).

4.2.3.6. Liquid chromatography-mass spectrometry analysis of GTE, MO and GMM

4.2.3.6.1. LCMS analysis of GTE

The total ion current (TIC) chromatogram of GTE revealed 5 major peaks at retention times of 0.826, 0.978, 2.346, 1.260 and

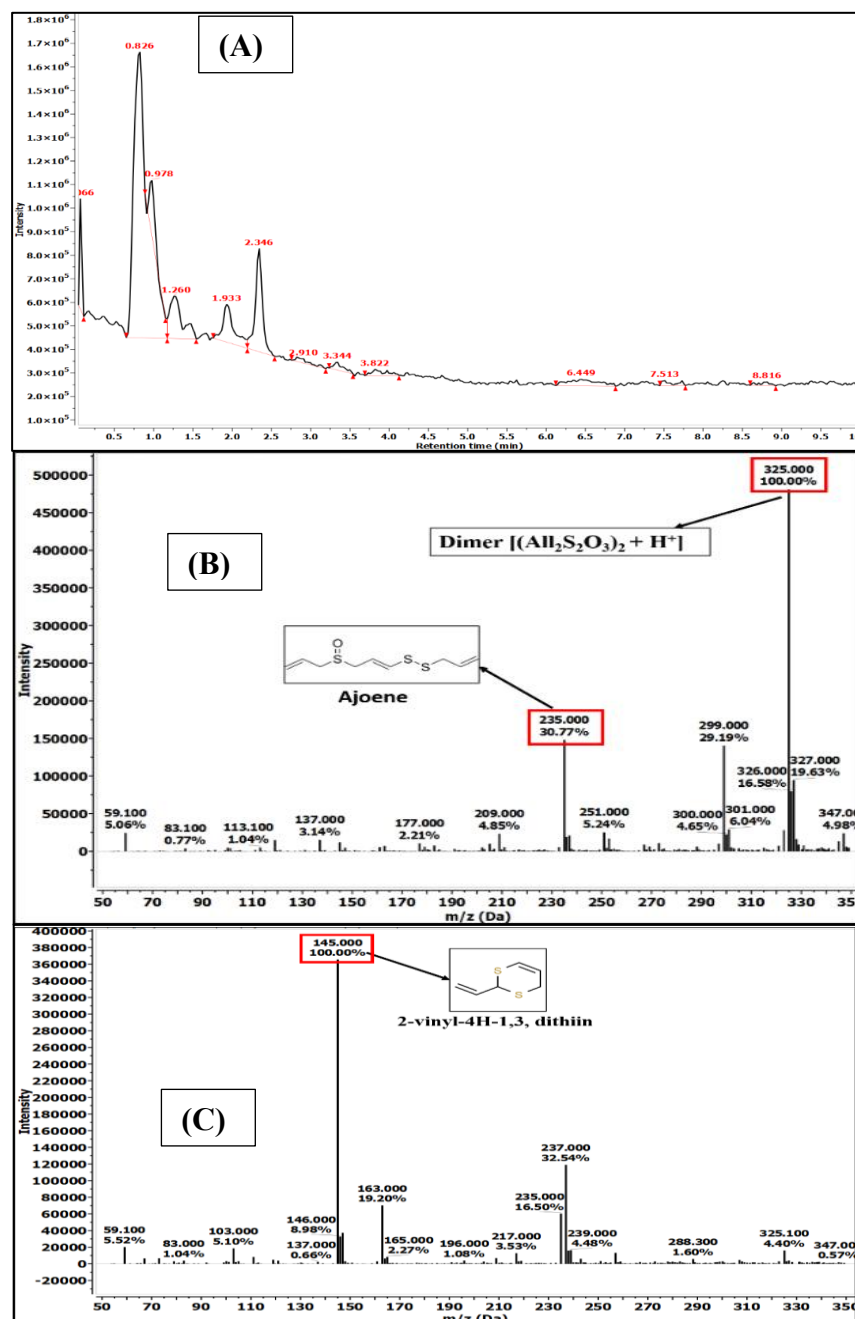
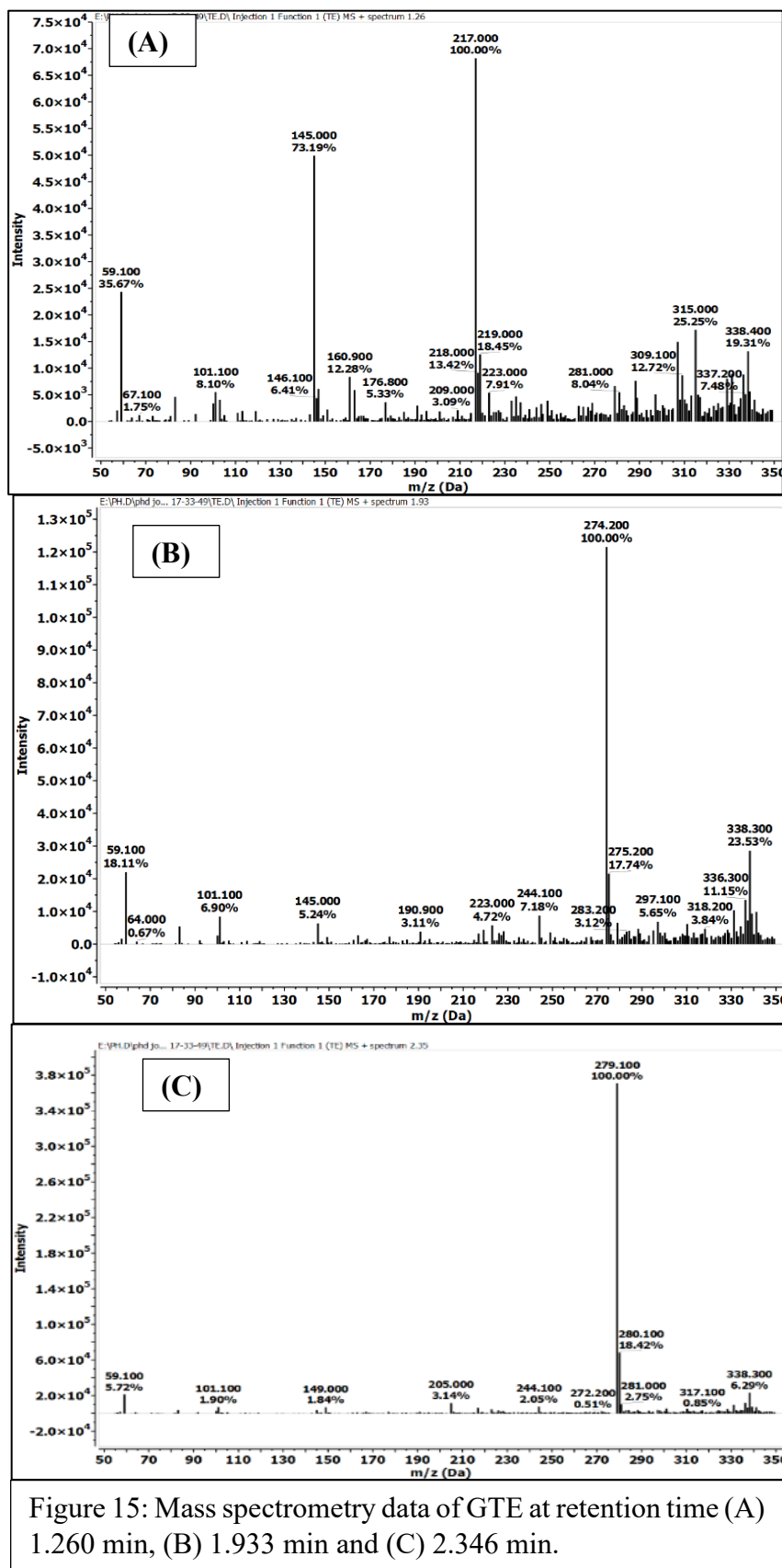


Figure 14: (A) Liquid chromatogram during LC/MS analysis of GTE; mass spectrometry data at retention time (B) 0.826 min (C) 0.978 min.

1.933 minutes (Figures 14 and 15). The mass spectrometry analysis of the major peaks is mentioned in the table 13.



4.2.3.6.2. LCMS analysis of MO

The chromatogram of MO revealed 7 major peaks at retention times of 0.804, 1.130, 1.26, 1.50, 5.34, 7.17 and 8.45 min (Figures 16, 17 and 18). The mass spectrometry analysis of the major peaks is mentioned in the table 13.

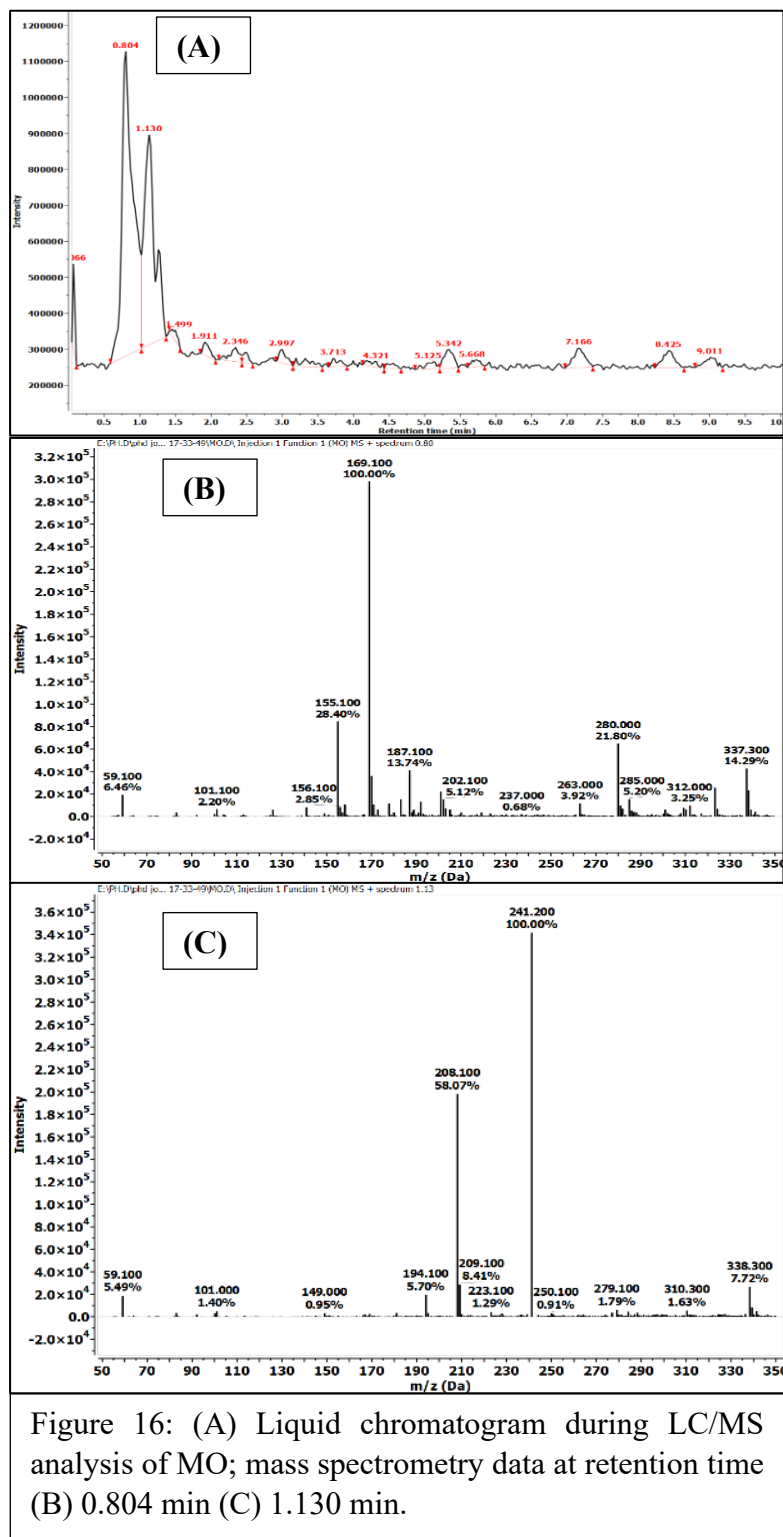


Figure 16: (A) Liquid chromatogram during LC/MS analysis of MO; mass spectrometry data at retention time (B) 0.804 min (C) 1.130 min.

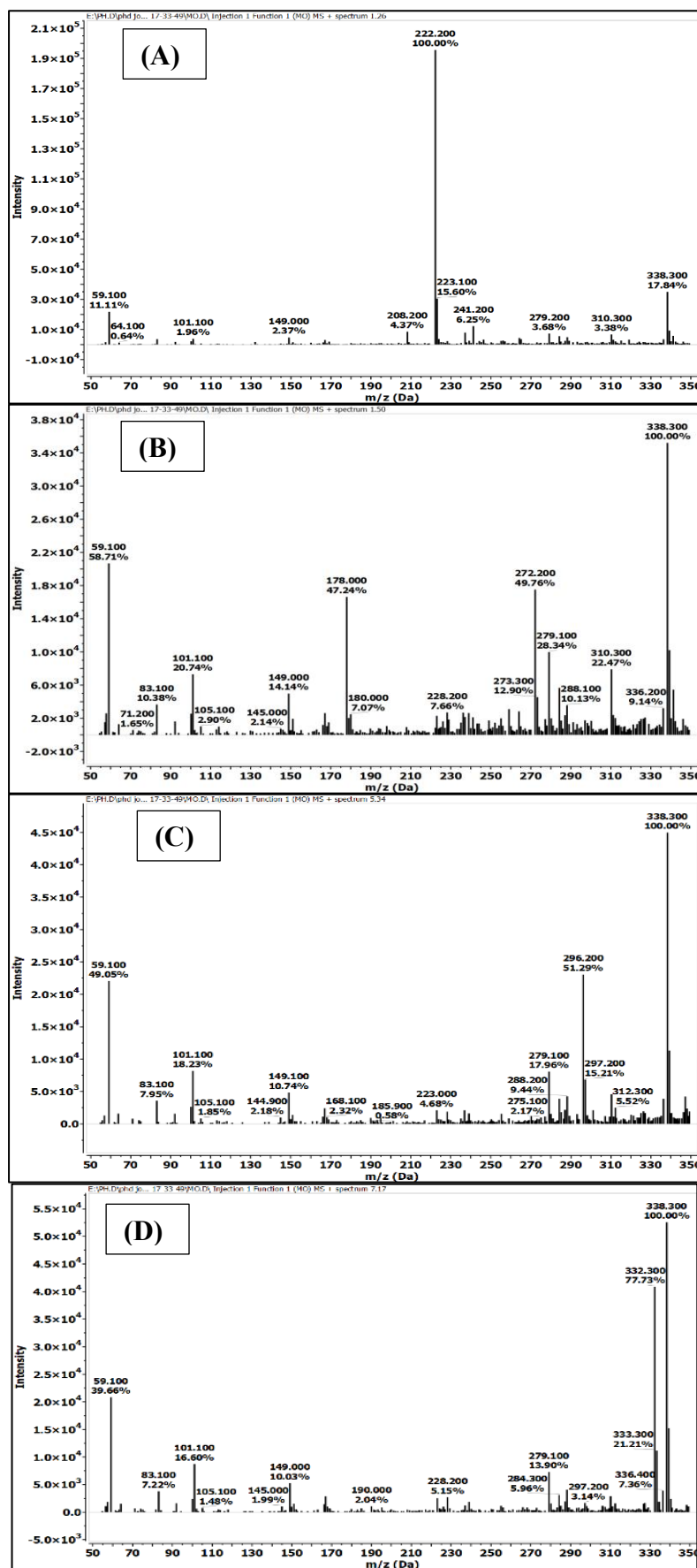


Figure 17: Mass spectrometry data of MO at retention time (A) 1.26; (B) 1.50; (C) 5.34; and (D) 7.17 min.

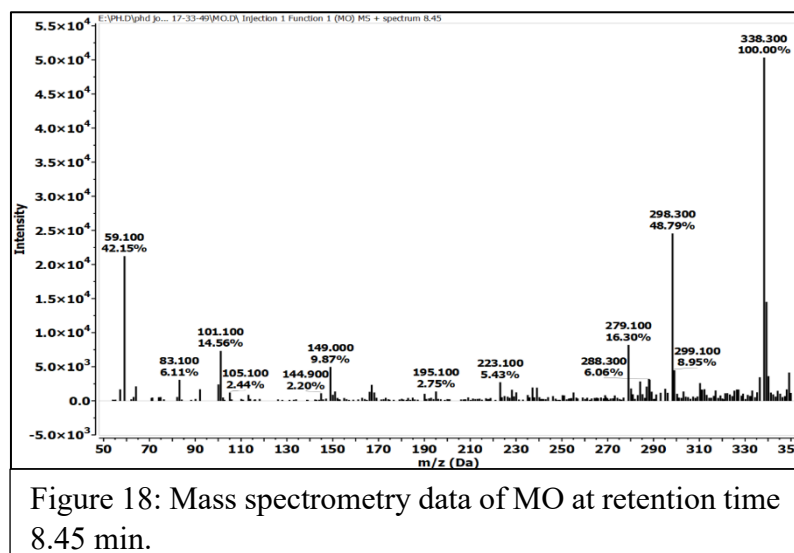


Figure 18: Mass spectrometry data of MO at retention time 8.45 min.

4.2.3.6.3. LCMS analysis of GMM

The total ionic current (TIC) chromatogram showed 9 major peaks at retention times 0.82, 0.85, 0.98, 1.09, 1.48, 3.00, 5.34, 7.14, 9.14 min (Figures 19, 20, 21 and 22). The mass spectrometry analysis of the peaks is shown in table 13.

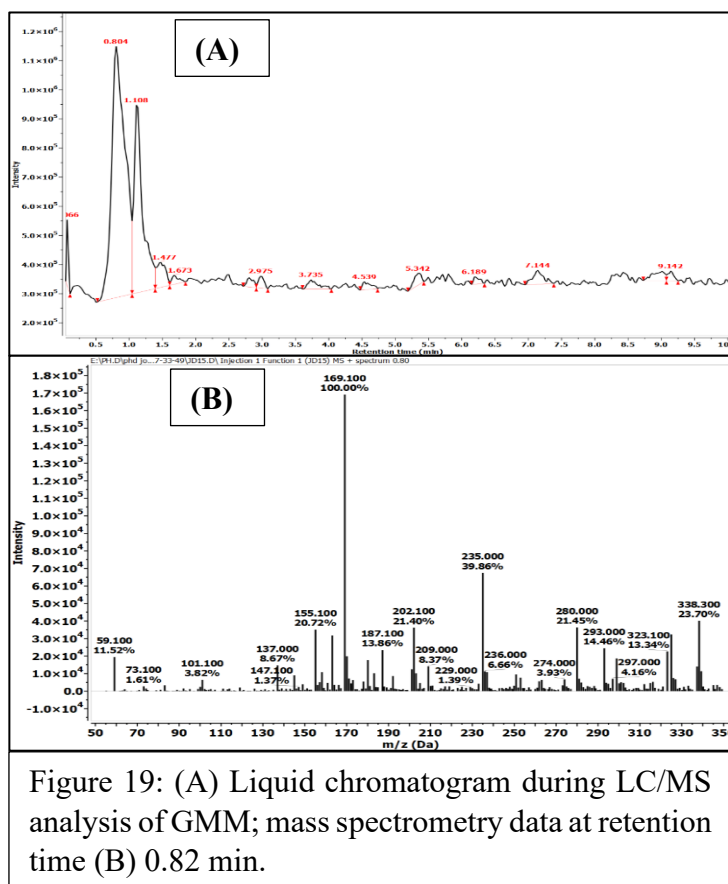


Figure 19: (A) Liquid chromatogram during LC/MS analysis of GMM; mass spectrometry data at retention time (B) 0.82 min.

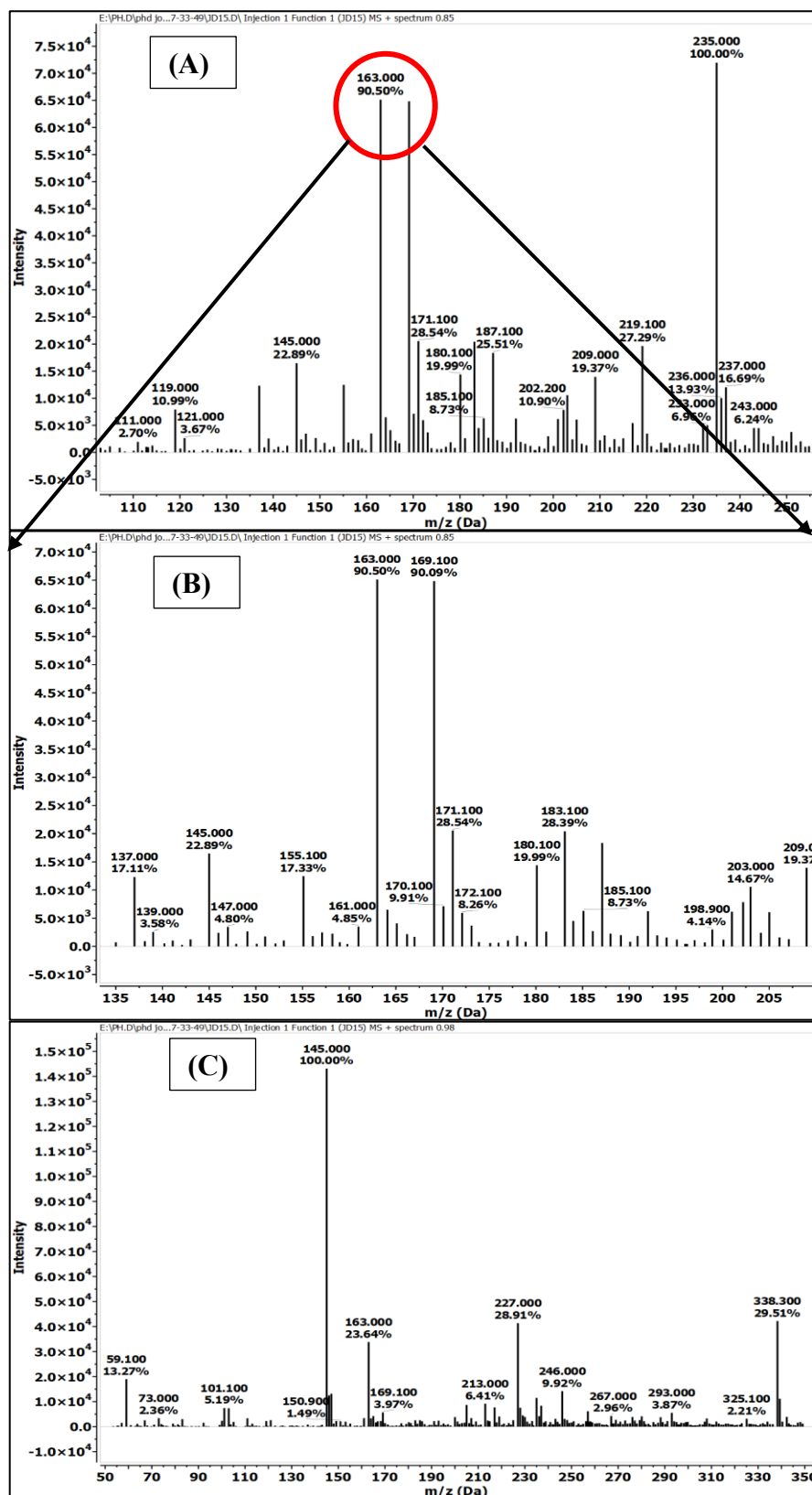


Figure 20: (A) Mass spectrometry data of GMM at retention time 0.85; (B) zoomed image of the region of 163.00 m/z at retention time 0.85 min; and (C) mass spectrometry data of GMM at retention time 0.98 min.

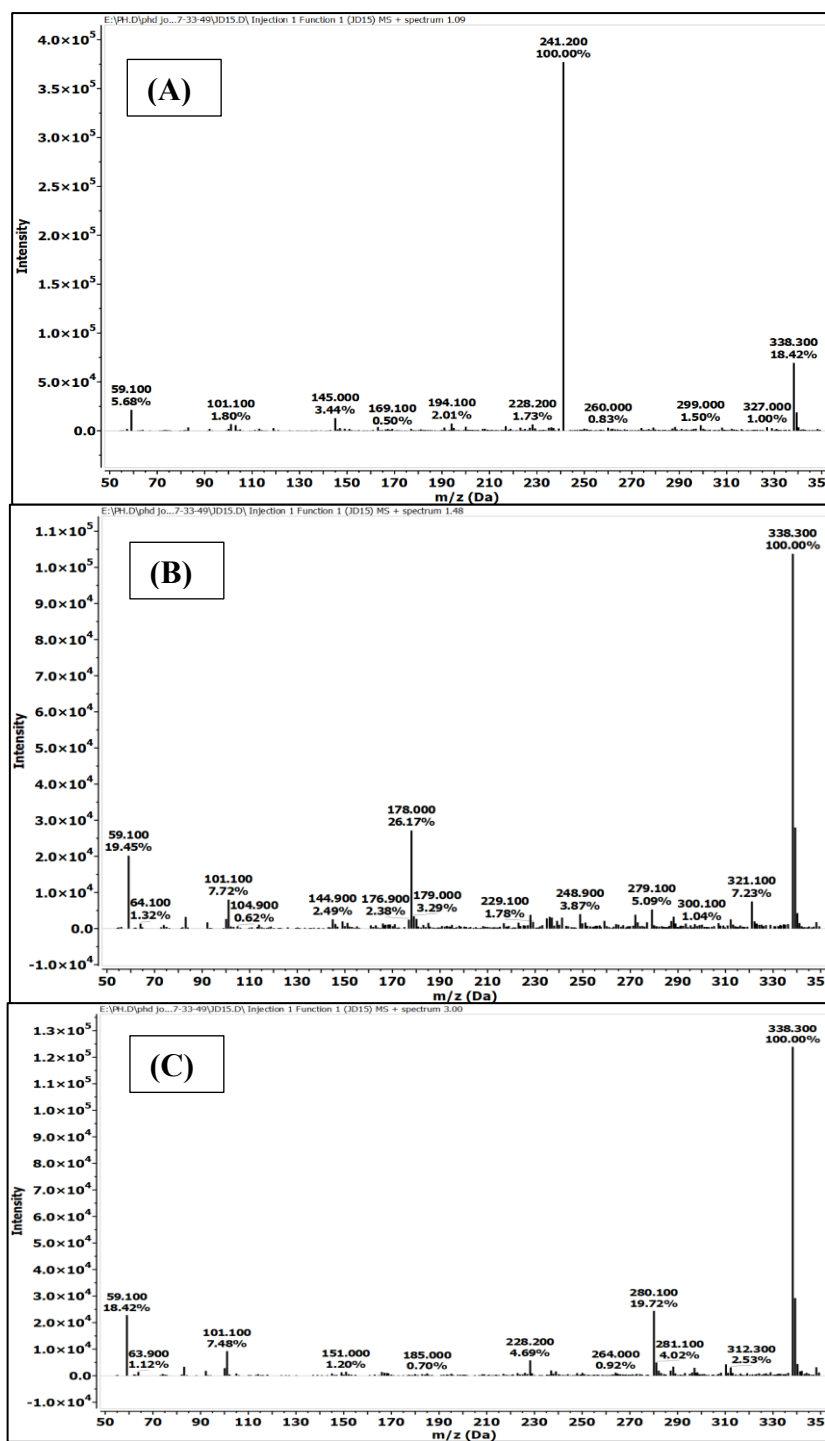


Figure 21: (A) Mass spectrometry data of GMM at retention time 1.09; (B) 1.48 min; and (C) 3.00 min.

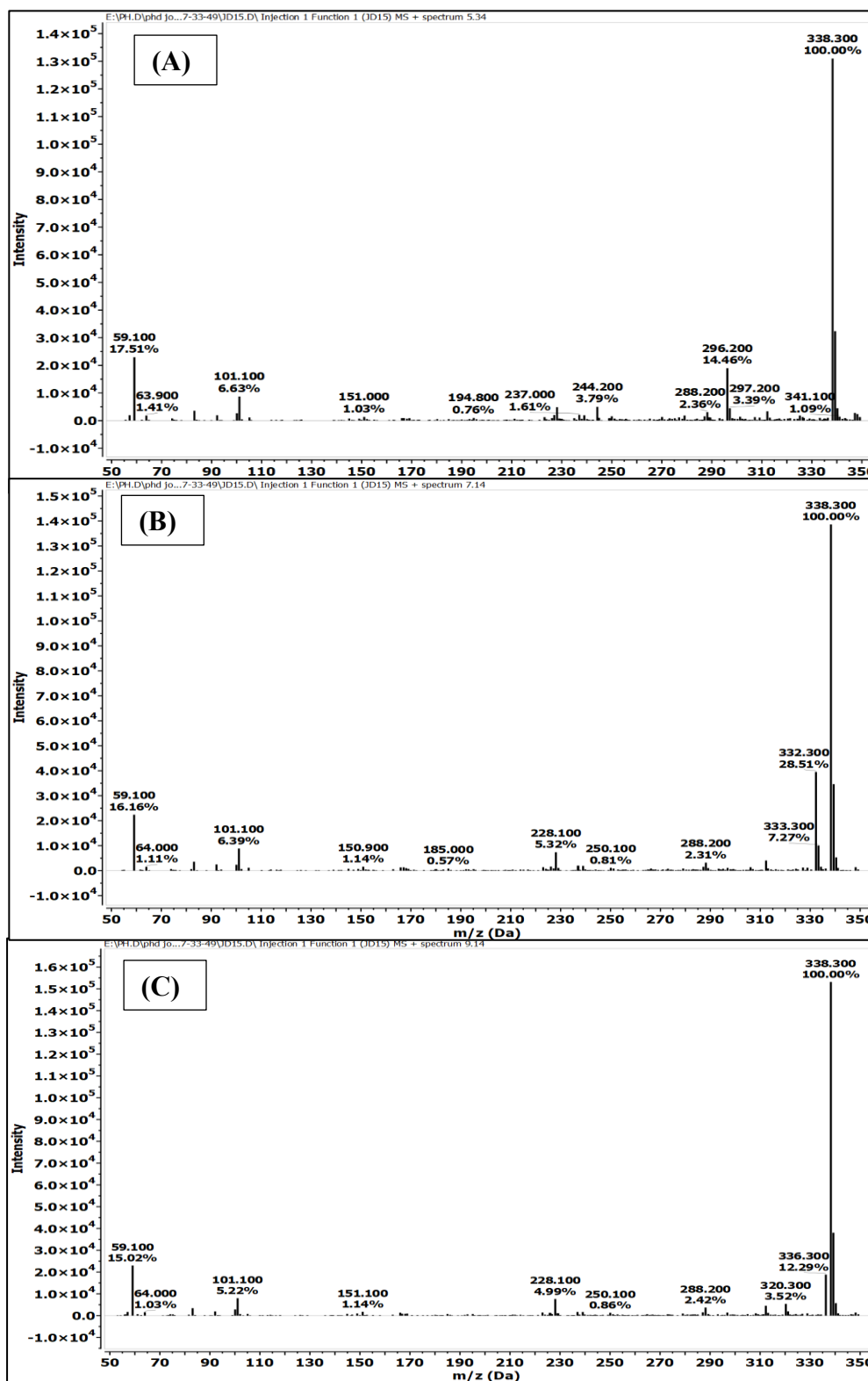


Figure 22: (A) Mass spectrometry data of GMM at retention time 5.34; (B) retention time 7.14 min; and (C) 9.14 min.

Table 13: LCMS analysis of GTE, MO and GMM

| Sample | Retention time (min) | m/z fractions |
|--------|----------------------|--|
| GTE | 0.826 | 325.00 (100.00%), 235.00 (30.77%) |
| | 0.978 | 145.00 (100.00%), 237.00 (32.54%) |
| | 2.346 | 217.00 (100.00%), 145.00 (73.19%) |
| | 1.260 | 274.20 (100.00%), 338.20 (23.53%) |
| | 1.933 | 279.10 (100.00%), 280.10 (18.42%) |
| MO | 0.804 | 169.10 (100.00%), 155.1 (28.4%), 288.0 (21.8%), 337.3 (14.29%). |
| | 1.130 | 241.20 (100.00%), 208.1 (58.07 %). |
| | 1.26 | 222.20 (100.00%), 338.30 (17.84 %), 223.10 (15.60 %). |
| | 1.50 | 338.30 (100.00%), 59.10 (58.71 %), 272.20 (49.76 %), 178.00 (47.24 %) |
| | 5.34 | 338.30 (100.00%), 296.20 (51.29 %), 59.10 (49.05 %). |
| | 7.17 | 338.30 (100.00%), 332.30 (77.73%), 59.10 (39.66%), 333.30 (21.21%) |
| | 8.45 | 338.30 (100.00%), 298.30 (48.79 %), 59.10 (42.15 %). |
| GMM | 0.80 | 169.10 (100.00%), 235.00 (39.86%), 338.30 (23.70%) |
| | 0.85 | 235.00 (100.00%), 163.00 (90.50%), 169.10 (90.09%), 171.10 (28.54%), 187.10 (25.51%), 219.10 (27.29%), 145.00 (22.89%) |
| | 0.98 | 145.00 (100.00%), 228.30 (29.51%), 227.00 (28.91%), 163.00 (23.64%) |
| | 1.09 | 241.00 (100.00%), 338.30 (18.24%) |
| | 1.48 | 338.30 (100.00%), 178.00 (26.17%), 59.10 (19.45%) |
| | 3.00 | 338.30 (100.00%), 280.10 (19.72%), 59.10 (18.42%) |
| | 5.34 | 338.30 (100.00%), 59.10 (17.51%), 296.20 (14.46%) |
| | 7.14 | 338.30 (100.00%), 59.10 (16.16%), 332.30 (28.51%) |
| | 9.14 | 338.30 (100.00%), 59.10 (15.02%), 336.30 (12.29%) |

4.2.3.7. Gas chromatography-mass spectrometry analysis

The GCMS analysis of MO and GMM showed 20 and 26 major peaks, respectively. The details of the identified compounds in both MO and GMM macerate are mentioned in table 14 below:

Table 14: Major compounds of mustard oil and garlic mustard oil macerate identified by GCMS analysis.

| Compounds | Mustard Oil (%) | Garlic Mustard Oil macerate (%) |
|---|-----------------|---------------------------------|
| 3-Hexanone | - | 0.69 |
| Hydroperoxide, 1- ethylbutyl | 0.12 | 0.30 |
| Isobutyl vinylacetate | - | 0.07 |
| Allyl isothiocyanate | 0.18 | 0.37 |
| Pentane,2,2,3,4-tetramethyl | - | 0.03 |
| 1-Butene, 4-isothiocyanato | 1.03 | 2.01 |
| undecane | - | 0.32 |
| Cyano-3,4-epithiobutane | - | 0.03 |
| 3-cyclopropylcarbonyloxypentadecane | - | 0.09 |
| 2-vinyl-4H-1,3-dithiine | - | 0.04 |
| Benzene,1,3-bis(1,1-dimethylethyl)- | 0.4 | 0.75 |
| Decane-2,3,5,8-tetramethyl- | 0.06 | 0.05 |
| Undecane,2-methyl- | - | 0.1 |
| Dodecane,26,11-trimethyl- | - | 0.12 |
| 1-iodo-2-methylundecane | - | 0.06 |
| Cyclopentaneundecanoic acid, methyl ester | 2.19 | 0.44 |
| 12,15-octadecadienoic acid, methyl ester | - | 90.25 |
| Cyclopentaneundecanoic acid, methyl ester | 3.13 | 0.77 |
| Cyclopentaneundecanoic acid | - | 0.99 |
| 7- Methyl-Z- tetradecen-1-ol acetate | - | - |
| 12-methyl-E,E,-2,13-octadecadien-a-ol | - | 0.03 |
| Cholestane-3-ol, 2-methylene- | - | 0.05 |
| 1-heptatriaotanol | - | 0.05 |
| Cis-13-eicosenoic acid | - | 0.03 |
| Cyclopropanedodecanoic acid, 2-octyl, methyl ester | 0.12 | 0.13 |
| Hexadecane, 1,1-bis (dodecyloxy)- | - | 0.05 |
| 17-pentatriacontene | - | 0.04 |
| 4-cyclopropylcarbonyloxytridecane | 0.08 | - |
| Tetradecane,2,6,10-trimethyl- | 0.13 | - |
| methoxyacetic acid, 2-tetradecyl ester | 0.03 | - |
| 3-cyclopropylcarbonyloxytridecane | 0.04 | - |
| Decane, 2,3,5,8-tetramethyl- | 0.14 | - |
| Methoxyacetic acid, 4-tetradecyl ester | 0.03 | - |
| 17-octadecyonic acid, methyl ester | 0.03 | - |
| 9-12-octadecadienoic acid (Z,Z)-, methyl ester | 34.3 | - |
| 8, 11-octadecadienoic acid, methyl ester | 6.67 | - |
| 10-octadecenoic acid, methyl ester, Isooleic acid. | 49.95 | - |
| 1- heptatriacotanol | 0.03 | - |
| Oxiraneundecanoic acid, 3-pentyl-, methyl ester, cis- | 0.12 | - |

4.3. Optimization of garlic mustard oil macerate

4.3.1. Optimization of garlic mustard oil macerate using response surface methodology

The range of concentration of ajoene and 2-vinyl-4H-1,3, dithiin yield in different prepared formulations of GMM were found to be between 1103.36-3212.906 $\mu\text{g/ml}$ of oil and 3474.06-6259.02 $\mu\text{g/ml}$ of oil, respectively (Table 15). In Table 7 the polynomial equation for the model is shown along with R^2 and P value. The R^2 values of the model for ajoene and 2-vinyl-4H-1,3, dithiin synthesis were found to be 0.93 and 0.72, respectively (Table 16). These show that the ajoene yield (Y_1) model is appropriate, but the dithiin yield (2-vinyl-4H-1,3 dithiin) model is not suitable. In future research, it is necessary to make modifications to the design to get a substantial p-value for the yield of 2-vinyl-4H-1,3-dithiin.

Table 15: Representing 17 different conditions for the garlic mustard oil macerate preparation designed by Central Composite Design along with the concentration of ajoene and 2-vinyl-4H-1,3, dithiin.

| Sl. No. | Factor 1 Temperature ($^{\circ}\text{C}$) | Factor 2 Time (Hr) | Factor 3 Oil volume (ml) | Response 1 Ajoene ($\mu\text{g/ml}$ of GMM) | Response 2 Ajoene ($\mu\text{g/ml}$ of GMM) |
|---------|---|--------------------------|--------------------------------|---|---|
| 1 | 55.00 | 4.50 | 4.00 | 1550.19 | 4959.94 |
| 2 | 70.00 | 3.00 | 3.00 | 1387.88 | 4361.35 |
| 3 | 85.00 | 4.50 | 2.00 | 1646.44 | 4717.34 |
| 4 | 100.00 | 3.00 | 3.00 | 1298.07 | 4517.05 |
| 5 | 70.00 | 3.00 | 3.00 | 1469.19 | 4371.71 |
| 6 | 55.00 | 4.50 | 2.00 | 2466.90 | 6259.02 |
| 7 | 55.00 | 1.50 | 4.00 | 1672.29 | 4870.83 |
| 8 | 85.00 | 1.50 | 2.00 | 1748.11 | 5000.93 |
| 9 | 70.00 | 6.00 | 3.00 | 1275.10 | 4052.47 |
| 10 | 40.00 | 3.00 | 3.00 | 1752.15 | 4783.77 |
| 11 | 85.00 | 1.50 | 4.00 | 1240.78 | 3956.95 |
| 12 | 70.00 | 3.00 | 3.00 | 1548.02 | 4551.55 |
| 13 | 70.00 | 3.00 | 5.00 | 1215.54 | 4018.85 |
| 14 | 70.00 | 3.00 | 1.00 | 3212.90 | 5522.14 |
| 15 | 70.00 | 0.00 | 3.00 | 2588.44 | 3474.06 |
| 16 | 85.00 | 4.50 | 4.00 | 1103.36 | 4051.47 |
| 17 | 55.00 | 1.50 | 2.00 | 2299.39 | 5340.81 |

Table 17 shows the ANOVA of the ajoene (Y_1) and 2-vinyl-4H-1,3, dithiin formation (Y_2). For Y_1 , the quadratic model was found to be significant at a

95% probability level with a p-value of 0.0051, whereas the quadratic model for Y_2 the model was not significant at a 95% probability level. The lack of fit signifies the fitness of the model (significant the p-value the less fit the model represents), Y_1 was found to be non-significant with a p-value of 0.089, whereas for Y_2 it was found to be significant with a p-value of 0.028. Upon examining the 3D model graph (Figure 23), it was determined that the levels of both ajoene and vinyl dithiin increased in response to a decreasing quantity of mustard oil (range from 1-2 times the weight of garlic paste), longer incubation periods (ranges from 3 and 4.5 h) and at lower temperatures (ranges from 55 to 70 °C).

Upon optimization, the optimum preparation condition for ajoene was at a temperature of 55 °C, a reaction time of 4.5 hours and an oil volume of 2.00 factor of weight of garlic; and for 2-vinyl-4H-1,3, dithiin, the conditions were a temperature of 77.51 °C, a reaction time of 2.22 hours and oil volume of 2.25 factor of weight of garlic. The predicted values of ajoene and 2-vinyl-4H-1,3, dithiin at the optimum conditions were 2387.24 µg/ml of GMM oil and 4806.11 µg/ml of GMM oil respectively. The experimental values were found to be 2186.58 ± 34.32 µg/ml of GMM and 4363.27 ± 32.50 µg/ml of GMM for ajoene and 2-vinyl-4H-1,3, dithiin respectively when synthesized in the above predicted optimal conditions (Table 18).

Table 16: Representing the polynomial equation for the synthesis of ajoene (µg/ml of GMM) (Y_1) and 2-vinyl-4H-1,3, dithiin (µg/ml of GMM) (Y_2).

| Response | Polynomial equation | R^2 | P value |
|---|--|--------|---------|
| Y1 | $Y = 5682.49950 - 31.63X_1 + 209.20X_2 - 1769.323X_3 - 1.59X_1X_2 + 4.14X_1X_3 - 27.34X_2X_3 + 0.076X_1^2 - 7.23X_2^2 + 190.95X_3^2$ | 0.9391 | 0.0051 |
| Y2 | $Y = 7722.69 - 43.85X_1 + 665.38X_2 - 937.91X_3 - 6.64X_1X_2 + 0.49X_1X_3 - 37.58X_2X_3 + 0.31X_1^2 - 14.01X_2^2 + 101.79X_3^2$ | 0.7297 | 0.2443 |
| Y1- ajoene (µg/ml of GMM), Y2- dithiin (µg/ml of GMM) | | | |

Table 17: ANOVA of the quadratic model for the optimization of ajoene ($\mu\text{g/ml}$ of GMM) (Y_1) and 2-vinyl-4H-1,3, dithiin ($\mu\text{g/ml}$ of GMM) (Y_2).

| Responses | Source | df | SS | Mean Square | F-value | P-value |
|-----------------------------------|-----------------|----|----------|-------------|---------|-------------------------|
| Ajoene (Y_1) | Model | 9 | 4.30E+06 | 4.78E+05 | 10.28 | 0.0051 ^a |
| | A-Temperature | 1 | 6.23E+05 | 6.23E+05 | 13.41 | 0.0106 |
| | B-Time | 1 | 15301.53 | 15301.53 | 0.3292 | 0.587 |
| | C-Amount of oil | 1 | 2.71E+06 | 2.71E+06 | 58.38 | 0.0003 ^{a,b,c} |
| | AB | 1 | 10118.28 | 10118.28 | 0.2177 | 0.6573 |
| | AC | 1 | 30429.29 | 30429.29 | 0.6546 | 0.4493 |
| | BC | 1 | 13232.19 | 13232.19 | 0.2847 | 0.6128 |
| | A ² | 1 | 5622.56 | 5622.56 | 0.121 | 0.7399 |
| | B ² | 1 | 2687.51 | 2687.51 | 0.0578 | 0.818 |
| | C ² | 1 | 6.93E+05 | 6.93E+05 | 14.91 | 0.0083 ^a |
| | Residual | 6 | 2.79E+05 | 46481.89 | | |
| | Lack of Fit | 4 | 2.66E+05 | 66517.06 | 10.37 | 0.0898 |
| | Pure Error | 2 | 12823.13 | 6411.56 | 7.28 | 0.0049 |
| | | | | | | |
| Dithiin (Y_2) | Model | 9 | 4.27E+06 | 4.74E+05 | 1.8 | 0.2443 |
| | A-Temperature | 1 | 1.12E+06 | 1.12E+06 | 4.26 | 0.0845 |
| | B-Time | 1 | 219.14 | 219.14 | 0.0008 | 0.9779 |
| | C-Amount of oil | 1 | 2.63E+06 | 2.63E+06 | 9.98 | 0.0196 ^a |
| | AB | 1 | 1.79E+05 | 1.79E+05 | 0.6795 | 0.4413 |
| | AC | 1 | 438.59 | 438.59 | 0.0017 | 0.9688 |
| | BC | 1 | 25424.12 | 25424.12 | 0.0966 | 0.7665 |
| | A ² | 1 | 99591.23 | 99591.23 | 0.3783 | 0.5611 |
| | B ² | 1 | 10249.91 | 10249.91 | 0.0389 | 0.8501 |
| | C ² | 1 | 2.00E+05 | 2.00E+05 | 0.7609 | 0.4166 |
| | Residual | 6 | 1.58E+06 | 2.63E+05 | | |
| | Lack of Fit | 4 | 1.56E+06 | 3.89E+05 | 34.03 | 0.0288 ^a |
| | Pure Error | 2 | 22876.29 | 11438.15 | | |
| | | | | | | |

a- P-value <0.05; b- P-value <0.005; c- P-value <0.001; Y_1 - ajoene ($\mu\text{g/ml}$ of GMM); Y_2 - dithiin ($\mu\text{g/ml}$ of GMM); df- degree of freedom; ss- sum of squares.

The actual value was in the range of the predicted values therefore the optimized conditions may be suitable for the synthesis of ajoene and 2-vinyl-4H-1,3, dithiin.

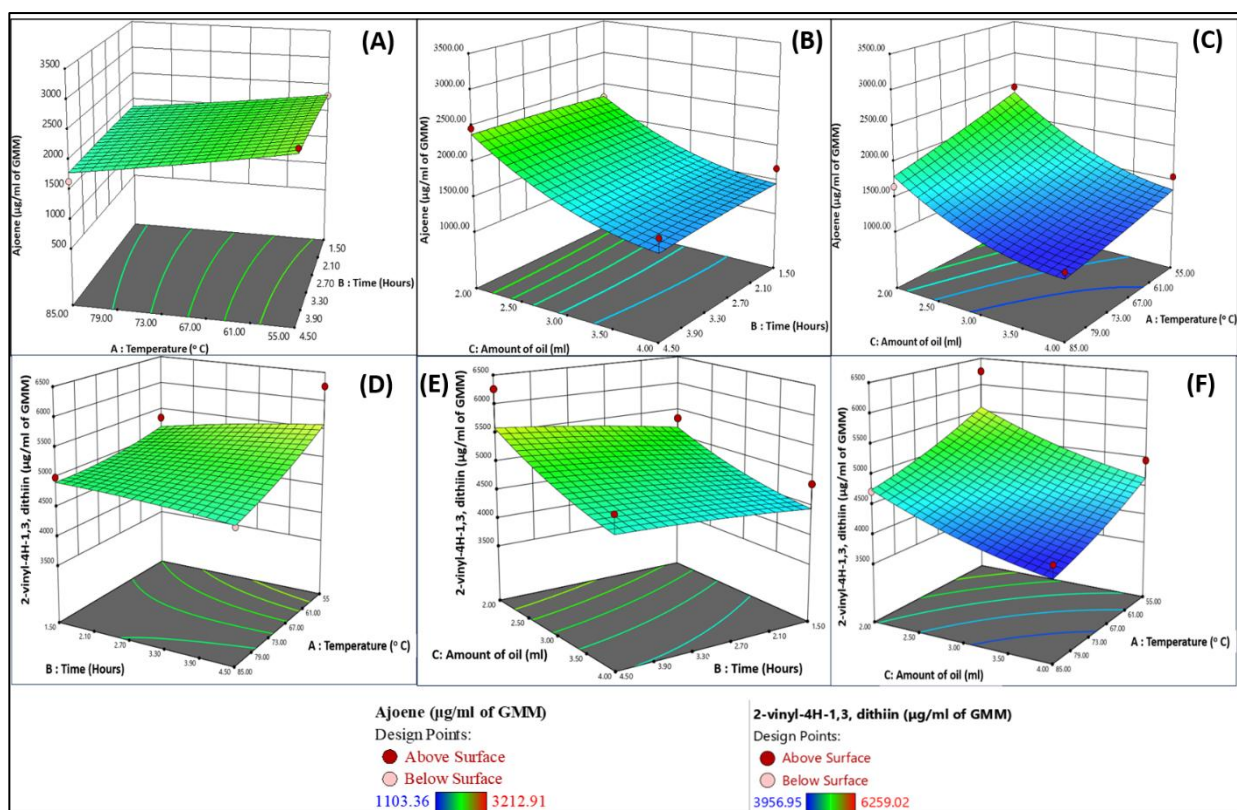


Figure 23: Shows a response surface plot for optimization of ajoene for (A) temperature and time, (B) time and amount of oil and (C) temperature and amount of oil for GMM preparation; and a response surface plot for 2-vinyl-4H-1,3, dithiin optimization with (D) temperature, (E) time and (F) amount of oil for GMM preparation (Picture courtesy: Singha, J., Dutta, N., and Saikia, J.P. A novel method to produce maximum ajoene and vinyl dithiin during garlic mustard oil macerate preparation. *Journal of Sulfur Chemistry*: 1-13, 2025.).

Table 18: Representing the predicted value and the experimental values of ajoene (μg/ml of GMM) (Y₁) and 2-vinyl-4H-1,3, dithiin (μg/ml of GMM) (Y₂).

| Response | Temperature (°C) | Time (Hours) | Amount of oil (ml) | Predicted Value (μg/ml of GMM) | Experimental value (μg/ml of GMM) | Results |
|-------------------------|------------------|--------------|--------------------|--------------------------------|-----------------------------------|----------|
| Ajoene | 55.00 | 4.5 | 2.00 | 2387.24 | 2186.58 ± 34.32 | In range |
| 2-vinyl-4H-1,3, dithiin | 77.51 | 2.22 | 2.25 | 4806.11 | 4363.27 ± 32.50 | In range |

4.3.2. Quantification of the amount of GMM oil required for antibacterial and antifungal activity during vapour diffusion assay

No bacterial colony was seen when 500 μl of GMM was used in all the bacterial species (*S. aureus* MTCC 3160, *K. pneumoniae* MTCC 618 and *E. coli*).

MTCC 40). However, the bacterial colony was visible when the same amount of mustard oil was used against *S. aureus* MTCC 3160, *K. pneumoniae* MTCC 618 and *E. coli* MTCC 40 (Figure 24, 25, 26). When 250 μ l of GMM oil was used, *E. coli* MTCC 40 and *S. aureus* MTCC 3160 showed a zone of inhibition in the centre of the plate whereas MO did not show any zone of inhibition against the two. The other volumes of GMM oil such as 100 and 50 μ l have not shown any significant difference in any of the strains with that of the mustard

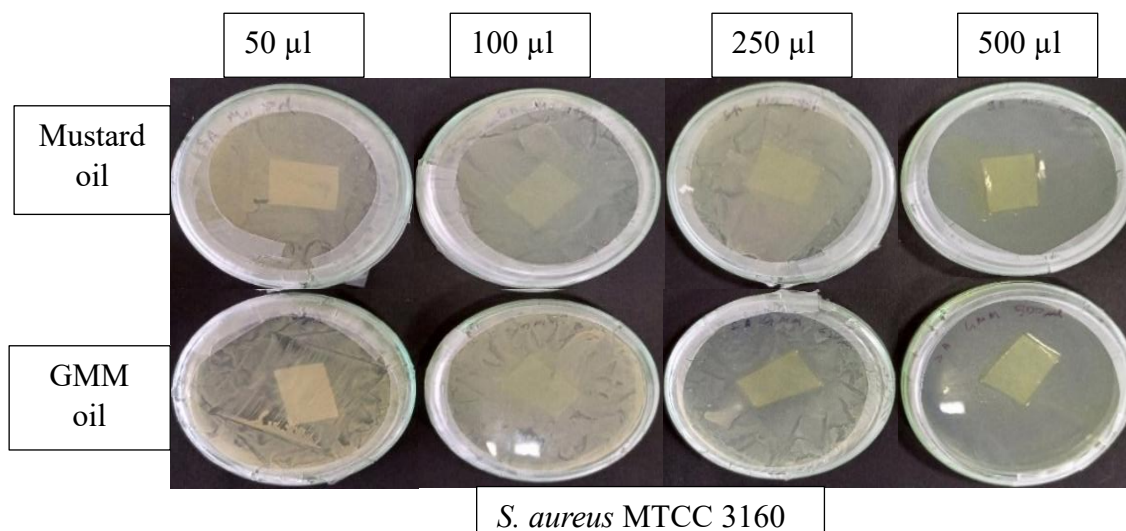


Figure 24: Showing the antibacterial activity against *S. aureus* MTCC 3160 when exposed to different volume of mustard oil and garlic mustard oil macerate vapour.

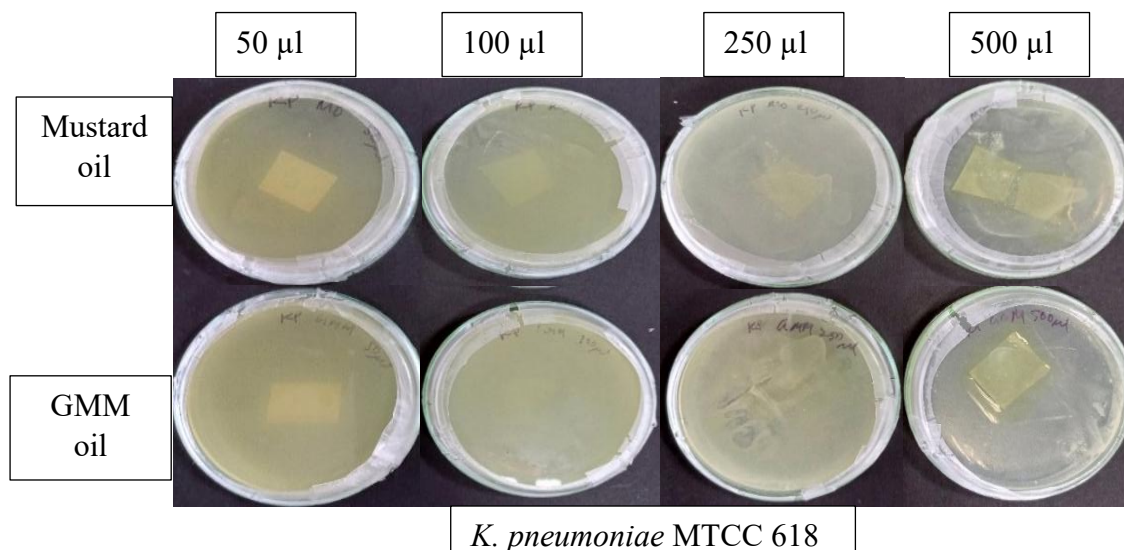


Figure 25: Showing the antibacterial activity against *K. pneumoniae* MTCC 618 when exposed to different volume of mustard oil and garlic mustard oil macerate vapour.

oil.

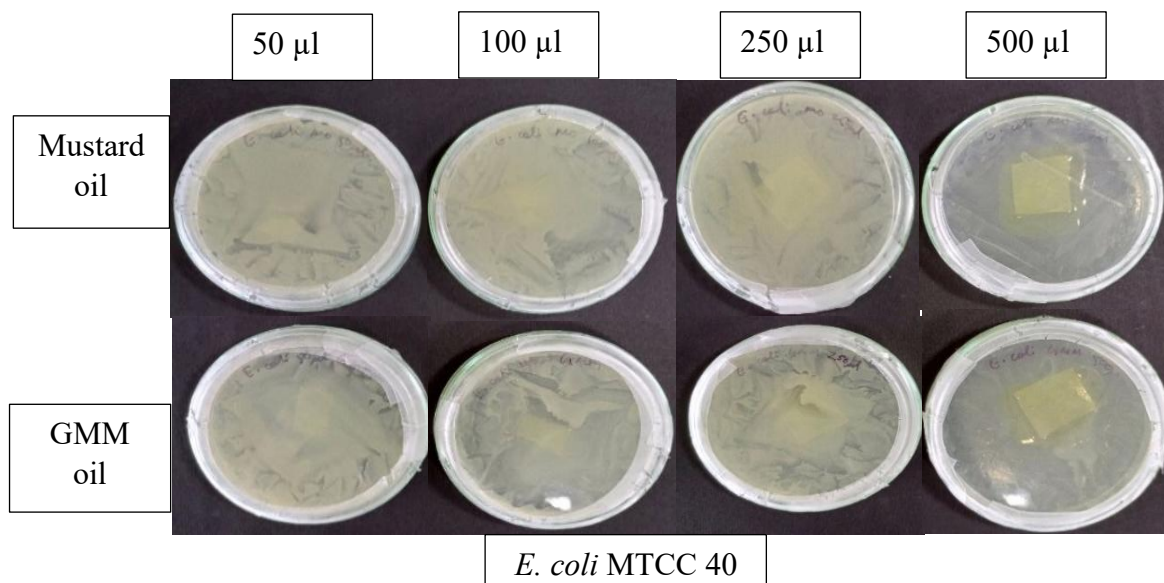


Figure 26: Showing the antibacterial activity against *E. coli* MTCC 40 when exposed to different volume of mustard oil and garlic mustard oil macerate vapour.

It was observed that both MO and GMM oil have antifungal properties against *C. albicans* MTCC 183. The volumes of 1000 μ l and 500 μ l of both the oil samples have shown no fungal colonies (Figure 27). At 250 μ l sample of MO and GMM oil, significantly less fungal colony was observed in the plates with garlic mustard oil macerate oil compared to mustard oil. There was no significant difference in the colony number seen between the plate containing 100 μ l of mustard oil and garlic mustard oil macerate. Therefore, 750 μ l 300 μ l of GMM was considered for antifungal assay.

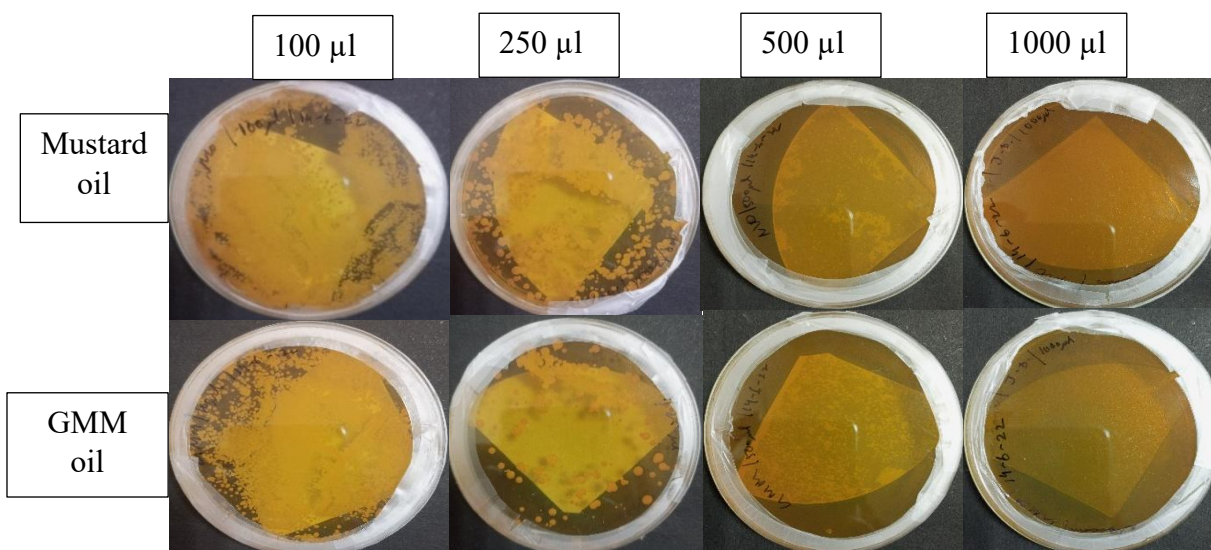


Figure 27: Showing the antifungal activity against *C. albicans* MTCC 183 when exposed to different volume of mustard oil and garlic mustard oil macerate vapour.

4.3.3. Optimization of GMM based on antibacterial activity against *S. aureus*

4.3.3.1. Antibacterial activity by vapour diffusion method

4.3.3.1.1. GMM based on the ratio of garlic and mustard oil

The macerate which was prepared with the ratio of garlic and mustard oil (1:4 and 1:8, w/v) has shown the maximum antibacterial activity (Figure 28). The relative scoring was done based on three parameters: the filter paper is visible (a), the shape of the filter paper is visible (b) and the bacterial colony colour is white (c). The order of antibacterial activity was found to be: G160/4/1 > G160/8/1 > G160/2/1 > G160/16/1 > GR160/2/1 (Table 19).

Table 19: Relative scoring of the antibacterial activity of prepared GMM based on ratio of garlic and MO against *S. aureus*

| Sample ID | G160/2/1 | G160/4/1 | G160/8/1 | G160/16/1 | GR160/2/1 |
|-----------|----------|-------------|-------------|-----------|-----------|
| Set 1 | +(a) | +++ (a,b,c) | +++ (a,b,c) | NA | ++ (a,b) |
| Set 2 | ++ (a,b) | +++ (a,b,c) | +++ (a,b,c) | NA | NA |

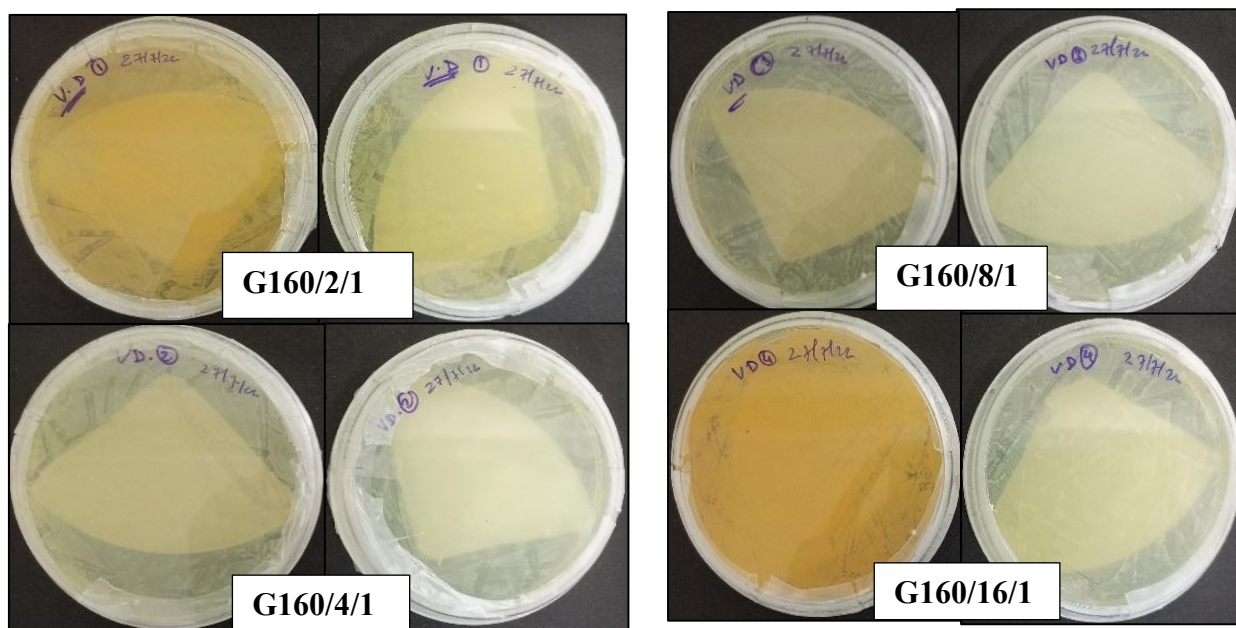


Figure 28: Antibacterial activity against *S. aureus* by prepared GMM at various ratio of garlic and mustard oil by vapour diffusion method.

4.3.3.1.2.

GMM based on time of heating of macerate at 80°C

The macerate which was prepared heated for 2 hours and 4 hours at 80°C has shown the maximum antibacterial activity (Figure 29). The order of antibacterial activity was found to be: G80/4/2 = G80/4/4 > G80/4/1 = G80/4/8 = G80/4/16 > G80/4/0 > MO (Table 20).

| Table 20: Relative scoring of the antibacterial activity of prepared GMM based on time of heating against <i>S. aureus</i> | | | | | | |
|--|---------|---------|---------|---------|---------|----------|
| Sample ID | G80/4/0 | G80/4/1 | G80/4/2 | G80/4/4 | G80/4/8 | G80/4/16 |
| Results | ++ | ++ | +++ | +++ | ++ | ++ |

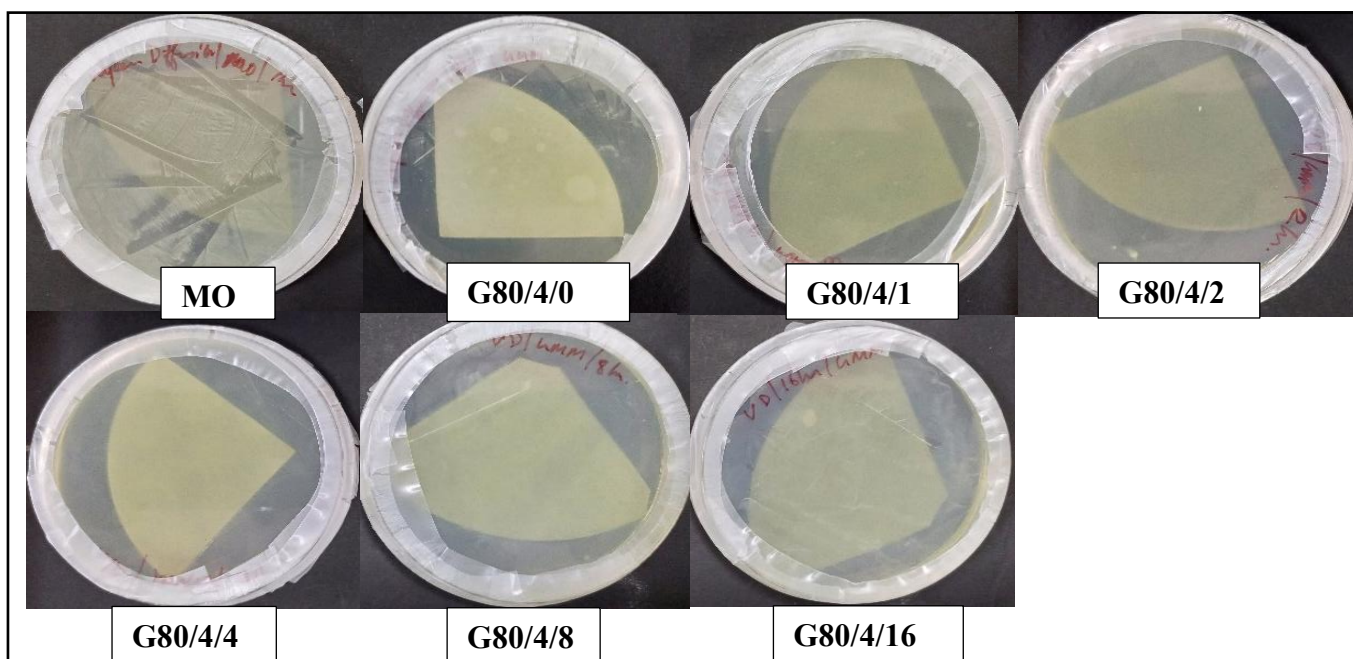


Figure 29: Antibacterial activity against *S. aureus* by prepared GMM sample based on time of heating through vapour diffusion method.

4.3.4. Optimization of garlic mustard oil macerate based on antifungal activity

4.3.4.1. Antifungal activity by agar diffusion method

4.3.4.1.1. GMM based on different preparation temperature

The antifungal activity of GMM prepared at different temperatures $55^{\circ}\text{C} > 80^{\circ}\text{C} > 160^{\circ}\text{C} > \text{MO}$ (Figures 30 and 31).

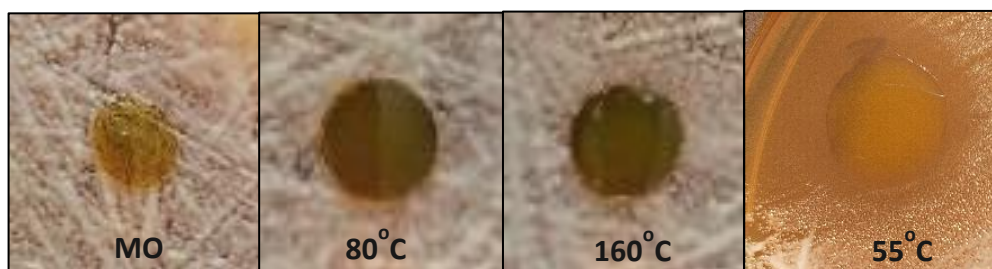


Figure 30: Antifungal activity of GMM prepared at different temperature against *C. albicans* (Image courtesy: Singha, J., and Saikia, J.P. Optimisation of garlic mustard oil macerate with respect to its antifungal activity against *Candida albicans* MTCC 183 and in-silico molecular docking of the volatile compounds with N-myristoyltransferase. *Natural Product Research*: 1-8, 2024.).

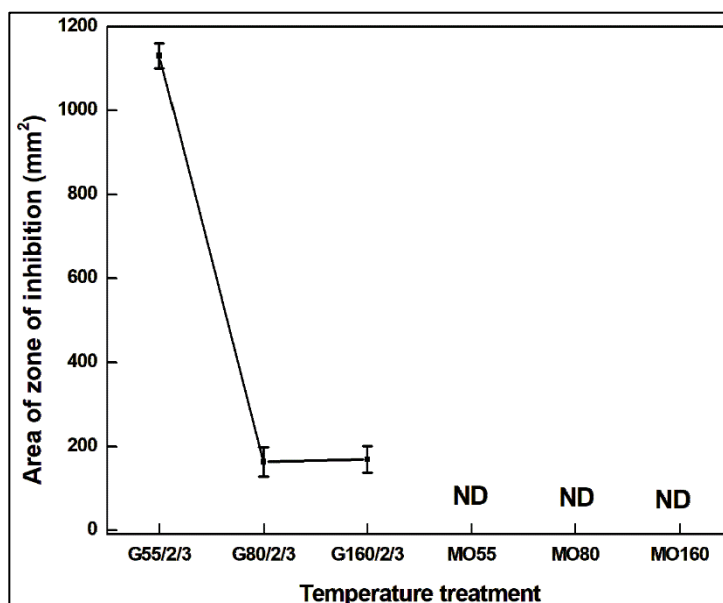


Figure 31: Line graph showing antifungal activity of GMM prepared at different temperature against *C. albicans* through agar diffusion method.

4.3.4.1.2. GMM based on the time of heating

The antifungal activity of GMM prepared at different times of heating 1Hr > 0Hr > 2Hr > 4Hr > 8Hr > 16Hr > MO (Figures 32 and 33).

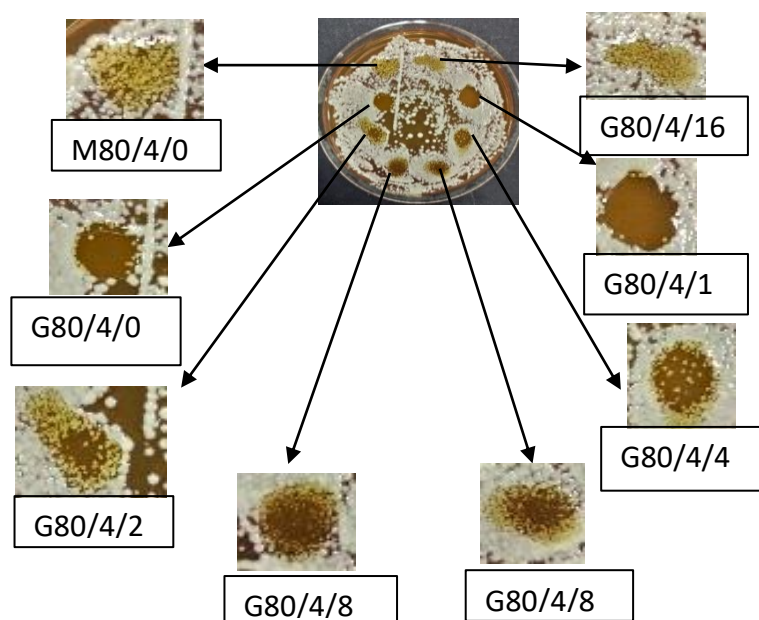
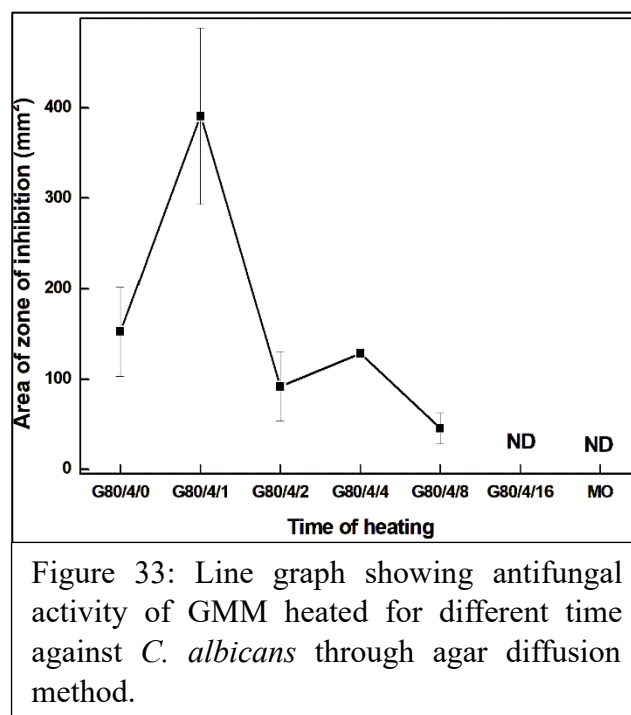


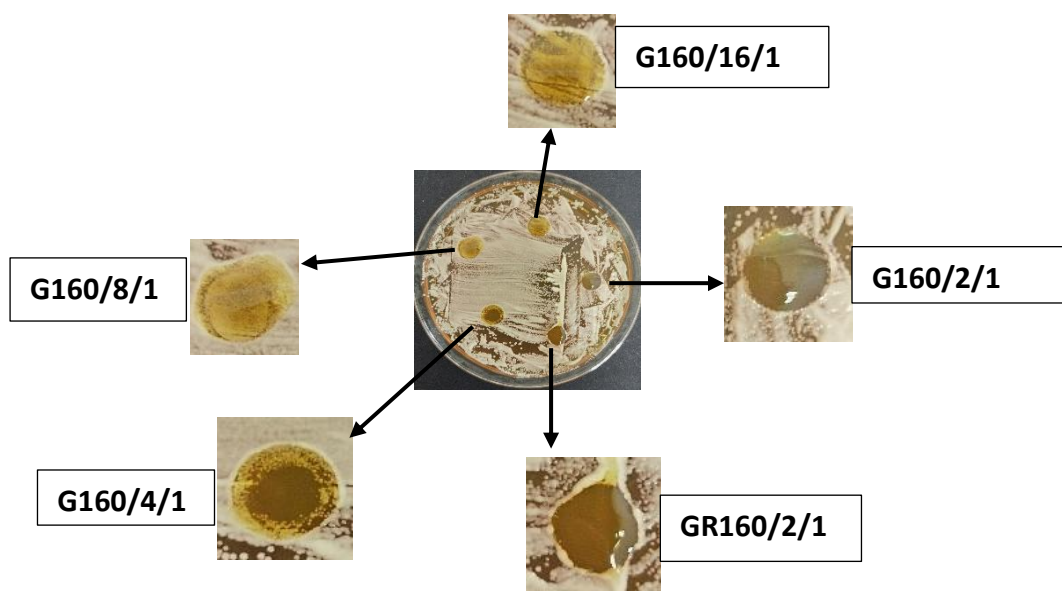
Figure 32: Antifungal activity of GMM heated for different time against *C. albicans* through agar diffusion method.



4.3.4.1.3.

GMM based on the ratio of garlic and mustard oil

The antifungal activity of GMM prepared with different ratios of garlic and mustard oil 1:2 > 1:4 > 1:8 > 1:16 > MO (Figures 34 and 35).



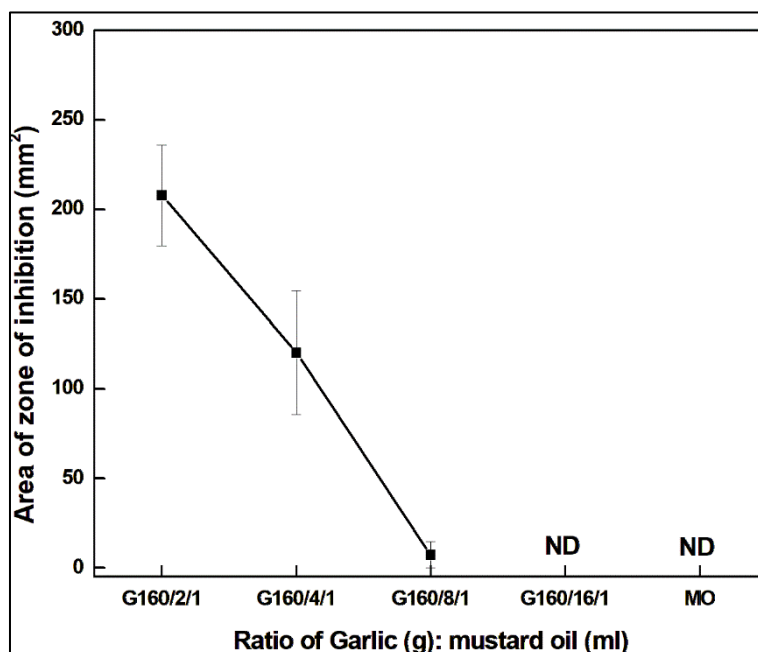


Figure 35: Line graph showing antifungal activity of GMM prepared with different ratio of garlic and mustard oil against *C. albicans* through agar diffusion method.

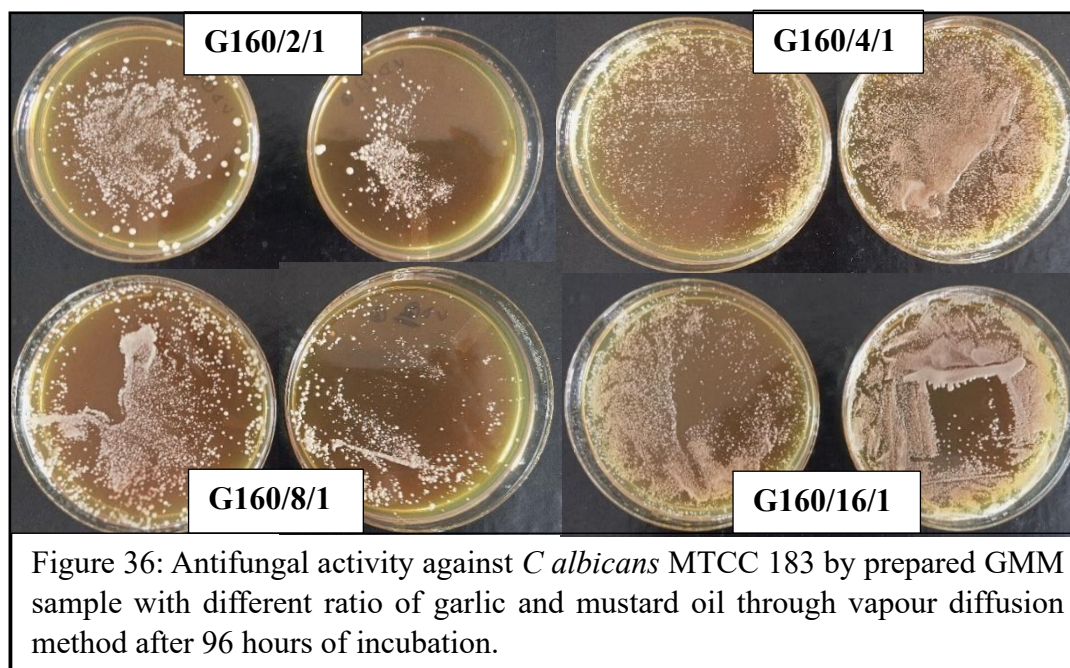
4.3.4.2. Antifungal activity by vapour diffusion method

4.3.4.2.1. GMM based on the ratio of garlic and mustard oil

The macerate which was prepared with the ratio of garlic and mustard oil (1:2 and 1:4, w/v) has shown the maximum antifungal activity because till 72 hours there was no fungal growth in the plates (Table 21). The order of antifungal activity was found to be: G160/2/1 > G160/4/1 > G160/8/1 > G160/16/1 (Figure 36).

| Table 21: Qualitative estimation of antifungal activity of GMM based on the ratio of garlic and MO. | | | | | |
|---|--------|----------|----------|----------|----------|
| Sample | Repeat | 24 hours | 48 hours | 72 hours | 96 hours |
| G160/2/1 | A | No | No | No | Yes |
| | B | No | No | No | Yes |
| G160/4/1 | A | No | No | No | Yes |
| | B | No | No | No | Yes |
| G160/8/1 | A | No | No | No | Yes |
| | B | No | No | Yes | Yes |

| | | | | | |
|-----------|---|----|----|-----|-----|
| G160/16/1 | A | No | No | No | Yes |
| | B | No | No | Yes | Yes |



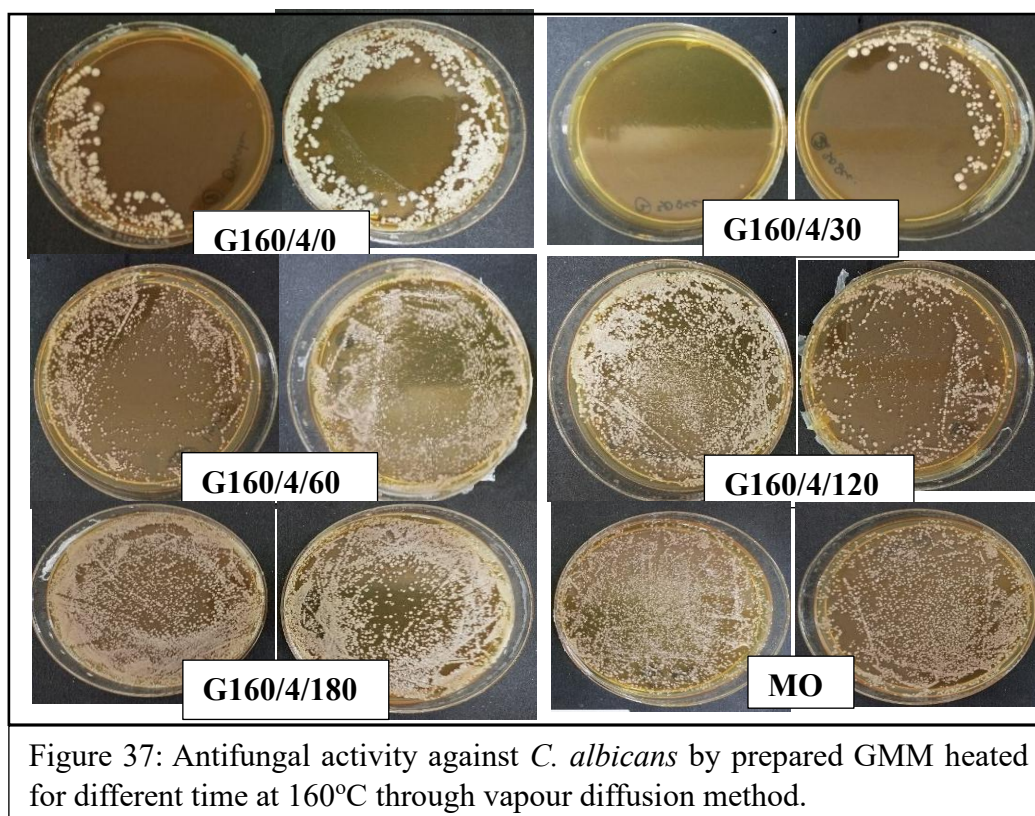
4.3.4.2.2.

GMM based on time of heating of macerate at 160°C

The macerate which was heated for 30 seconds at 160°C showed the maximum antifungal activity (Figure 37 and Table 22). The order of antifungal activity was found to be: G160/4/30 > G160/4/0 > G160/4/60 > G160/4/120 > G160/4/180.

Table 22: Qualitative estimation of antifungal activity of GMM heated for different times at 160°C through vapour diffusion method.

| Sample ID | GMM |
|------------|-----|
| G160/4/0 | ++ |
| G160/4/30 | +++ |
| G160/4/60 | + |
| G160/4/120 | + |
| G160/4/180 | NA |
| MO | NA |



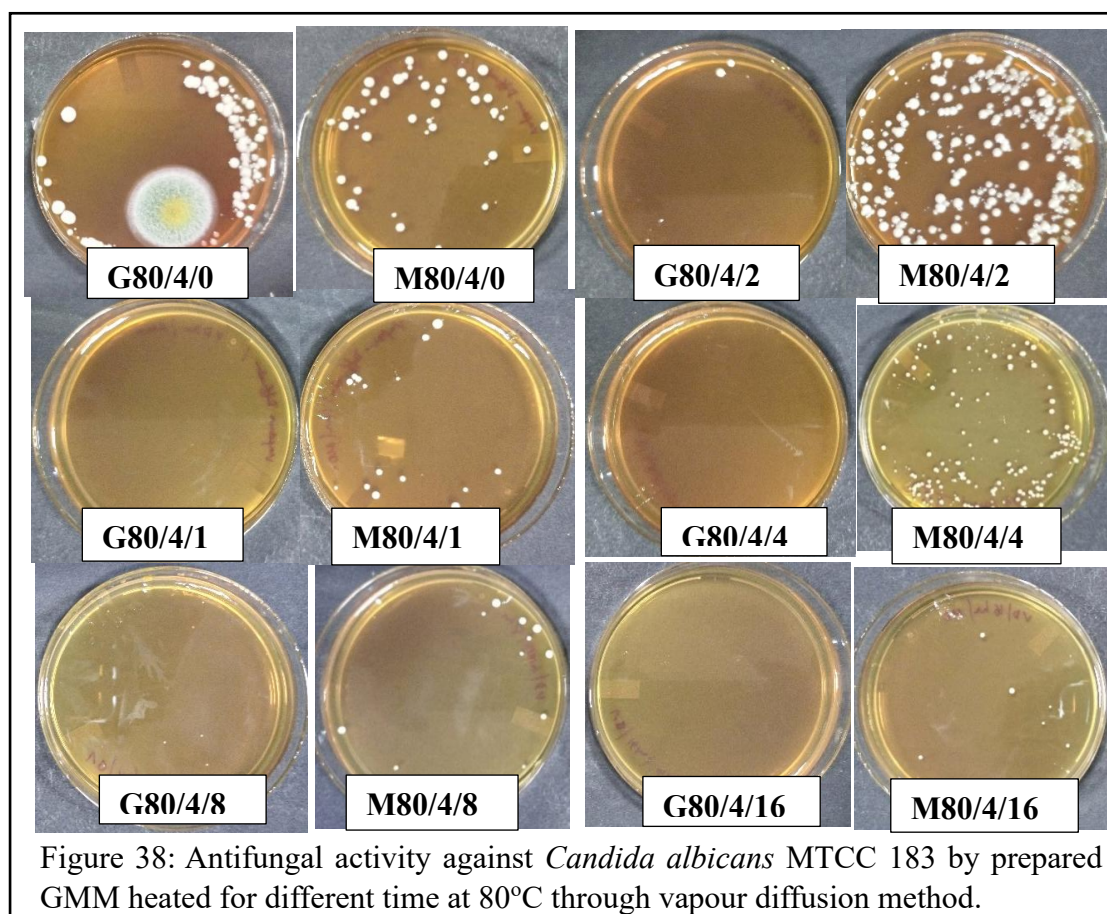
4.3.4.2.3.

GMM based on time of heating of macerate at 80°C

The macerate which was heated for two hours and 4 hours at 80°C has shown the maximum antifungal activity (Figure 38 and Table 23). The order of antifungal activity was found to be: G80/4/2 > G80/4/4 > G80/4/1=G80/4/8> G80/4/16> G80/4/0.

Table 23: Number of colonies of *C. albicans* after the treatment by prepared GMM heated for different times at 80°C through vapour diffusion method.

| Sample ID | GMM | MO |
|-----------|-------------|---------------|
| G80/4/0 | 58 colonies | 88 colonies |
| G80/4/1 | No colonies | 13 colonies |
| G80/4/2 | 6 colonies | >200 colonies |
| G80/4/4 | No colonies | 159 colonies |
| G80/4/8 | No colonies | 13 colonies |
| G80/4/16 | No colonies | 8 colonies |



4.3.5. Optimization of garlic mustard oil macerate based on DPPH scavenging activity

4.3.5.1. GMM based on the ratio of garlic and mustard oil

From the results the order of DPPH scavenging activity of prepared GMM at various ratios of garlic: mustard oil was found to be 1:4 > 1:16 > 1:2 > 1:8 > 1:1 > MO (Figure 39).

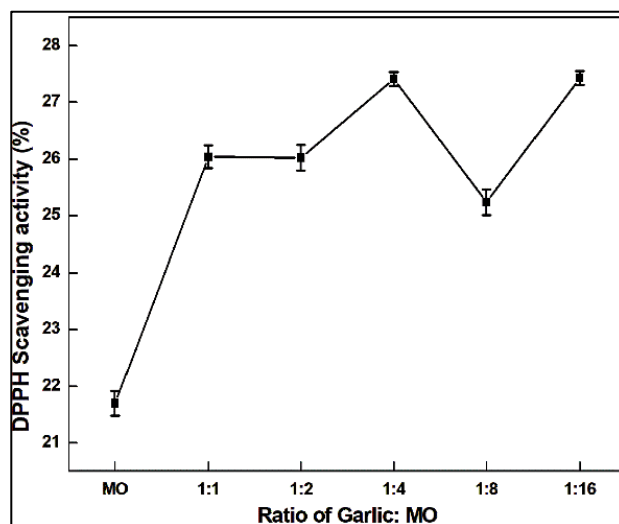


Figure 39: DPPH scavenging activity by prepared GMM with different ratio of garlic and mustard oil.

4.3.5.2. GMM based on the temperature of heating

From the results, the order of DPPH scavenging activity of prepared GMM at different temperatures was found to be 100°C > 180°C > 30°C > 60°C (Figure 40).

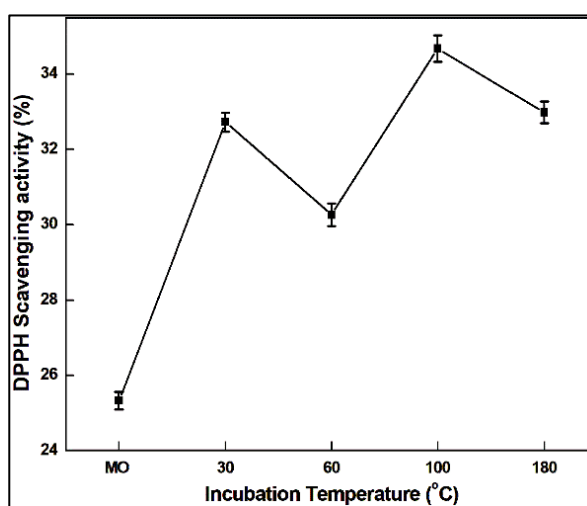
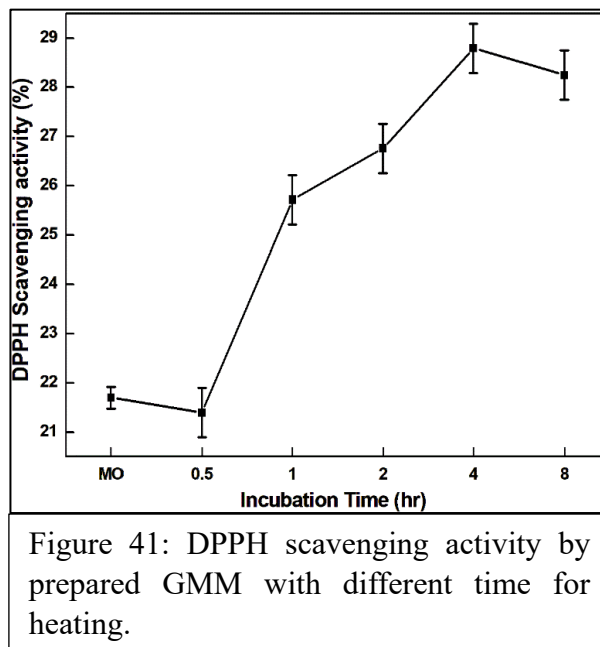


Figure 40: DPPH scavenging activity by prepared GMM with different temperature of heating.

4.3.5.3. GMM based on incubation time

From the results, the order of DPPH scavenging activity of prepared GMM at different temperatures was found to be 4hrs > 8hrs > 2hrs > 1hrs > 0.5hrs > MO (Figure 41).

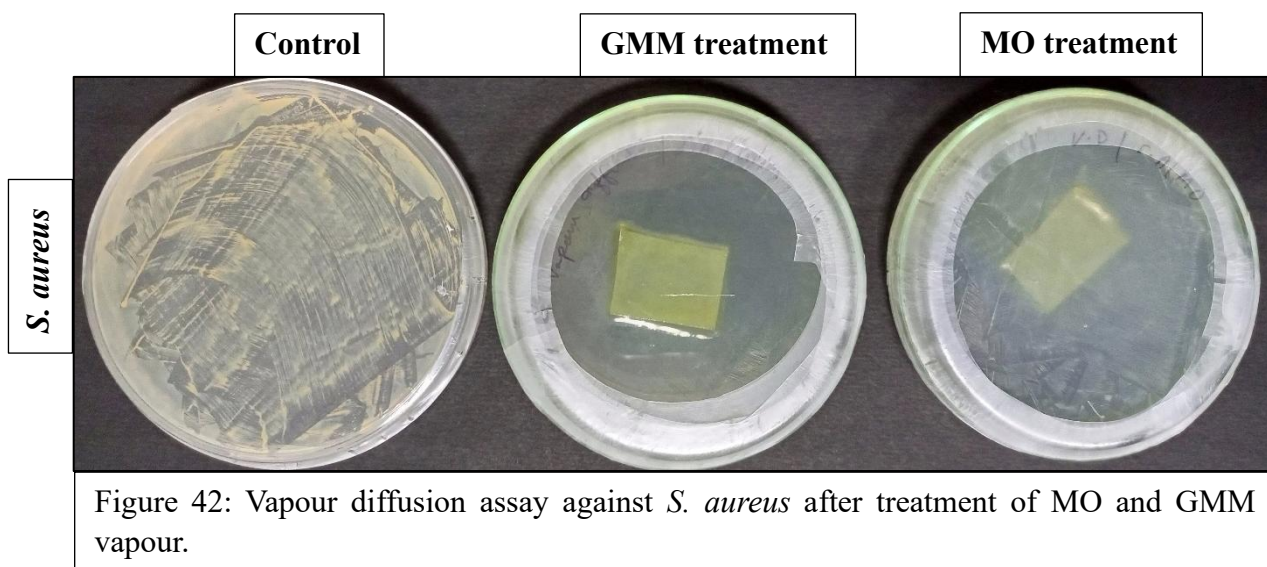


4.4. Bioactivity of optimized garlic mustard oil macerate

4.4.1. Antibacterial activity

4.4.1.1. Vapour diffusion assay

During the vapour diffusion assay of optimized GMM against *S. aureus* no bacterial colony was observed after 24 hours of incubation, whereas



the plate exposed to the vapour of MO showed a lawn of bacteria in the plate (Figure 42).

A similar result was observed during the vapour diffusion assay against *B. cereus*. Optimized GMM has shown higher antibacterial activity then compared to MO against *B. cereus* (Figure 43).

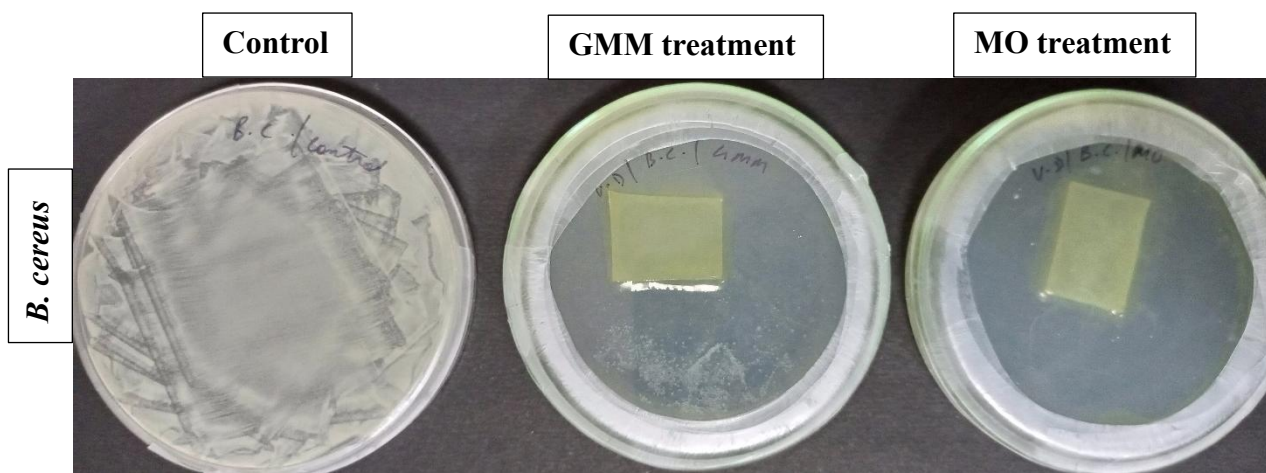


Figure 43: Vapour diffusion assay against *B. cereus* after treatment of MO and GMM vapour.

A similar result was observed during the vapour diffusion assay against *K. pneumoniae*. Optimized GMM has shown higher antibacterial activity than compared to MO against *K. pneumoniae* (Figure 44).

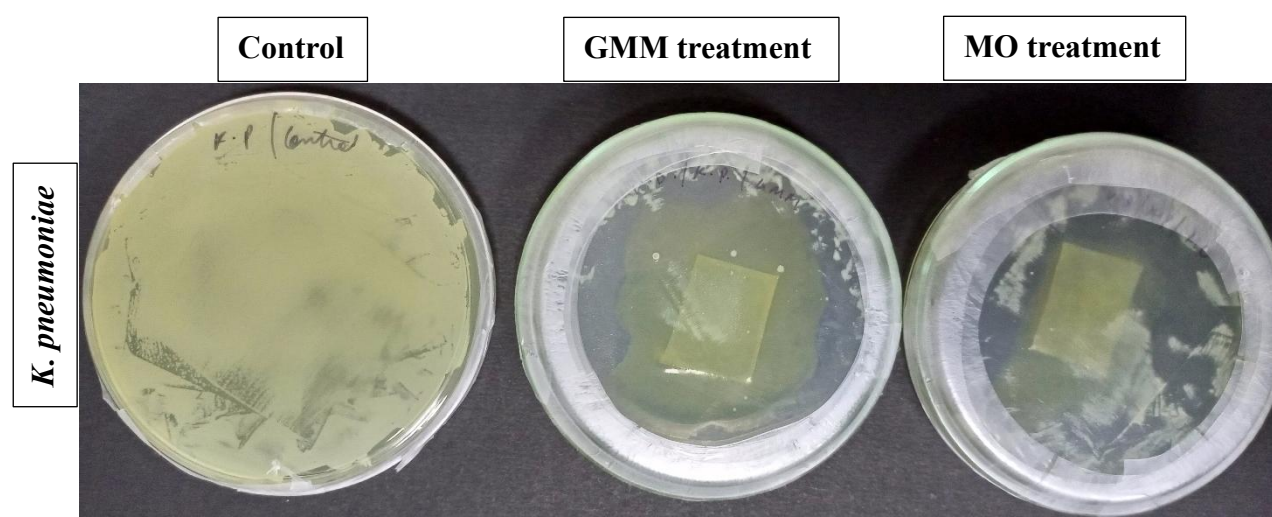
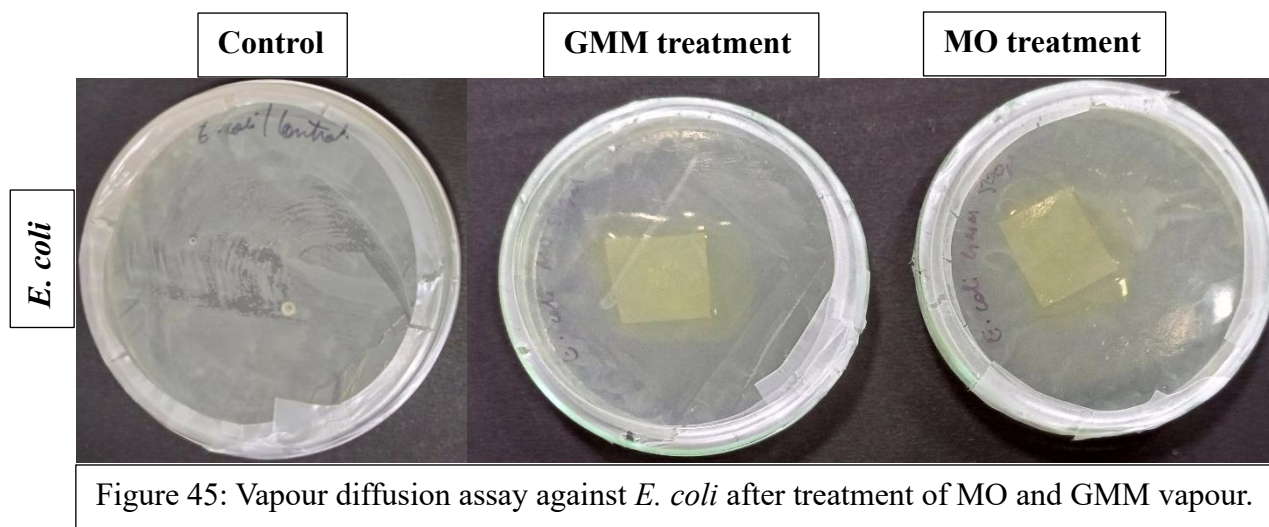


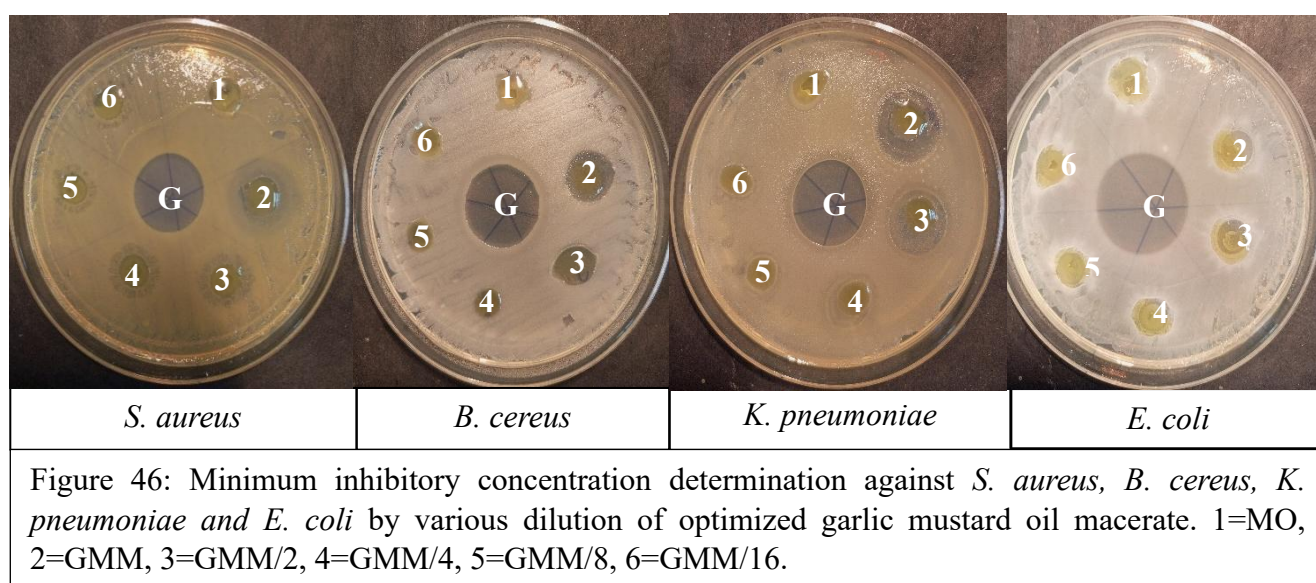
Figure 44: Vapour diffusion assay against *K. pneumoniae* after treatment of MO and GMM vapour.

A similar result was observed during the vapour diffusion assay against *E. coli*. Optimized GMM has shown higher antibacterial activity than compared to MO against *E. coli* (Figure 45).

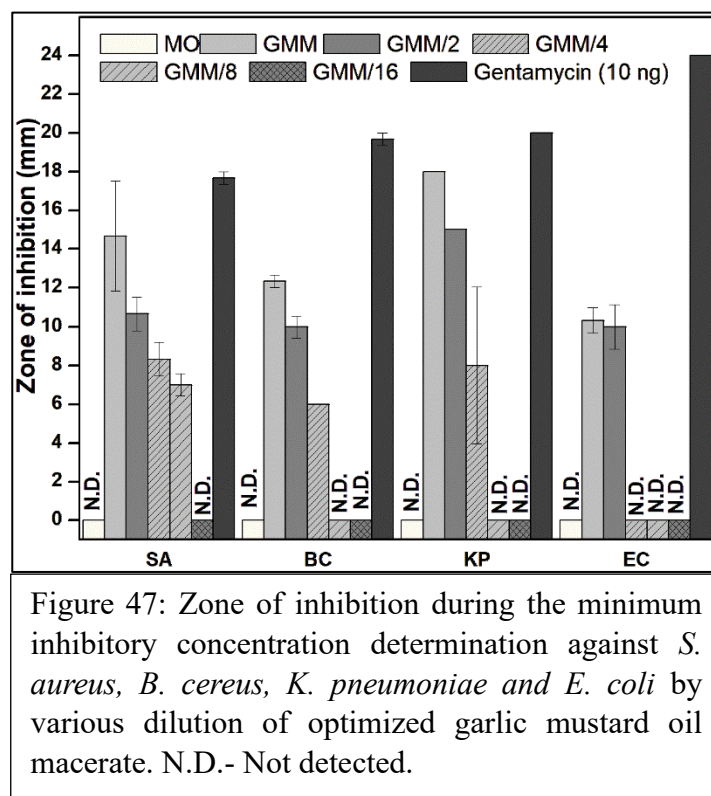


4.4.1.2. Minimum inhibitory concentration and minimum bactericidal concentration using agar diffusion assay

The zone of inhibition was found to decrease with a decrease in dilution. MIC against *S. aureus*, *B. cereus*, *K. pneumoniae* and *E. coli* was found to be GMM/8 (0.125% v/v), GMM/4 (0.250% v/v), GMM/2 (0.500%) and GMM/2 (0.500%), respectively. MBC was not detected for any of the test samples of GMM (Figure 46-47 and Table 24).



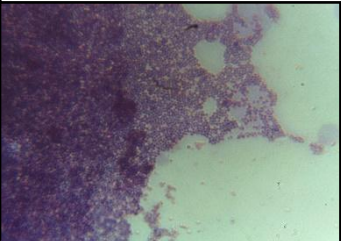
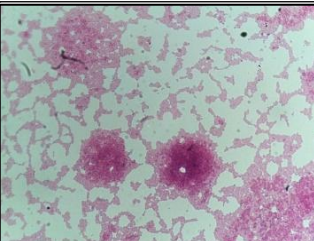
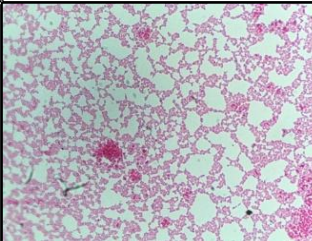
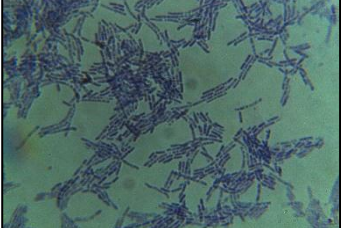

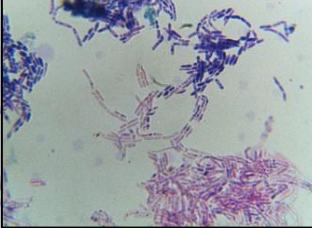
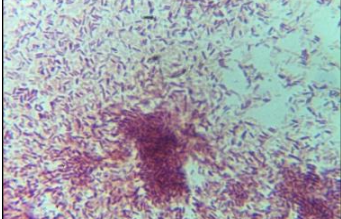
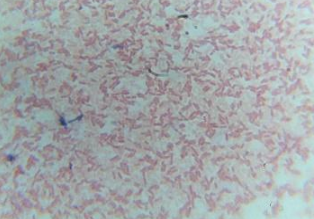
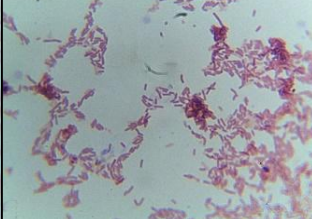
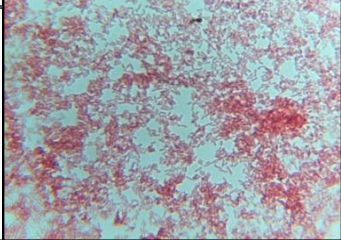
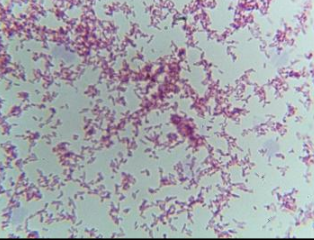
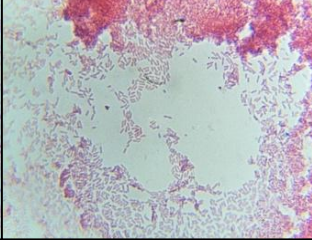
| Table 24: MIC and MBC against gram-positive and gram-negative bacteria | | |
|--|---------------------|-----|
| Bacteria | MIC | MBC |
| <i>S. aureus</i> MTCC 3160 | GMM/8 (0.125%, v/v) | ND |
| <i>B. cereus</i> MTCC 430 | GMM/4 (0.250%, v/v) | ND |
| <i>K. pneumoniae</i> MTCC 618 | GMM/4 (0.250%, v/v) | ND |
| <i>E. coli</i> MTCC 40 | GMM/2 (0.50%, v/v) | ND |



4.4.1.3. Gram staining

In the case of *S. aureus*, a pink colour colony was observed in the samples treated with MO and GMM. A similar result was observed in the case of *B. cereus* samples which were exposed to GMM oil, but a violet colony was seen in the case of the bacteria treated with MO treatment. Next, in the case of both the gram-negative bacteria *K.*

pneumoniae and *E. coli* no such morphological change was observed (Figure 48).

| Bacteria | Control | MO | GMM |
|---|---|--|---|
| <i>S. aureus</i> |  |  |  |
| <i>B. cereus</i> |  |  |  |
| <i>K. pneumoniae</i> |  |  |  |
| <i>E. coli</i> |  |  |  |
| Figure 48: Gram staining of different bacterial species after agar diffusion with MO and GMM. | | | |

4.4.1.4. Staphyloxanthin inhibition by GMM against *S. aureus*

Figure 49 shows that upon simultaneous exposure of the GMM VOCs to *S. aureus*, the zone of inhibition by gentamycin, tetracycline and kanamycin increased by 41.17, 38.89 and 43.75%, respectively compared to blank. Likewise, as compared to a blank, the VOCs in mustard oil increased the zone of inhibition for gentamycin, tetracycline and kanamycin by 33.33, 33.33 and 39.58%, respectively (Figure 50). Surprisingly, during the antibacterial assay a reduction in

staphyloxanthin pigment was observed after the *S. aureus* was exposed to the VOCs of GMM and MO (Figure 49)

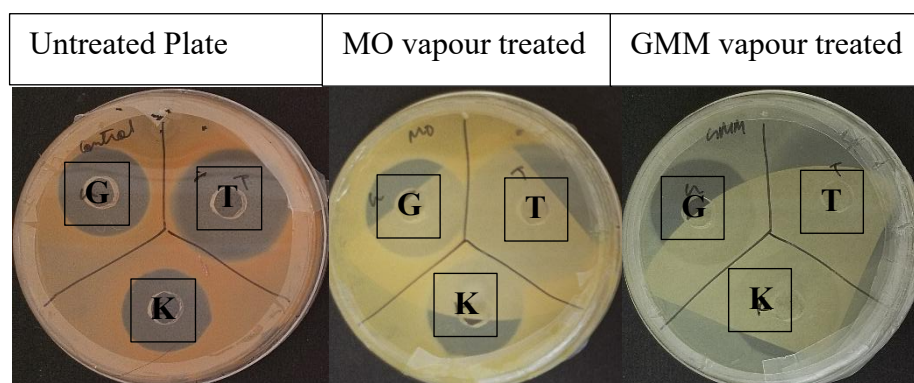


Figure 49: Showing the increase in zone of inhibition by Gentamycin (G) (10 ng), Tetracycline (T) (10 ng) and kanamycin (K) (10 ng) against *S. aureus* MTCC 3160 when treated with vapour of mustard oil and garlic mustard oil macerate (Image courtesy: Singha, J., Dutta, N., and Saikia, J.P. A novel volatile staphyloxanthin biosynthesis inhibitor against *Staphylococcus aureus*. *Microbial Pathogenesis*: 107489, 2025).

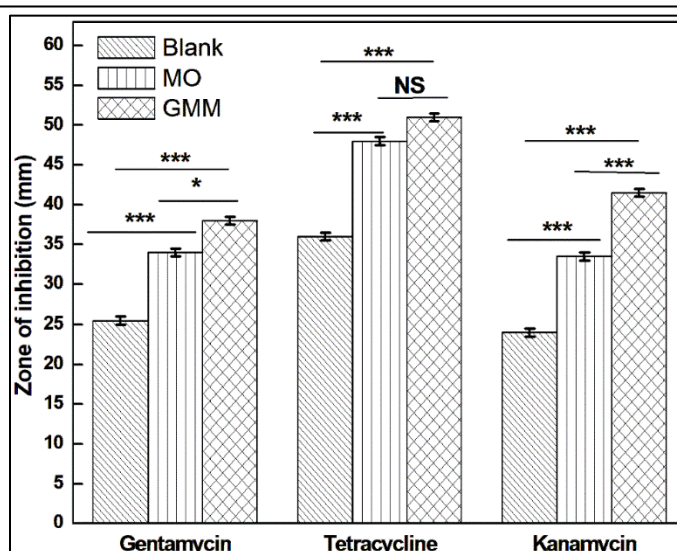


Figure 50: Representation of the increase in zone of inhibition when *S. aureus* when exposed to VOCs of MO and GMM (Image courtesy: Singha, J., Dutta, N., and Saikia, J.P. A novel volatile staphyloxanthin biosynthesis inhibitor against *Staphylococcus aureus*. *Microbial Pathogenesis*: 107489, 2025).

4.4.1.4.1. Inhibition percentage of staphyloxanthin

Surprisingly, during the antibacterial assay a reduction in staphyloxanthin pigment was observed after the *S. aureus* was exposed to the VOCs of GMM and MO. Using spectrophotometric analysis on a methanolic extract of bacterial cells, it was found that *S. aureus* cells exposed to GMM VOCs produced $44.23 \pm 0.14\%$ less staphyloxanthin.

4.4.1.4.2. Fourier-transform infrared spectroscopy (FTIR) analysis

Upon FTIR analysis of staphyloxanthin extract, the spectral intensity of the extract from GMM VOCs exposed *S. aureus* was found to be significantly reduced in 3370, 2947, 2835, 1656, 1450, 1027 cm^{-1} wavenumbers compared to that of the untreated cells (Figure 51 (A)). The FTIR analysis of the *S. aureus* cell treated with GMM vapour showed minimum transmittance at 3437, 2085, 1645, 1077 and 773 cm^{-1} (Figure 51 (B)).

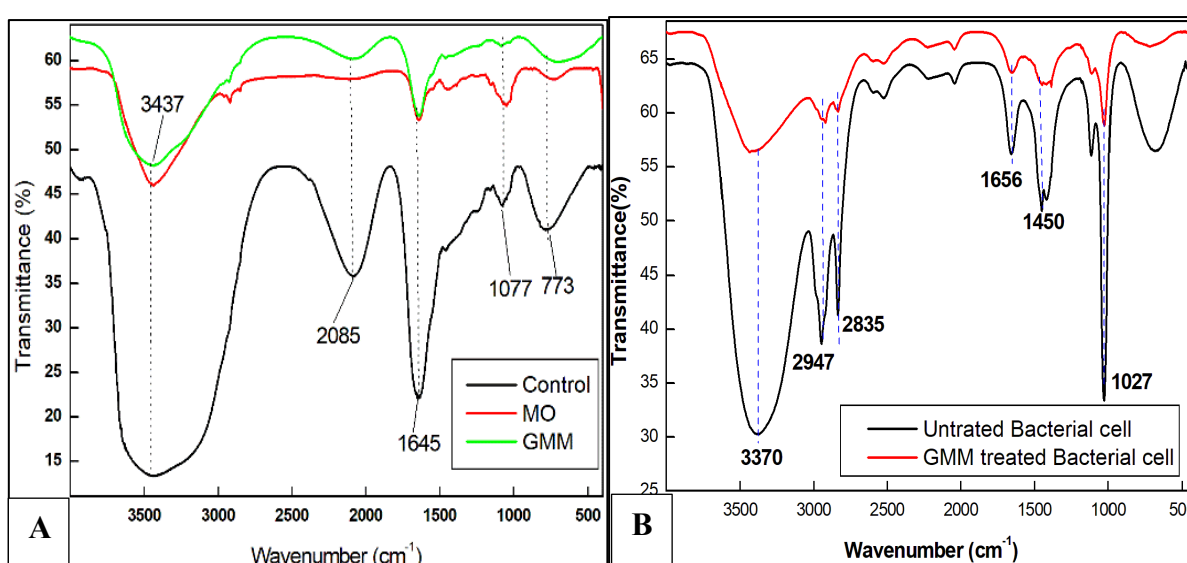
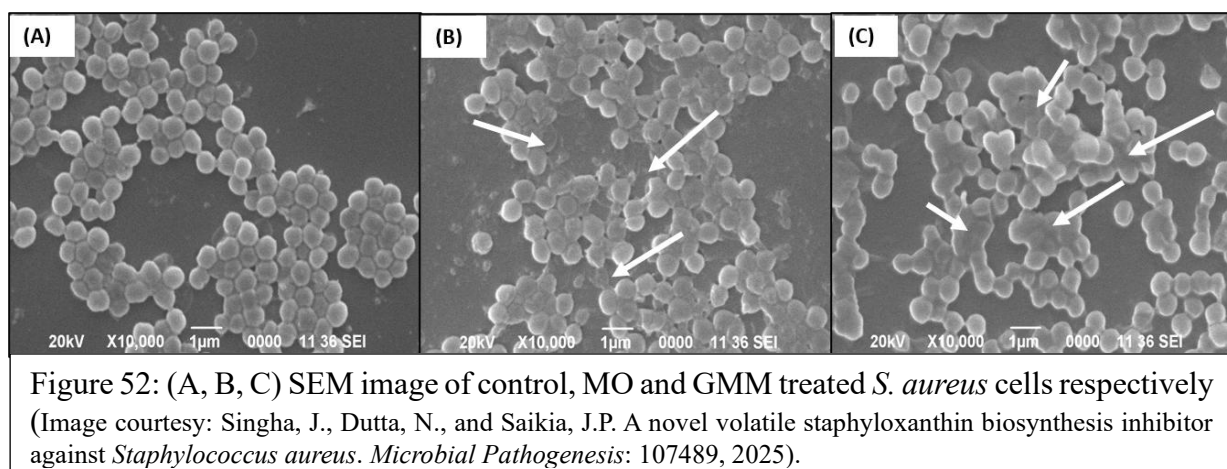


Figure 51:(A) FTIR analysis of the staphyloxanthin pigment extract from MO and GMM VOCs treated *S. aureus* cells; (B) FTIR analysis of *S. aureus* cells treated with VOCs of MO and GMM (Image courtesy: Singha, J., Dutta, N., and Saikia, J.P. A novel volatile staphyloxanthin biosynthesis inhibitor against *Staphylococcus aureus*. *Microbial Pathogenesis*: 107489, 2025).

4.4.1.4.3. Scanning electron microscopy (SEM) analysis

The coccus structure of the bacteria was shown to be visible, spherical and intact in the untreated *S. aureus* sample (Figure 52 A). Although there was noticeable cell debris in the cells exposed to the volatiles in MO, intact cells were also visible with their spherical, intact globular structures (Figure 52 B). Bacterial cells were shown to be elongated and to have lost their ability to form spherical, globular formations after being exposed to GMM

volatiles. This could be because the membrane fluidity had increased (Figure 52 C).



4.4.1.4.4. Molecular docking

Sinigrin showed the lowest binding energy of -6.9 Kcal/mol with crtM then followed by ajoene > allicin > dithiin > AITC. Ajoene (ASN A:168) and sinigrin (HIS A:18, GLN A:165, ARG A:171, ASN A:168, ARG A:45) exhibited conventional hydrogen bonding with the crtM protein. The detailed interaction between crtM-ligands along with binding energy is shown in Table 25 and Figure 53-57 (3D and 2D structure).

Table 25: Showing binding energy and type of molecular interaction of the phytochemicals with the protein dehydroxysqualene synthase crtM.

| Sl. No. | Phytochemicals | Lowest Binding Energy (Kcal/mol) with crtM | Types of interaction with crtM protein |
|---------|-----------------------------|--|--|
| 1 | Allyl Isothiocyanate (AITC) | -3.6 | Pi-Alkyl |
| 2 | Ajoene | -5.0 | Hydrogen bonding, pi-sulfur, Alkyl and pi alkyl |
| 3 | Allicin | -4.6 | Van der walls, alkyl and pi-alkyl |
| 4 | Dithiin | -4.5 | Pi-sigma, pi-sulfur, alkyl, pi-alkyl |
| 5 | Sinigrin | -6.9 | Hydrogen bond, carbon-hydrogen bond, pi-sulfur, pi-alkyl |

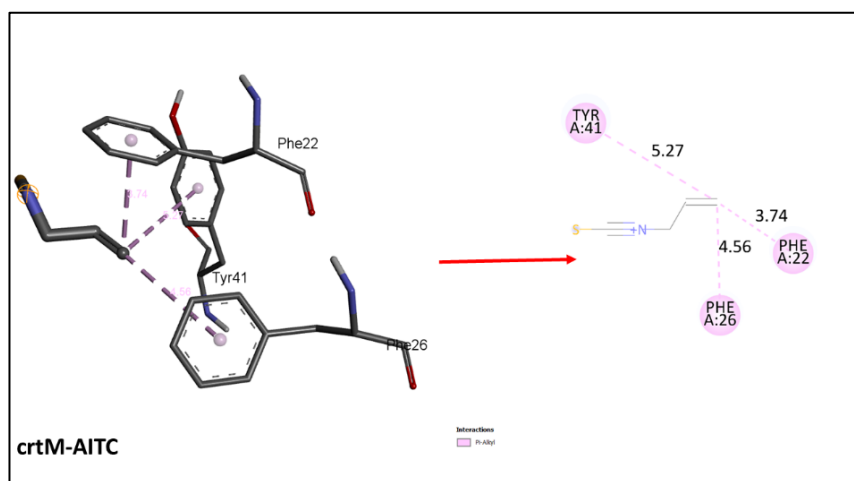


Figure 53: Representation of 3D and 2D interaction of crtM with AITC. (Image courtesy: Singha, J., Dutta, N., and Saikia, J.P. A novel volatile staphyloxanthin biosynthesis inhibitor against *Staphylococcus aureus*. *Microbial Pathogenesis*: 107489, 2025.

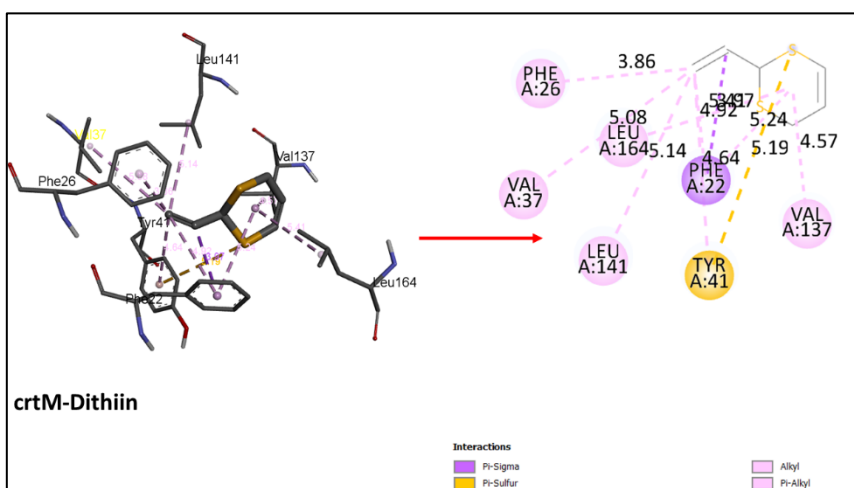


Figure 54: Representation of 3D and 2D interaction of crtM with Dithiin. (Image courtesy: Singha, J., Dutta, N., and Saikia, J.P. A novel volatile staphyloxanthin biosynthesis inhibitor against *Staphylococcus aureus*. *Microbial Pathogenesis*: 107489, 2025

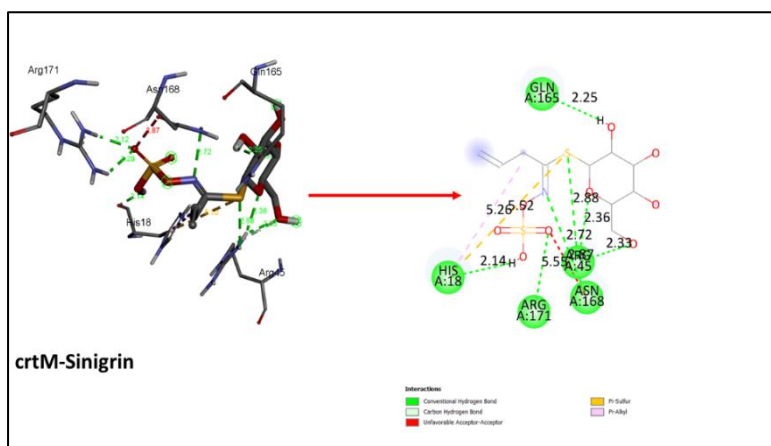


Figure 55: Representation of 3D and 2D interaction of crtM with sinigrin. (Image courtesy: Singha, J., Dutta, N., and Saikia, J.P. A novel volatile staphyloxanthin biosynthesis inhibitor against *Staphylococcus aureus*. *Microbial Pathogenesis*: 107489, 2025)

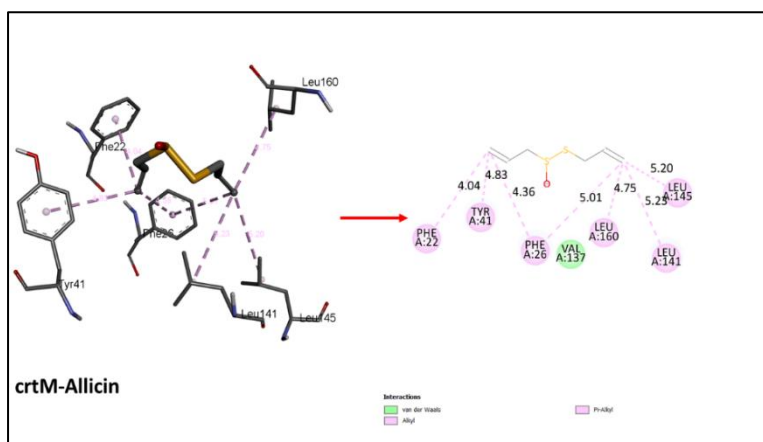


Figure 56: Representation of 3D and 2D interaction of crtM with alliin. (Image courtesy: Singha, J., Dutta, N., and Saikia, J.P. A novel volatile staphyloxanthin biosynthesis inhibitor against *Staphylococcus aureus*. *Microbial Pathogenesis*: 107489, 2025)

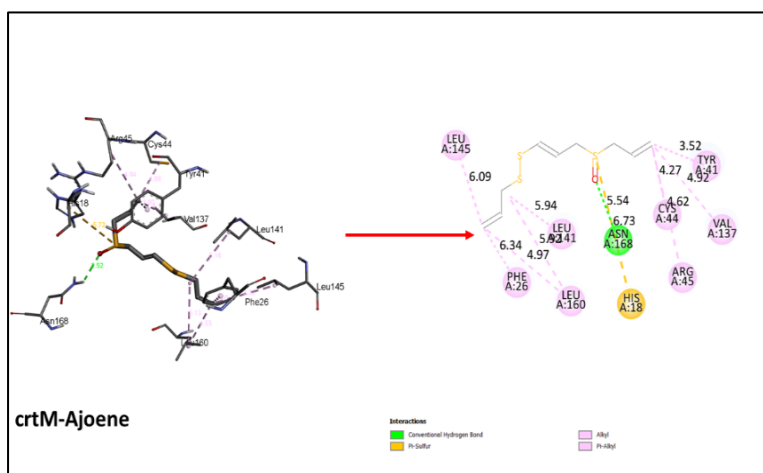


Figure 57: Representation of 3D and 2D interaction of crtM with ajoene. (Image courtesy: Singha, J., Dutta, N., and Saikia, J.P. A novel volatile staphyloxanthin biosynthesis inhibitor against *Staphylococcus aureus*. *Microbial Pathogenesis*: 107489, 2025)

4.4.2. Antibiofilm analysis

4.4.2.1. Screening of bacteria producing biofilm

Out of the four selected bacteria, *S. aureus* had shown a positive biofilm formation which was confirmed by slime mold formation on the CRA plate (Figure 58 A). Whereas, *B. cereus*, *K. pneumoniae* and *E. coli* did not form a biofilm (Figure 58 B, C, D).

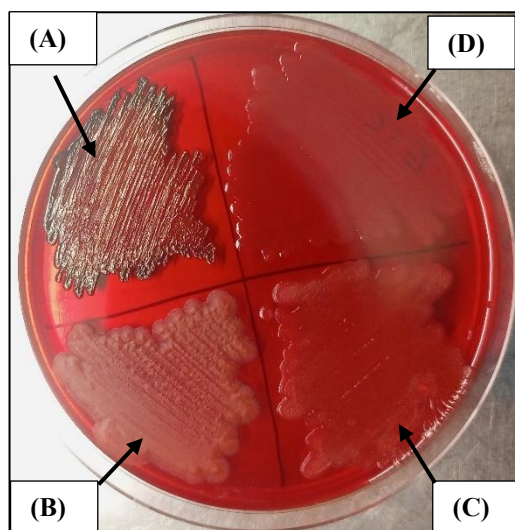


Figure 58: (A) Biofilm production by *S. aureus*; (B, C, D) no biofilm production by *B. cereus*, *K. pneumoniae* and *E. coli*, respectively.

4.4.2.2. Antibiofilm assay against *S. aureus*

4.4.2.2.1. Agar diffusion assay

In Figure 59, the inhibition of *S. aureus* bacterial growth was observed under the GMM oil but not under MO oil where a dark stain could be observed.

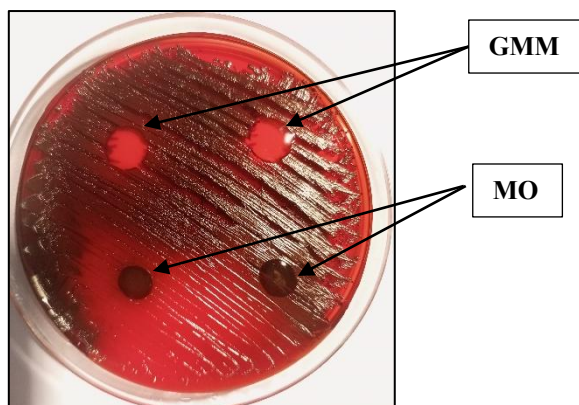


Figure 59: GMM inhibiting the *S. aureus* while no antibacterial activity was observed under the MO.

4.4.2.2.2. Vapour diffusion assay

During the vapour diffusion assay, *S. aureus* when treated with GMM vapour no biofilm formation was observed (Figure 60 C) then compared to the untreated blank plate where due to the biofilm formation dark black stain was observed (Figure 60 A). Less biofilm formation by *S. aureus* was observed in the CRA plates when treated with MO vapour (Figure 60 B).

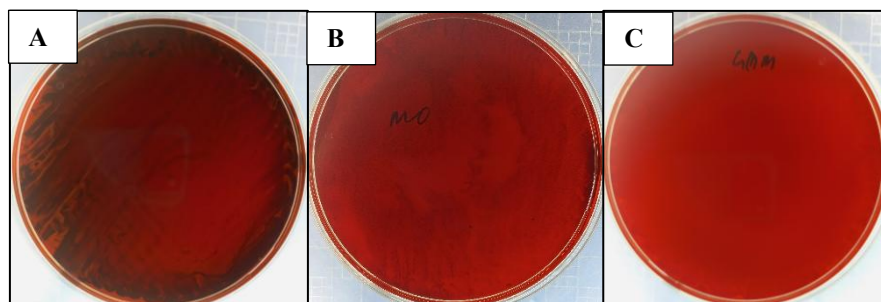


Figure 60: (A) *S. aureus* spread on CRA plate forming biofilm without any treatment; (B) *S. aureus* forming patches of biofilm in CRA after treatment of MO vapour; and (C) *S. aureus* forming no biofilm in CRA after treatment of GMM vapour.

4.4.2.2.3. Ring Biofilm inhibition assay

In Figure 61, concentration-dependent reduction in ring formation was observed in *S. aureus* during test tube ring assay. No ring formation was observed at the concentration of 50 $\mu\text{l/ml}$ of MO in MHB. In GMM-treated test tubes, no ring formation was observed at 25 $\mu\text{l/ml}$ concentration (Figure 62).

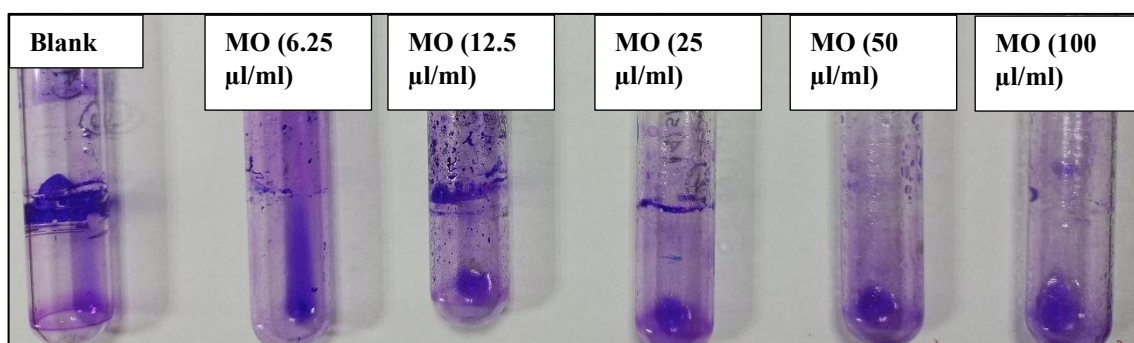


Figure 61: Effect of MO treatment on *S. aureus* biofilm formation on glass test tubes.

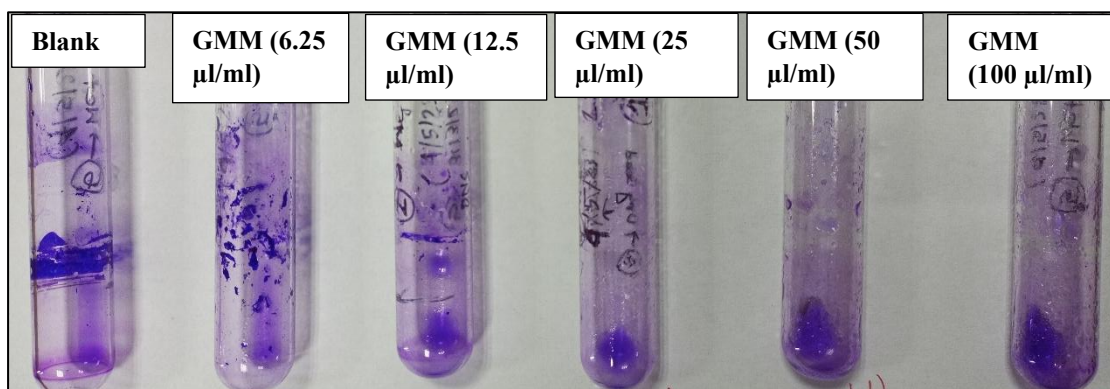


Figure 62: Effect of GMM treatment on *S. aureus* biofilm formation on glass test tubes.

4.4.2.3. Antibiofilm activity against *Pseudomonas aeruginosa* MTCC 2297

4.4.2.3.1. Vapour diffusion assay

During the vapour diffusion assay, inhibition of pyocyanin pigment was observed when *P. aeruginosa* MTCC 2297 was exposed to GMM vapour. This was not observed in the plates treated with MO vapour and control (Figure 63).

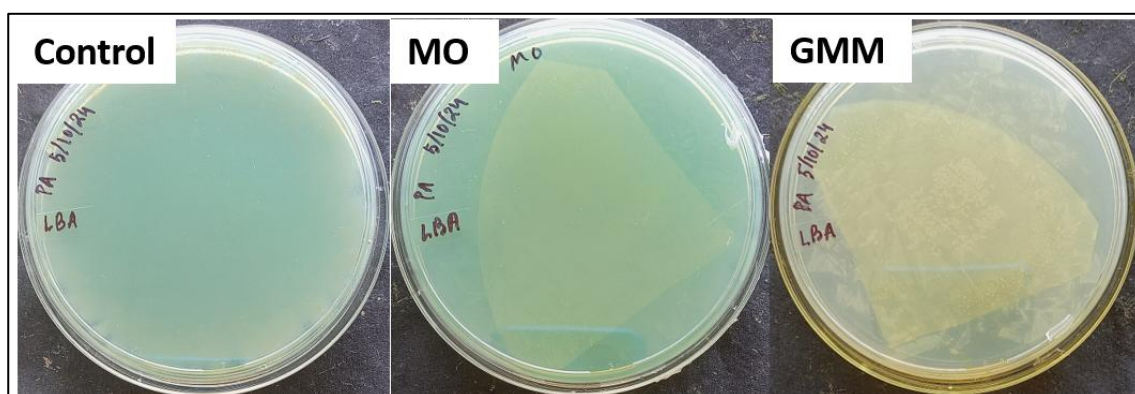


Figure 63: Vapour diffusion assay using MO and GMM against *P. aeruginosa*.

4.4.2.3.2. Microscopic assay

A microscopic assay using crystal violet has shown a significant reduction in biofilm formation by *P. aeruginosa* after GMM treatment at the concentration of 100 µl/ml which was followed by MO (Figure 64).

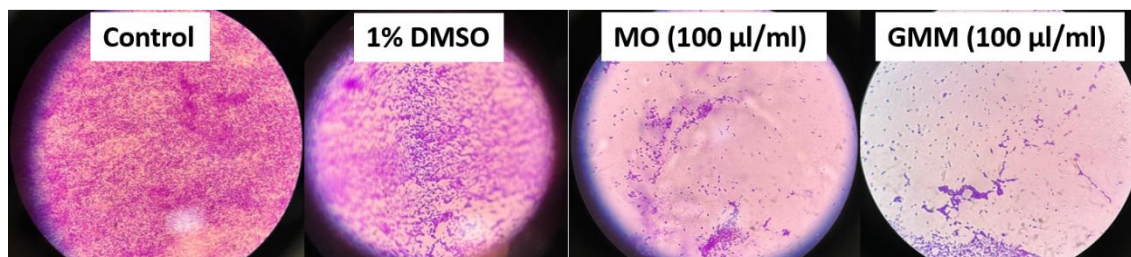


Figure 64: Microscopic assay using crystal violet for biofilm inhibition assay using GMM and MO against *P. aeruginosa*.

4.4.2.3.3. Estimation of total carbohydrate in EPS

A significant reduction in the carbohydrate concentration in EPS was observed at 100 µl/ml concentration of GMM and then compared to MO (Figure 65).

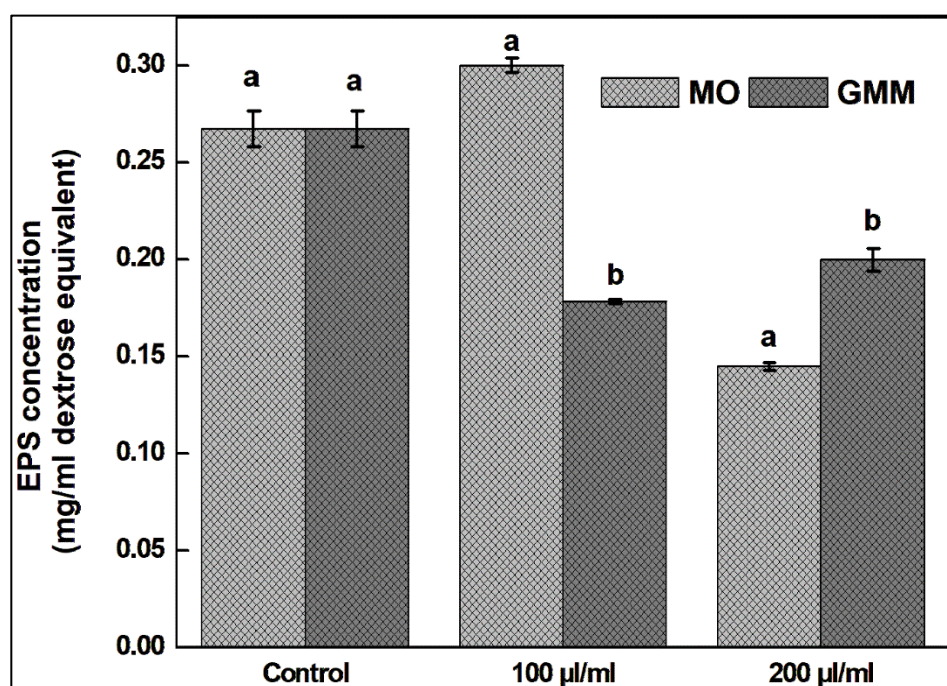


Figure 65: EPS inhibition assay using GMM and MO against *P. aeruginosa*. Bars with different alphabet labels in each group are significantly different ($P \leq 0.05$).

4.4.2.3.4. Quantification of pyocyanin

Dose-dependent inhibition of pyocyanin production by *P. aeruginosa* was observed for both the GMM and MO during the broth dilution method (Figure 66).

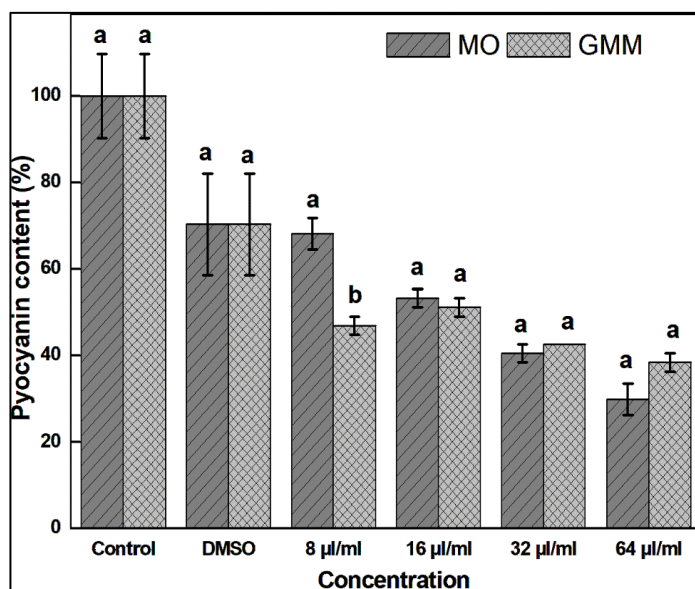


Figure 66: Pyocyanin inhibition assay against *P. aeruginosa* using GMM and MO against. Bars with different alphabet labels in each group are significantly different ($P \leq 0.05$).

4.4.2.4. Violacein inhibition assay in *Chromobacterium violaceum* MTCC 12472

4.4.2.4.1. Vapour diffusion assay

During vapour diffusion assay, MO and GMM vapour were found to inhibit the violet pigment of violacein (Figure 67).

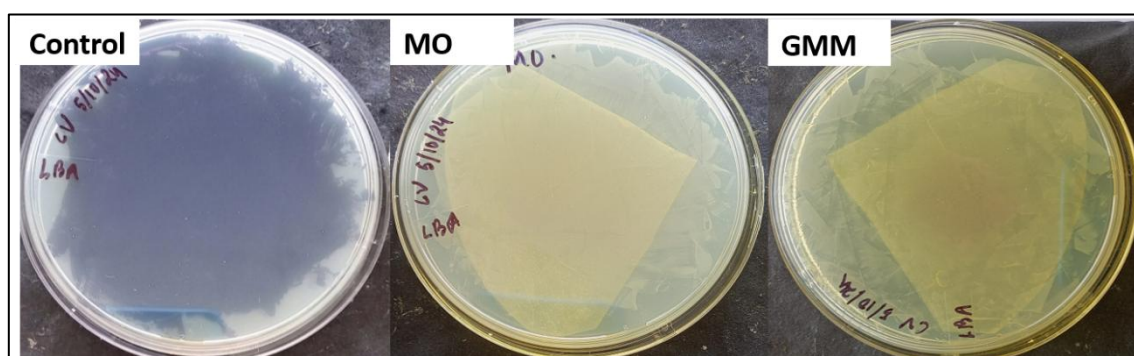


Figure 67: Vapour diffusion assay using MO and GMM against *Chromobacterium violaceum*.

4.4.2.4.2. Violacein inhibition

During the broth dilution method, with an increase in the concentration of GMM, a decrease in violacein concentration in the broth was observed. A significant difference between GMM and MO was observed at the concentrations of 16 and 32 $\mu\text{l/ml}$ (Figure 68).

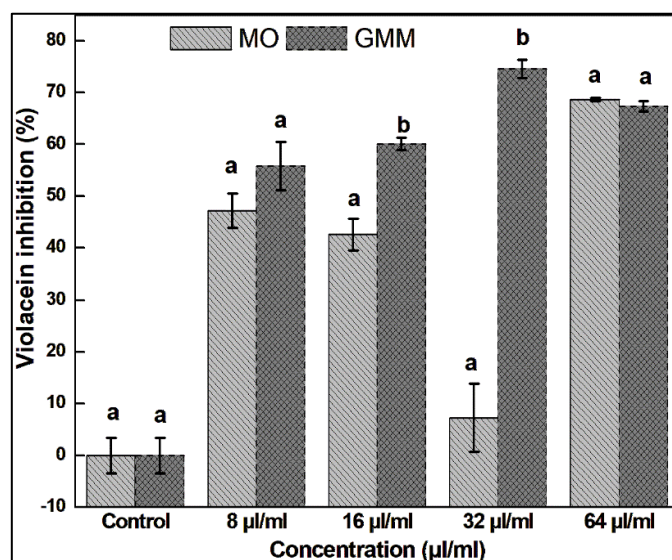


Figure 68: Violacein inhibition assay using various concentration of MO and GMM against *Chromobacterium violaceum*. Bars with different alphabet labels in each group are significantly different ($P \leq 0.05$).

4.4.3. Antifungal activity

4.4.3.1. Vapour diffusion assay

After 7 days of incubation, 6 colonies of *C. albicans* were observed in the plate treated with MO vapour (Figure 69 B), no fungal colonies were

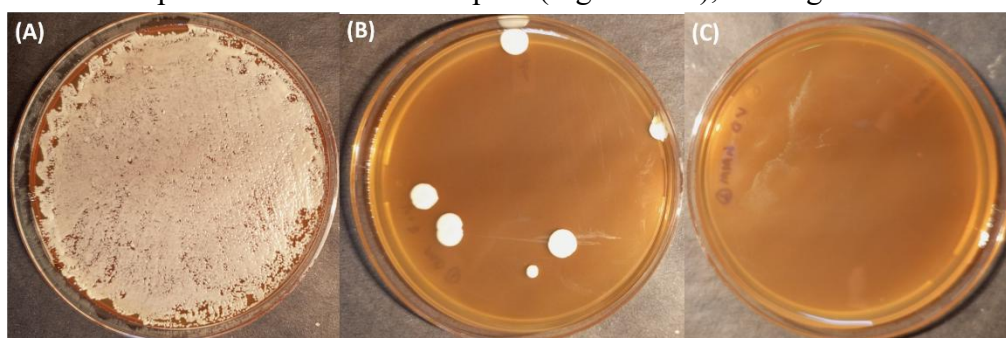


Figure 69: (A) Control plate with *C. albicans*; antifungal assay against *C. albicans* using (B) MO; (C) optimized GMM using vapour diffusion method (Image courtesy: Singha, J., and Saikia, J.P. Optimisation of garlic mustard oil macerate with respect to its antifungal activity against *Candida albicans* MTCC 183 and in-silico molecular docking of the volatile compounds with N-myristoyltransferase. *Natural Product Research*: 1-8, 2024.)

observed for the plates treated with the vapour of GMM (Figure 69 C) and the fungal lawn was observed for untreated plates (Figure 69 A).

4.4.3.2. MIC and MBC determination by agar diffusion assay

The order of antifungal activity to the diameter of ZOI was GMM (26.33 ± 0.33 mm) > GMM/2 (11.67 ± 0.33 mm) > GMM/4 (10.67 ± 0.33 mm) > GMM/8 (8 ± 0.11 mm) > GMM/16 (0 mm) > MO (0 mm) (Figure 70 A and Figure 71). The MFC was found to be GMM/ 4 (Figure 70 B).

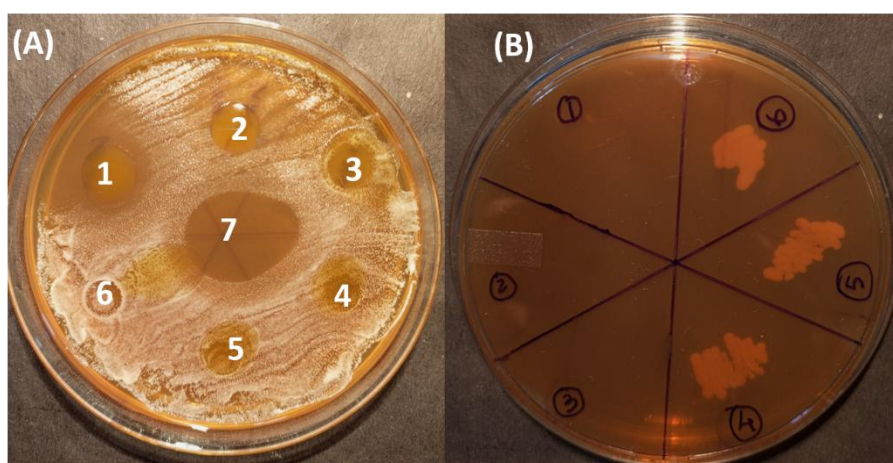


Figure 70: (A) Minimum inhibitory concentration of optimized GMM against *C. albicans*; (B) steaking of fungal colony from below the oil sample from the plate in (A) for determination of minimum fungicidal concentration. Note: 1 (GMM), 2(GMM/2), 3 (GMM/4), 4 (GMM/8), 5 (GMM/16), 6 (MO).

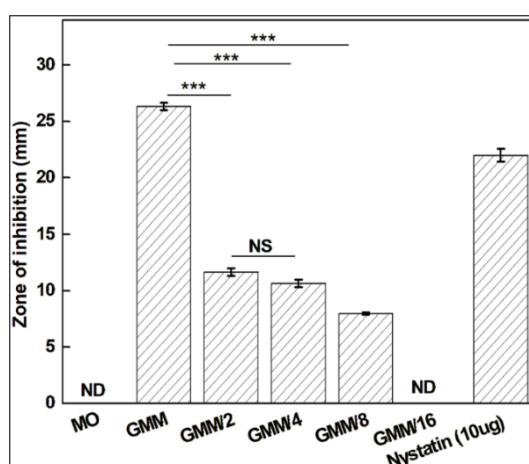


Figure 71: Zone of inhibition of optimized GMM against *C. albicans* during MIC determination. Note: NS- Not significant, ***- $p < 0.001$.

4.4.3.3. Lactophenol blue staining

The microscopy result showed a significant reduction in fungal cell count when treated with optimized GMM (Figure 72A) and then compared to blank (Figure 72C) and MO (Figure 72B) treated cells. The average cell size of the cells was also found to be reduced when observed under 1000X magnification.

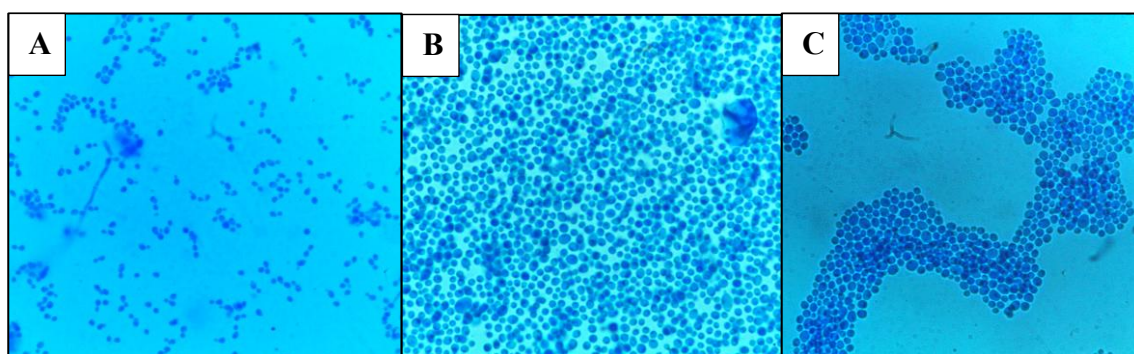


Figure 72: Lactophenol blue staining of *C. albicans* treated with (A) GMM/8 dilution, (B) MO and (C) no treatment.

4.4.3.4. Poison food assay

During the present experiment, the MIC of GMM was found to be 20 $\mu\text{l/ml}$ and for MO at the maximum concentration of 20 $\mu\text{l/ml}$ fungal colony was observed. Whereas for all the other concentrations, fungal growth was observed for both MO and GMM (Figure 74). Reduction in fungus growth was observed for 10, 5, 2.5 and 1.25 $\mu\text{l/ml}$ of GMM then compared to control after 14 days of incubation (Figure 73).

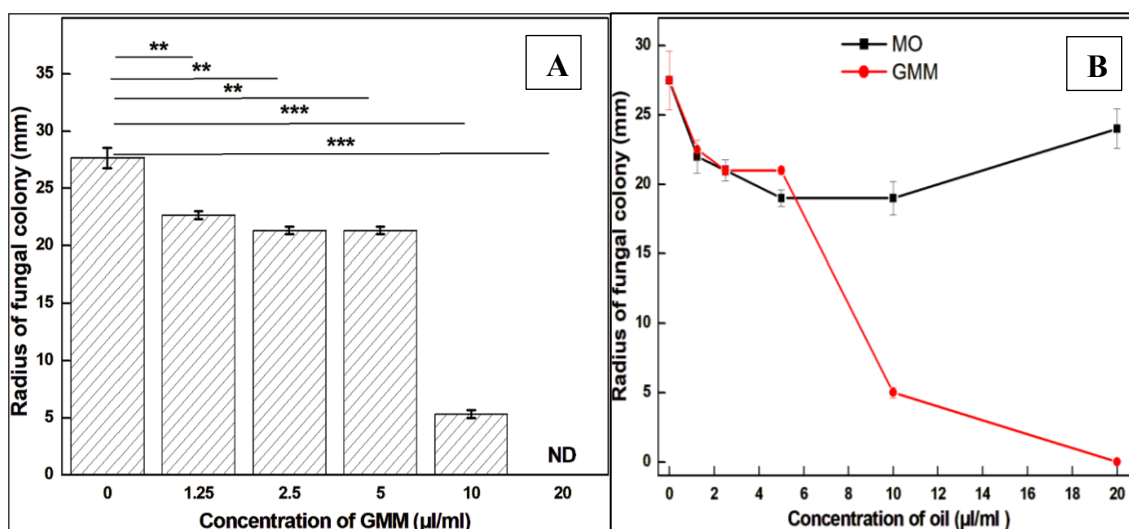


Figure 73: (A) Poison food assay against *C. albicans* using optimized GMM. Note: NS- Not significant, **- $p < 0.01$, ***- $p < 0.001$; (B) Line graph showing the inhibition of *C. albicans* by various concentration of MO and GMM (Image courtesy: Singha, J., and Saikia, J.P. Optimisation of garlic mustard oil macerate with respect to its antifungal activity against *Candida albicans* MTCC 183 and in-silico molecular docking of the volatile compounds with N-myristoyltransferase. *Natural Product Research*: 1-8, 2024.).

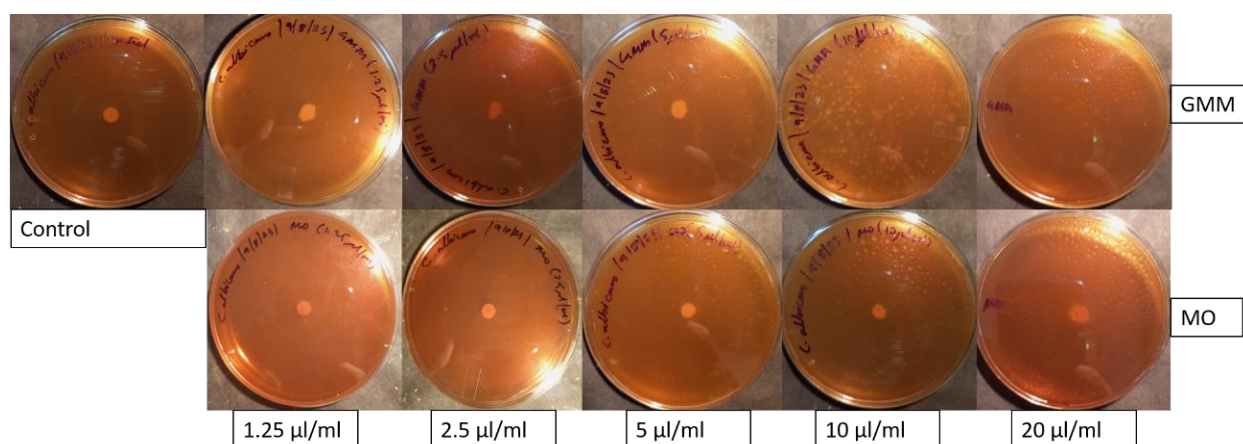


Figure 74: Showing the growth of *C. albicans* using various concentration of MO and GMM during poison food assay after 48 hours of incubation.

4.4.3.5. Scanning electron microscopy

SEM analysis showed clear changes in the cellular morphology between the untreated and GMM/2 (50%, v/v) treated fungi upon agar diffusion assay, where cell membrane disruption was observed which could cause leakage to cytoplasmic content and may lead to cell death (Figure 75 C). When the cells were treated with non-diluted GMM, no live cells were observed and cell debris could be seen (Figure 75 D). However, the untreated and MO-treated fungal cells showed no visible physical damage or alteration in the structure (Figure 75 A and B, respectively). Under both conditions, the cells were found to be ovular in structure with smooth cell walls.

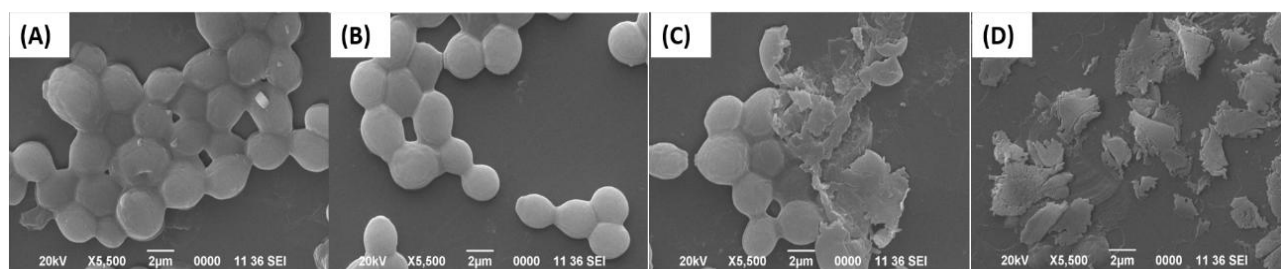


Figure 75: (A) Scanning electron micrographs of *C. albicans* with magnification of 5500X; (B) Scanning electron micrographs of *C. albicans* treated with MO (direct contact) with magnification of 5500X; (C) Scanning electron micrographs of *C. albicans* treated with GMM/2 (0.50%, v/v) dilution (direct contact) with magnification of 5500X; and (D) Scanning electron micrographs of *C. albicans* treated with GMM without dilution (direct contact) with magnification of 5500X (Image courtesy: Singha, J., and Saikia, J.P. Optimisation of garlic mustard oil macerate with respect to its antifungal activity against *Candida albicans* MTCC 183 and in-silico molecular docking of the volatile compounds with N-myristoyltransferase. *Natural Product Research*: 1-8, 2024.)

4.4.3.6. Molecular docking

Out of all the eight compounds, sinigrin showed the minimum binding energy of -7.0 kCal/mol with N-myristoyltransferase (1 nmt) followed by Z-ajoene (-4.5 kCal/mol) > E-ajoene (-4.2 kCal/mol) > 3-Vinyl dithiin (-4.1 kCal/mol) > 1-Butene-4-isothiocyanato (-4.0 kCal/mol) > Allicin (-3.9 kCal/mol) = 2-vinyl dithiin (-3.9 kCal/mol) > AITC (-3.4 kCal/mol) with binding energy shown in Table 26. The maximum number of

hydrogen bonding was shown by sinigrin followed by E-ajoene (4)>Allicin (3)> 1-Butene-4-isothiocyannato (3) (Figure 76- 83).

Table 26: Showing the binding energy, number of hydrogen bonds and type of interactions of selected molecules with N-myristoyltransferase (nmt, PDB ID: 1nmt) during the molecular docking study

| Sl. No | Compound | Binding energy (kCal/mol) | No. of Hydrogen bonds (Interaction residues) | Types of interactions |
|--------|----------------------------|---------------------------|---|---|
| 1 | 3-Vinyl dithiin | -4.1 | 0 | Van der Waals, Alkyl, Pi-alkyl |
| 2 | Allyl isothiocyanate | -3.4 | 0 | Van der Waals, carbon-hydrogen, Pi-alkyl |
| 3 | Allicin | -3.9 | 3 (GLY B:413) (HIS B:227) (ASP B:412) | Hydrogen bond, Van der Waals, Attractive charge |
| 4 | E ajoene | -4.2 | 4 (HIS B:227) (ASP B:412) (TYP B:354) (ASN B:392) | Hydrogen bond, Pi-alkyl, Van der Waals, pi-sulfur |
| 5 | Sinigrin | -7.0 | 7 (THR A:218) (LEU A:419) (LYS B:167) (VAL B:168) (ARG A:423) (ASN B:166) (LYS B:161) | Hydrogen bond, Pi-alkyl |
| 6 | Z- ajoene | -4.5 | 1 (ASN B:392) | Hydrogen bond, Pi-alkyl, alkyl, pi-sulfur |
| 7 | 2- Vinyl dithiin | -3.9 | 0 | Van der Waals, pi-sulfur, alkyl, pi-alkyl |
| 8 | 1-Butene-4-isothiocyannato | -4.0 | 3 (LEU A:419) (ASN B:166) (LYS B:161) | Hydrogen bond, carbon-hydrogen bond, unfavourable positive-positive |

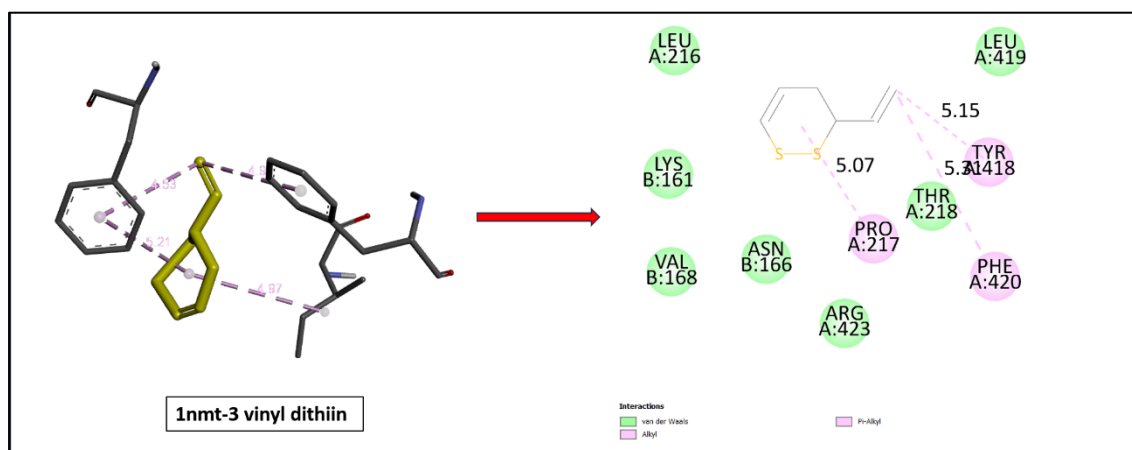


Figure 76: Representation of 3D and 2D interaction of 1nmt with 3-vinyl dithiin. (Image courtesy: Singha, J., and Saikia, J.P. Optimisation of garlic mustard oil macerate with respect to its antifungal activity against *Candida albicans* MTCC 183 and in-silico molecular docking of the volatile compounds with N-myristoyltransferase. *Natural Product Research*: 1-8, 2024.)

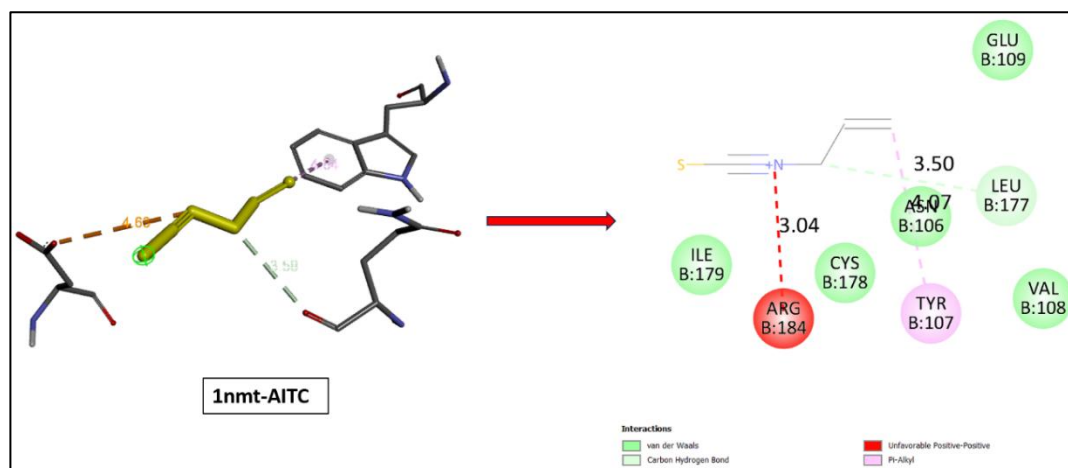


Figure 77: Representation of 3D and 2D interaction of 1nmt with AITC. (Image courtesy: Singha, J., and Saikia, J.P. Optimisation of garlic mustard oil macerate with respect to its antifungal activity against *Candida albicans* MTCC 183 and in-silico molecular docking of the volatile compounds with N-myristoyltransferase. *Natural Product Research*: 1-8, 2024.)

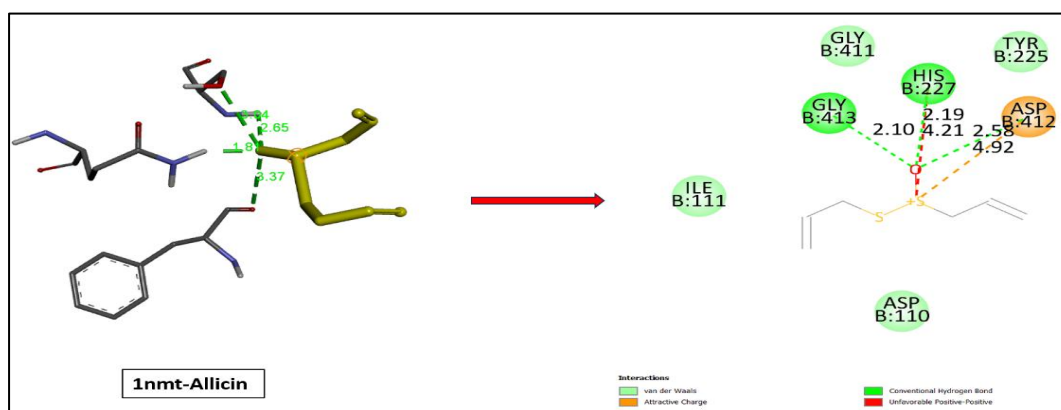


Figure 78: Representation of 3D and 2D interaction of 1nmt with allicin. (Image courtesy: Singha, J., and Saikia, J.P. Optimisation of garlic mustard oil macerate with respect to its antifungal activity against *Candida albicans* MTCC 183 and in-silico molecular docking of the volatile compounds with N-myristoyltransferase. *Natural Product Research*: 1-8, 2024.)

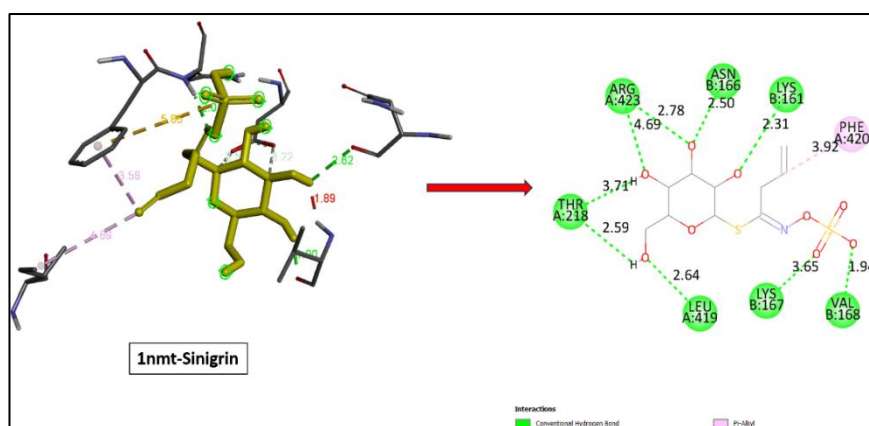


Figure 79: Representation of 3D and 2D interaction of 1nmt with sinigrin. (Image courtesy: Singha, J., and Saikia, J.P. Optimisation of garlic mustard oil macerate with respect to its antifungal activity against *Candida albicans* MTCC 183 and in-silico molecular docking of the volatile compounds with N-myristoyltransferase. *Natural Product Research*: 1-8, 2024.)

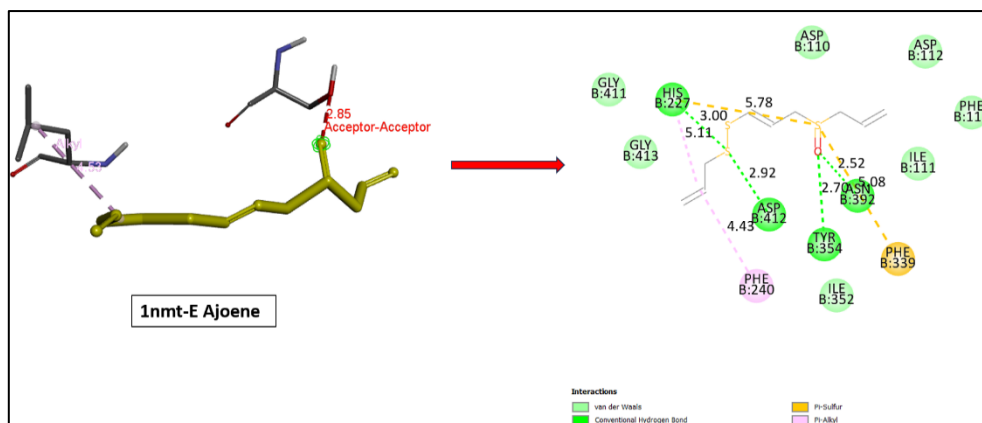


Figure 80: Representation of 3D and 2D interaction of 1nmt with E-ajoene. (Image courtesy: Singha, J., and Saikia, J.P. Optimisation of garlic mustard oil macerate with respect to its antifungal activity against *Candida albicans* MTCC 183 and in-silico molecular docking of the volatile compounds with N-myristoyltransferase. *Natural Product Research*: 1-8, 2024.)

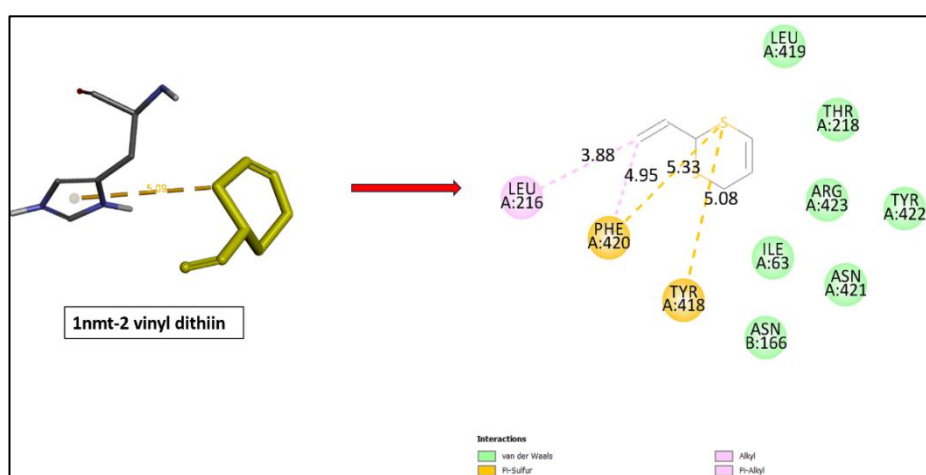


Figure 81: Representation of 3D and 2D interaction of 1nmt with 2-vinyl-dithiin. (Image courtesy: Singha, J., and Saikia, J.P. Optimisation of garlic mustard oil macerate with respect to its antifungal activity against *Candida albicans* MTCC 183 and in-silico molecular docking of the volatile compounds with N-myristoyltransferase. *Natural Product Research*: 1-8, 2024.)

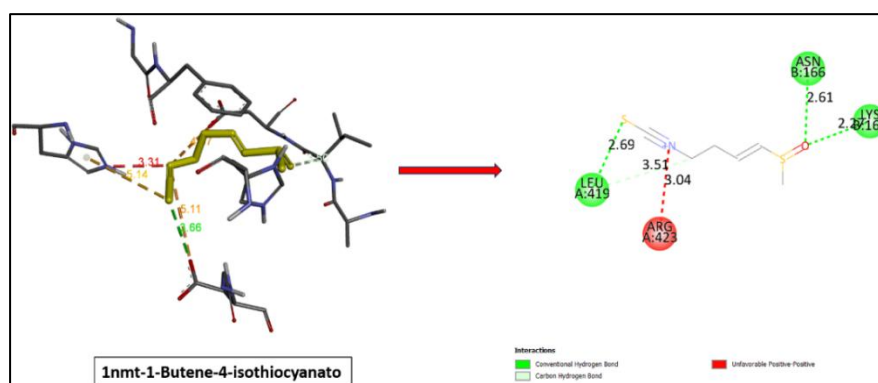


Figure 82: Representation of 3D and 2D interaction of 1nmt with i-butene-4-isothiocyanato. (Image courtesy: Singha, J., and Saikia, J.P. Optimisation of garlic mustard oil macerate with respect to its antifungal activity against *Candida albicans* MTCC 183 and in-silico molecular docking of the volatile compounds with N-myristoyltransferase. *Natural Product Research*: 1-8, 2024.)

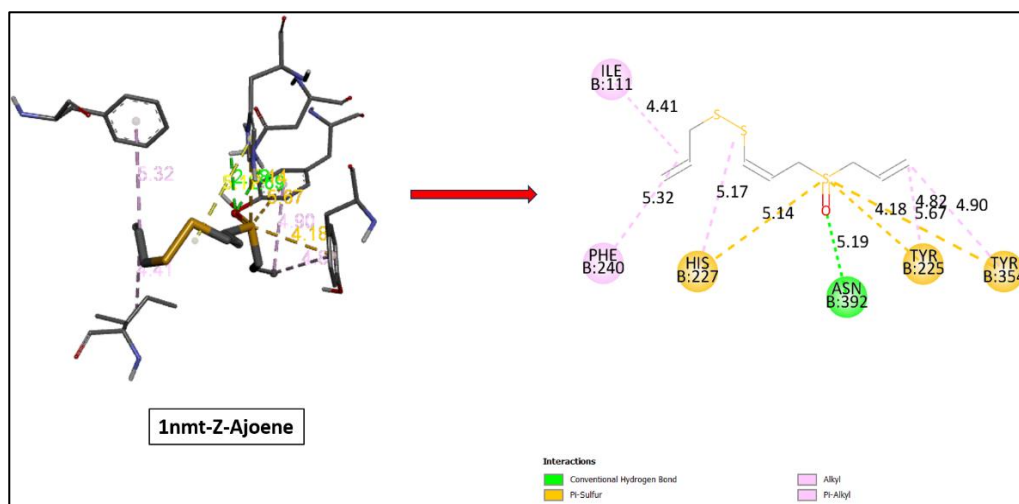


Figure 83: Representation of 3D and 2D interaction of 1nmt with Z-ajoene. (Image courtesy: Singha, J., and Saikia, J.P. Optimisation of garlic mustard oil macerate with respect to its antifungal activity against *Candida albicans* MTCC 183 and in-silico molecular docking of the volatile compounds with N-myristoyltransferase. *Natural Product Research*: 1-8, 2024.)

4.4.4. Cell viability assay against HEK293 normal cell line, THP-1 cell line and MCF7 breast cancer cell line

This study was undertaken to utilize the HEK cell line as a model for assessing the cytotoxicity of a tested concentration range on normal cell lines. The IC_{50} value for both MO and GMM was determined to be greater than 400 $\mu\text{g/ml}$ concentration. At a concentration of 400 $\mu\text{g/ml}$, the highest level of cytotoxicity was seen for both MO and GMM, resulting in viable cell percentages of 84.98% and 89.98%, respectively (Figures 84-85). Therefore, the measured concentration range did not exhibit any notable cytotoxic effects against normal cell lines.

The THP-1 cell line is commonly employed in research on anti-inflammatory investigations. Consistent with the current body of literature, our study was centred on the analysis of gene expression. Consequently, an initial evaluation was carried out to examine the cytotoxic effects of MO/GMM on the THP-1 cell line. After doing the cell viability assessment, it was discovered that the IC_{50} value for both MO and GMM surpassed a concentration of 400 $\mu\text{g/ml}$ (Figures 84 and 85). The viability of THP-1 cells was seen to be high, with MO and GMM exhibiting viabilities of 78.96% and 73.63% respectively. These results indicate the absence of harmful effects for both the preparation. Against

the MCF7 breast cancer cell line IC_{50} value of both GMM and MO was found to be $>400 \mu\text{g/ml}$ and $391.9 \mu\text{g/ml}$ respectively (Figures 84 and 85).

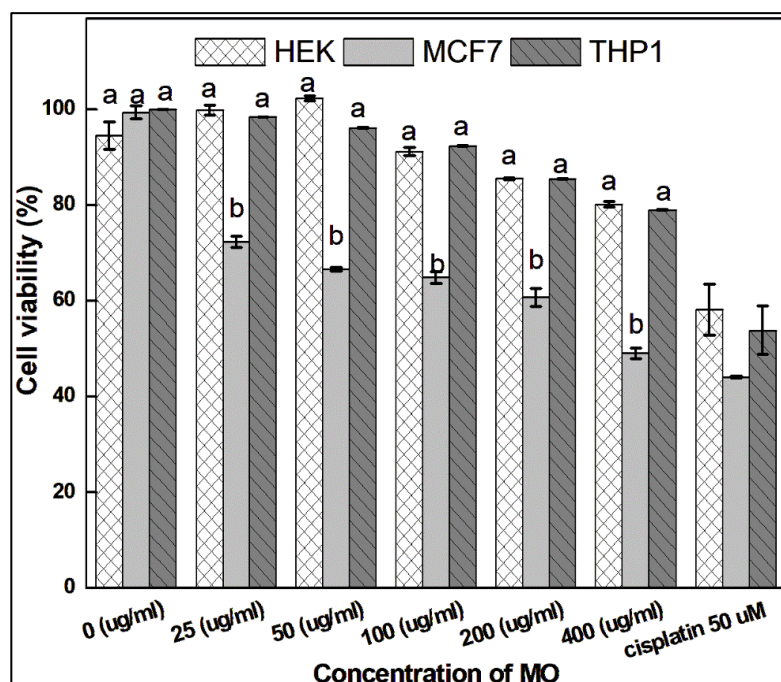


Figure 84: Cytotoxicity activity of MO against HEK 293 cell, MCF7 and THP1 cell lines. Bars with different alphabet labels in each group are significantly different ($P \leq 0.05$).

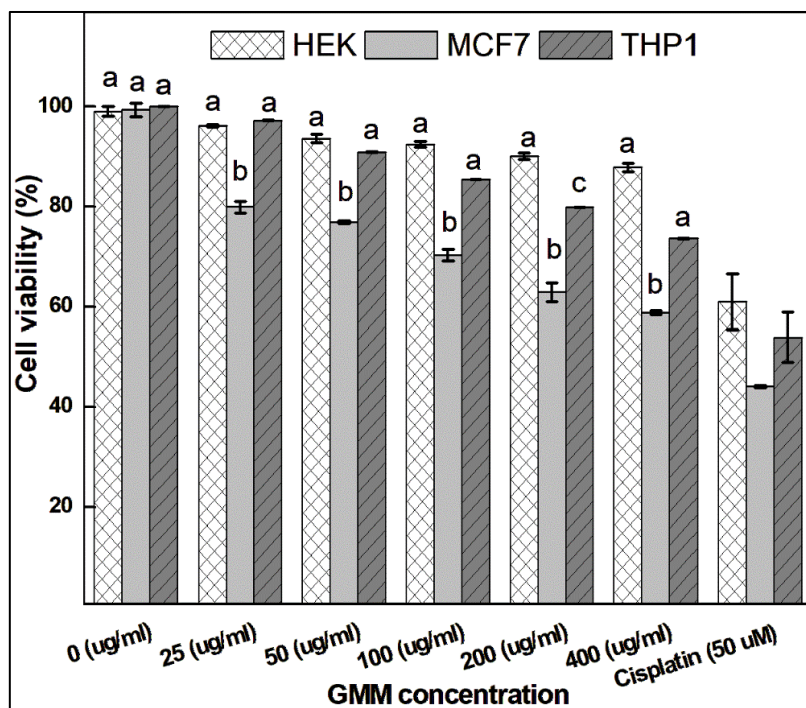


Figure 85: Cytotoxicity activity of GMM against HEK 293 cell, MCF7 and THP1 cell lines. Bars with different alphabet labels in each group are significantly different ($P \leq 0.05$).

4.4.5. Anti-inflammatory activity

4.4.5.1. Semi-quantitative PCR

TNF- α exhibited a notable 7.74-fold upregulation in response to LPS stimulation. Pretreatment with GMM (200 μ g/ml) and MO (200 μ g/ml) resulted in significant downregulation of TNF- α to 5.53-fold and 2.99-fold respectively (Figure 86A). LPS treatment induced a significant 2.22-fold increase in IL-1 β expression. IL-1 β expression was markedly downregulated, decreasing to 0.07-fold and 0.15-fold, respectively, following pretreatment with GMM (200 μ g/ml) and MO (200 μ g/ml) (Figure 86B). In the presence of LPS, IL-6 exhibited a marked 7.74-fold increase in expression. Pre-treatment with MO (200 μ g/ml) resulted in a 1.80-fold decrease in IL-6 synthesis. However, while GMM (200 μ g/ml) did decline the IL-6 expression levels, the reduction was found to be insignificant (Figure 86C). LPS stimulation led to a significant 1.98-fold upregulation in IL-8 expression. Interestingly, pretreatment with GMM (200 μ g/ml) and MO (200 μ g/ml) led to a significant downregulation of 0.33-fold and 1.52-fold (Figure 86D). To our surprise, a similar pattern was not observed in the instance of COX-2. LPS pre-treatment resulted in a 3.94-fold upregulation. Pretreatment with GMM at 200 μ g/ml led to a marked decrease in COX-2 expression, lowering it to 0.27-fold, but mustard oil (200 μ g/ml) treatment, triggered an unexpected upregulation of COX-2, surpassing even the magnitude of upregulation induced by LPS, with a 4.10-fold increase (Figure 86E).

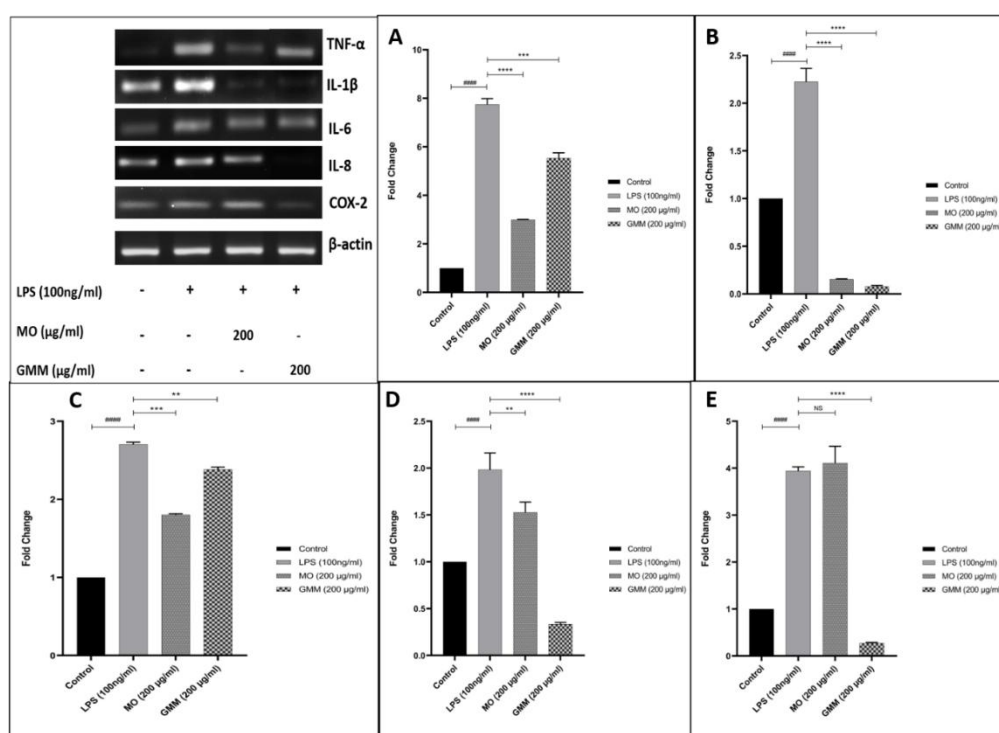


Figure 86: Relative gene expression of A. TNF- α , B. IL-1 β , C. IL-6, D. IL-8 and E. COX-2 checked by semi-quantitative PCR using gene-specific primers. The band intensities were quantitated and data are presented as mean \pm SEM of three independent experiments. One-way ANOVA and post hoc Bonferroni Comparison test were performed between control vs. LPS (#) and LPS vs. MO and GMM (*), representing statistical significance: ** $p < 0.01$; *** $p < 0.001$; ###, **** $p < 0.0001$; and NS: Non-significant.

4.4.5.2. ADME (Absorption, Distribution, Metabolism and Excretion) and drug-likeness analysis

The results for ADME and drug-likeness analysis of the selected compounds of GMM in mentioned in Table 27.

Table 27: SwissADME analysis results of the volatile compounds present in garlic mustard oil macerate

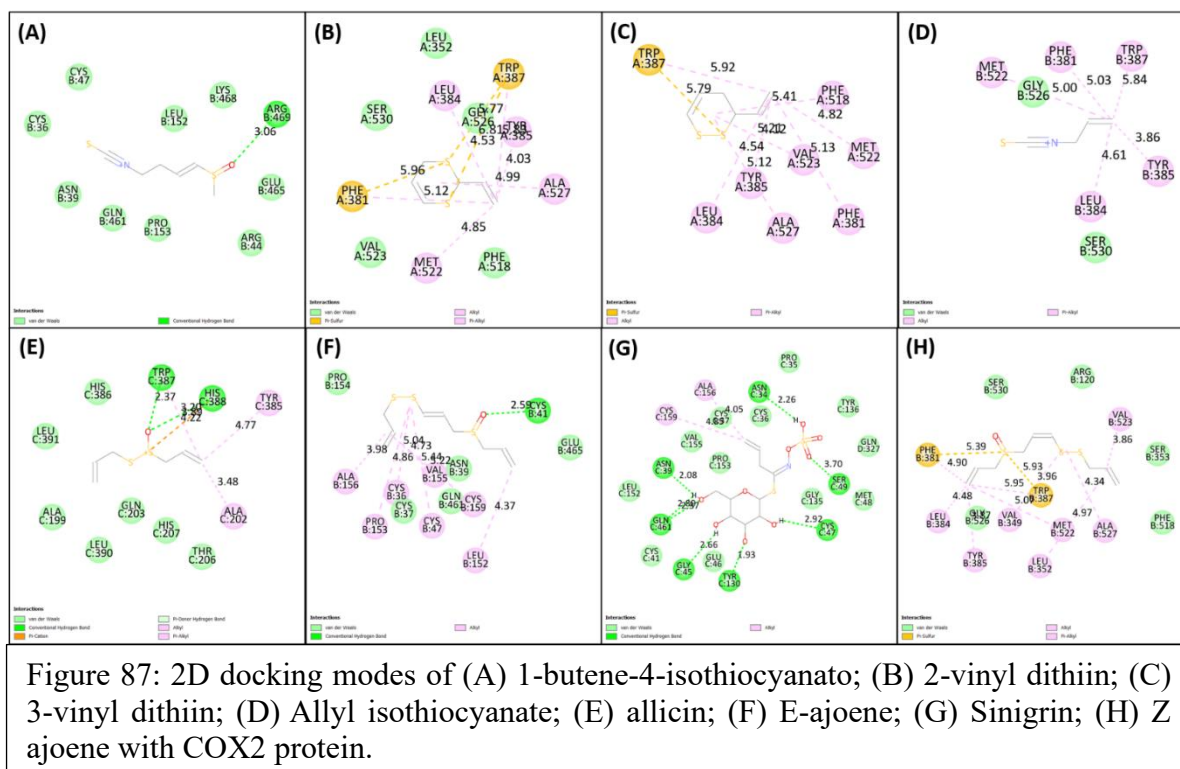
| | Molecules | 1-Butene, 4- isothiocy- nato | 2 vinyl dithii n | 3 vinyl dithii n | Allyl isothiocy- anate | Allicin | Sinigrin | E ajoene | Z ajoene |
|---------------------------|-------------------------------|--|---|---|----------------------------------|---|---|---|---|
| Physiochemical properties | Formula | C ₆ H ₉ NOS 2 | C ₆ H ₈ S ₂ | C ₆ H ₈ S ₂ | C ₄ H ₅ NS | C ₆ H ₁₀ OS ₂ | C ₁₀ H ₁₇ NO ₉ S ₂ | C ₉ H ₁₄ OS ₃ | C ₉ H ₁₄ OS ₃ |
| | MW | 175.27 | 144.2 6 | 144.2 6 | 99.15 | 162.27 | 359.37 | 234.4 | 234.4 |
| | #Heavy atoms | 10 | 8 | 8 | 6 | 9 | 22 | 13 | 13 |
| | #Aromatic heavy atoms | 0 | 0 | 0 | 0 | 0 | 0 | 0 | 0 |
| | Fraction Csp ³ | 0.5 | 0.33 | 0.33 | 0.25 | 0.33 | 0.7 | 0.33 | 0.33 |
| | #Rotatable bonds | 4 | 1 | 1 | 2 | 5 | 7 | 8 | 8 |
| | #H-bond acceptors | 2 | 0 | 0 | 1 | 1 | 10 | 1 | 1 |
| | #H-bond donors | 0 | 0 | 0 | 0 | 0 | 5 | 0 | 0 |
| | MR | 47.92 | 43.08 | 43.08 | 30.03 | 45.88 | 76.22 | 67.41 | 67.41 |
| | TPSA | 80.73 | 50.6 | 50.6 | 44.45 | 61.58 | 199.79 | 86.88 | 86.88 |
| Lipophilicity | iLOGP | 2.17 | 1.97 | 2.15 | 1.93 | 1.87 | 0.42 | 2.74 | 2.67 |
| | XLOGP3 | 1.48 | 2.3 | 2.05 | 2.41 | 1.31 | -1.07 | 1.71 | 1.71 |
| | WLOGP | 2.24 | 2.49 | 2.84 | 1.28 | 2.62 | -0.69 | 3.87 | 3.87 |
| | MLOGP | 1.75 | 1.96 | 1.96 | 1.98 | 1.18 | -2.59 | 2.1 | 2.1 |
| | Silicos-IT Log P | 1.99 | 2.34 | 2.34 | 2.37 | 0.96 | -2.39 | 2.2 | 2.2 |
| | Consensus Log P | 1.92 | 2.21 | 2.27 | 1.99 | 1.59 | -1.26 | 2.52 | 2.51 |
| Water solubility | ESOL Log S | -1.6 | -2.12 | -1.96 | -1.84 | -1.34 | -0.93 | -1.84 | -1.84 |
| | ESOL Solubility (mg/ml) | 4.45 | 1.1 | 1.58 | 1.43 | 7.39 | 42 | 3.37 | 3.37 |
| | ESOL Solubility (mol/l) | 0.0254 | 0.007 63 | 0.011 | 0.0144 | 0.0456 | 0.117 | 0.0144 | 0.0144 |
| | ESOL Class | Very soluble | Solub le | Very solubl e | Very soluble | Very soluble | Very soluble | Very soluble | Very soluble |
| | Ali Log S | -2.78 | -3 | -2.74 | -2.99 | -2.2 | -2.64 | -3.15 | -3.15 |
| | Ali Solubility (mg/ml) | 0.289 | 0.144 | 0.262 | 0.103 | 1.02 | 0.83 | 0.166 | 0.166 |
| | Ali Solubility (mol/l) | 0.0017 | 0.001 | 0.001 82 | 0.00103 | 0.0062 6 | 0.00231 | 0.0007 08 | 0.0007 1 |

| | | | | | | | | | |
|-------------------|-------------------------------|---------|---------|---------|---------|---------|---------|---------|---------|
| | Ali Class | Soluble | Soluble | Soluble | Soluble | Soluble | Soluble | Soluble | Soluble |
| | Silicos-IT LogSw | -1.38 | -0.93 | -0.93 | -0.85 | -1.7 | 1.94 | -2.32 | -2.32 |
| | Silicos-IT Solubility (mg/ml) | 7.34 | 16.8 | 16.8 | 14.1 | 3.24 | 31200 | 1.11 | 1.11 |
| | Silicos-IT Solubility (mol/l) | 0.0419 | 0.116 | 0.116 | 0.142 | 0.02 | 86.7 | 0.00475 | 0.00475 |
| | Silicos-IT class | Soluble | Soluble | Soluble | Soluble | Soluble | Soluble | Soluble | Soluble |
| Pharmacokinetics | GI absorption | High | High | High | High | High | Low | High | High |
| | BBB permeant | No | Yes | Yes | Yes | Yes | No | No | No |
| | Pgp substrate | No | No | No | No | No | Yes | No | No |
| | CYP1A2 inhibitor | No | No | No | No | No | No | No | No |
| | CYP2C19 inhibitor | No | No | No | No | No | No | No | No |
| | CYP2C9 inhibitor | No | No | No | No | No | No | Yes | Yes |
| | CYP2D6 inhibitor | No | No | No | No | No | No | No | No |
| | CYP3A4 inhibitor | No | No | No | No | No | No | No | No |
| | log Kp (cm/s) | -6.32 | -5.55 | -5.72 | -5.19 | -6.36 | -9.25 | -6.52 | -6.52 |
| | | | | | | | | | |
| Druglikeness | Lipinski #violations | 0 | 0 | 0 | 0 | 0 | 0 | 0 | 0 |
| | Ghose #violations | 1 | 2 | 2 | 3 | 1 | 1 | 0 | 0 |
| | Veber #violations | 0 | 0 | 0 | 0 | 0 | 1 | 0 | 0 |
| | Egan #violations | 0 | 0 | 0 | 0 | 0 | 1 | 0 | 0 |
| | Muegge #violations | 1 | 1 | 1 | 2 | 1 | 1 | 0 | 0 |
| | | | | | | | | | |
| | Bioavailability Score | 0.55 | 0.55 | 0.55 | 0.55 | 0.55 | 0.11 | 0.55 | 0.55 |
| Medical Chemistry | | | | | | | | | |
| | PAINS #alerts | 0 | 0 | 0 | 0 | 0 | 0 | 0 | 0 |
| | Brenk #alerts | 2 | 1 | 2 | 3 | 2 | 5 | 2 | 2 |
| | Leadlikeness #violations | 1 | 1 | 1 | 1 | 1 | 1 | 2 | 2 |
| | Synthetic Accessibility | 3.46 | 3.91 | 4.27 | 2.2 | 3.6 | 5.35 | 4.33 | 4.33 |

4.4.5.3. Molecular docking analysis of GMM volatile compounds with Cox2, IL1 β , IL6, TNF α and IL-8

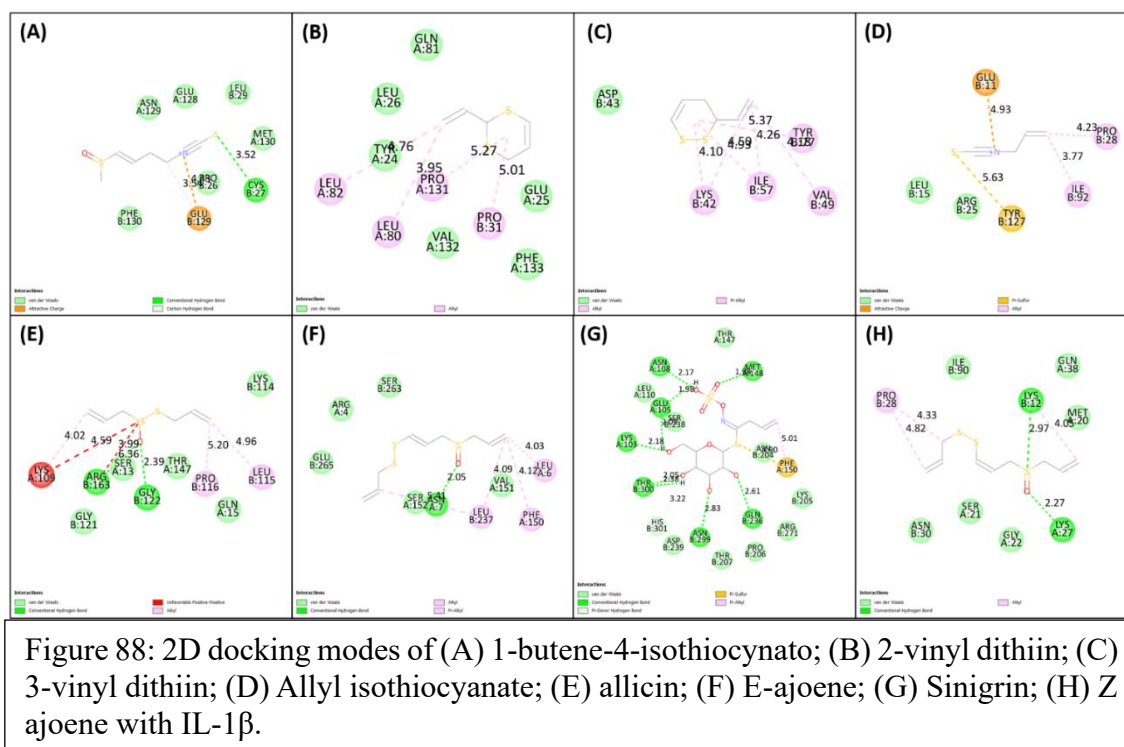
4.4.5.3.1. Cox2 (PDB ID: 4cox)

Out of all the eight compounds, sinigrin showed the minimum binding energy of -7.6 kcal/mol followed by Z-ajoene > 3-vinyl dithiin > 2-vinyl-dithiin > allicin = E-ajoene > 1-butene-4-isothiocyanato > AITC (Figure 87 and Table 28).



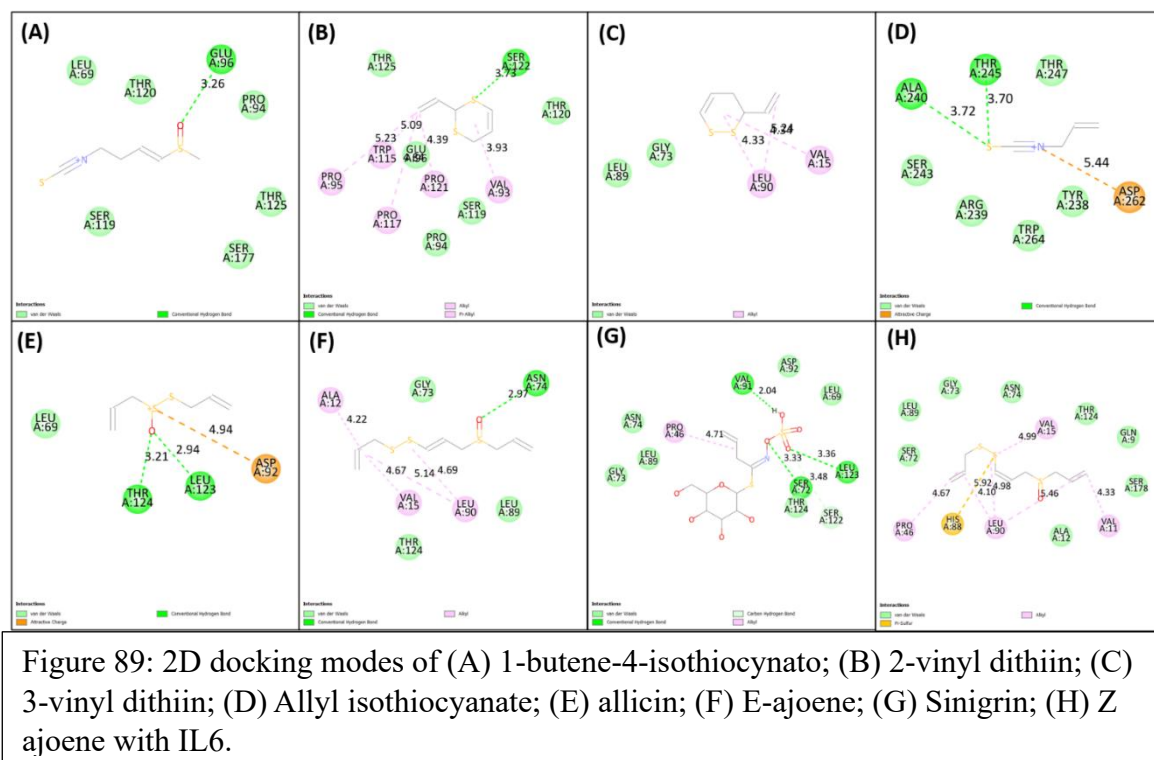
4.4.5.3.2. IL-1 β (PDB ID: 1itb)

Out of all the eight compounds, sinigrin showed the minimum binding energy of -7.3 kcal/mol followed by 3-vinyldithiin > 1-butene-4-isothiocyanato > Z-ajoene > allicin > 2-vinyl dithiin > E ajoene > AITC (Figure 88 and Table 28).



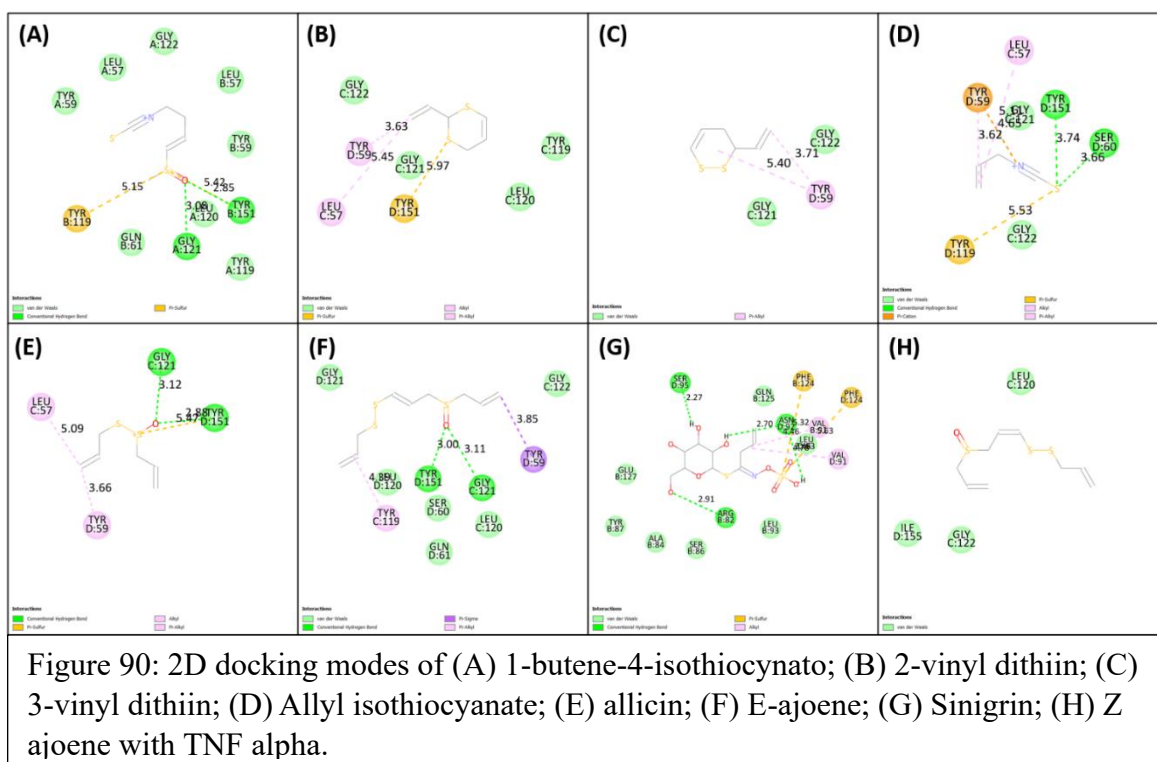
4.4.5.3.3. IL-6 (PDB ID: 1n26)

Out of all the eight compounds, sinigrin showed the minimum binding energy of -5.3 kcal/mol followed by 3-Vinyl-dithiin>allicin=2-vinyl-dithiin>Z-ajoene>E-ajoene>1-Butene-4-isothiocyanato>AITC (Figure 89 and Table 28).



4.4.5.3.4. TNF- α (PDB ID: 2az5)

Out of all the eight compounds, sinigrin showed the minimum binding energy of -6.4 kcal/mol followed by allicin=3-vinyl dithiin=E-ajoene> Z-ajoene=2-vinyl dithiin>1-butene-4-isothiocyannato>AITC (Figure 90 and Table 28).



4.4.5.3.5. IL-8 (PDB ID: 4xdx)

Out of all the eight compounds, sinigrin showed the minimum binding energy of -5.7 kcal/mol followed by 3-vinyl dithiin> Z-ajoene> E-ajoene> allicin=2-vinyl dithiin>1-butene-4-isothiocyannato>AITC with binding energy and 2D structure are shown in Figure 91 and Table 28.

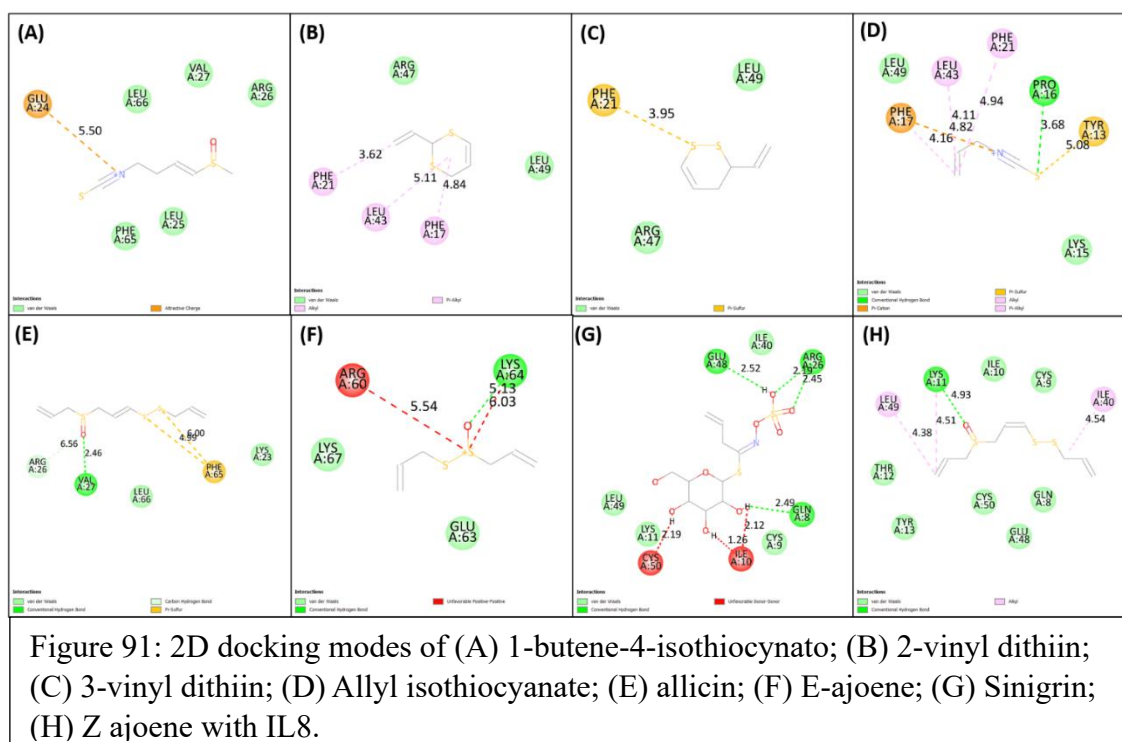


Table 28: Showing the binding energy of selected volatile molecules present in GMM with pro-inflammatory cytokines (COX-2, IL1 β , IL6, IL8, TNF α) during molecular docking study.

| Sl. No | Compounds | Binding affinity ((kcal/mol)) | | | | |
|--------|---------------------------|-------------------------------|-------------------------------|-----------------------|-----------------------|--------------------------------|
| | | COX2 (PDB ID: 4cox) | IL1 β (PDB ID: 1itb) | IL6 (PDB ID: 1n26) | IL8 (PDB ID: 4xdx) | TNF α (PDB ID: 2az5) |
| 1 | Z Ajoene | -5.4 | -3.7 | -3.4 | -4.2 | -4.2 |
| 2 | Allicin | -4.9 | -3.6 | -3.6 | -3.6 | -4.3 |
| 3 | 1-Butene-4-isothiocyanato | -4.2 | -3.9 | -3.1 | -3.4 | -3.9 |
| 4 | Allyl isothiocyanate | -3.7 | -3.2 | -2.8 | -3.1 | -3.3 |
| 5 | Sinigrin | -7.6 | -7.3 | -5.3 | -5.7 | -6.4 |
| 6 | 3 vinyl dithiin | -5.3 | -4.0 | -3.7 | -4.3 | -4.3 |
| 7 | E Ajoene | -4.9 | -3.5 | -3.3 | -4.1 | -4.3 |
| 8 | 2 vinyl dithiin | -5.0 | -3.6 | -3.6 | -3.6 | -4.2 |

4.4.6. Transdermal activity

During the transdermal activity, it was observed that the GMM/ MO oil had diffused through the eggshell membrane over the time of 2 hours during incubation at 37°C (Figure 92). However, the membrane absorbed some amount of oil during the diffusion. The pre-weight of the membrane with a surface area of 226.98 mm² was found to be 18.3 mg and the post-weight of the membrane was found to be 35.85 mg (amount of oil retained in the membrane 17.55 mg) which was 95.92% weight of the dry membrane. The FTIR results of blank eggshell membrane showed minimum transmittance at wavenumbers 3459, 1635, 1400, 1091 and 648 cm⁻¹. For the membranes used for the diffusion of MO and GMM, minimum transmittance was observed at 3008, 2925, 2854, 1465 and 722 cm⁻¹ (Figure 93). The liquid chromatogram for diffused MO and GMM is shown in Figure 94 and the mass spectrometric result at retention time 2.77 minutes and 7.43 minutes are shown in Figure 95 and Figure 96, respectively. The LCMS analysis of the oil diffused showed the presence of allicin (m/z=163.00), ajoene (m/z=235) and vinyl dithiin (m/z=145) in the GMM oil which supports the fact that the mustard oil helps in facilitating the transfer of the thiosulfinate compounds from the stratum corneum.

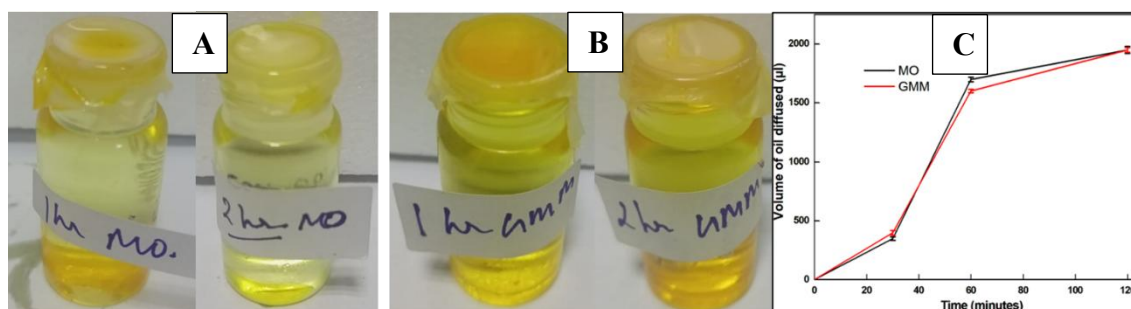


Figure 92: (A) Showing diffusion of MO through the eggshell membrane during 1hr and 2hr of incubation; (B) Showing diffusion of GMM through the eggshell membrane during 1hr and 2hr of incubation; (C) line graph showing the volume of oil diffused through eggshell membrane during the 2hr incubation time.

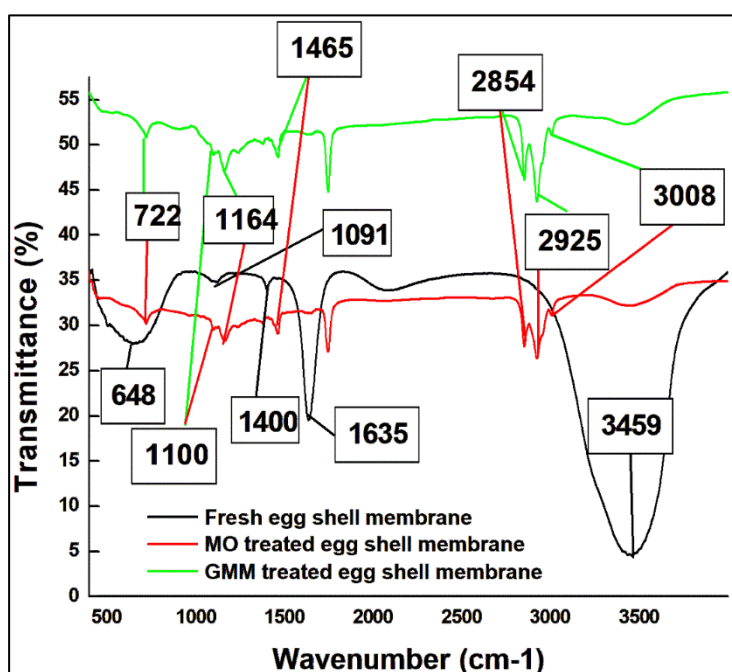


Figure 93: Showing the FTIR results of the untreated egg shell membrane (black), MO treated membrane (red) and GMM treated membrane.

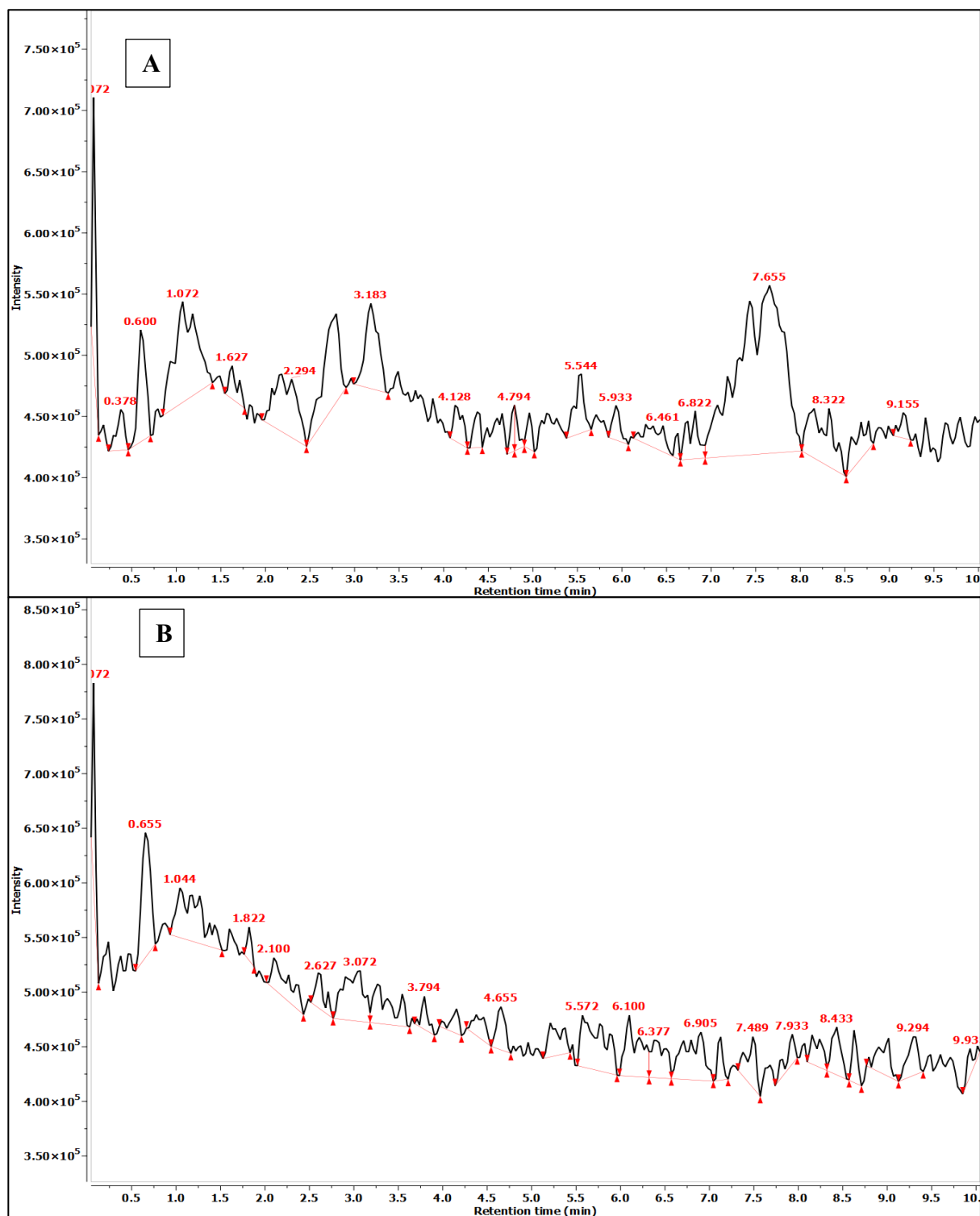
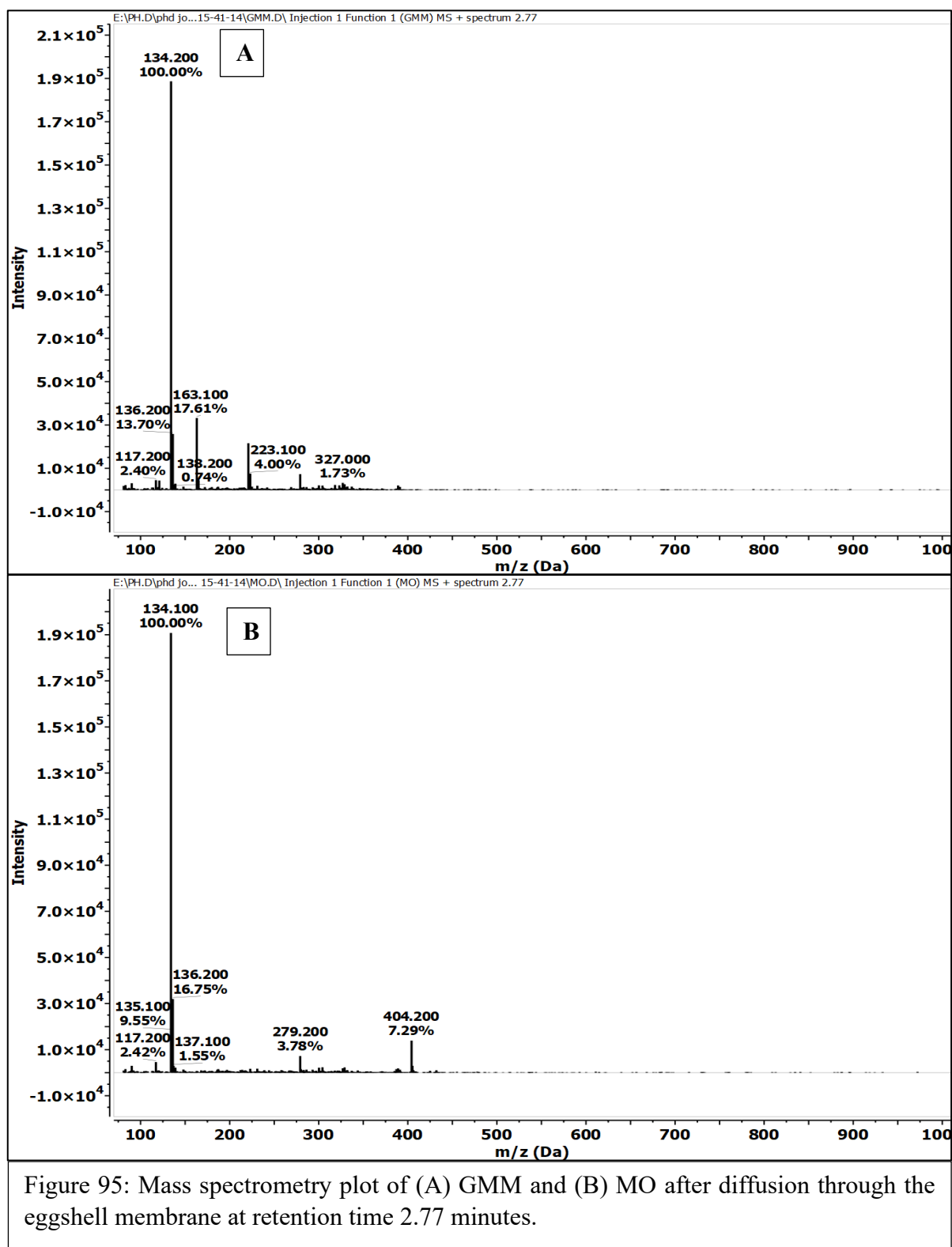


Figure 94: Liquid chromatogram of (A) diffused MO through eggshell membrane after extraction in acetonitrile; (B) diffused MO through eggshell membrane after extraction in acetonitrile.



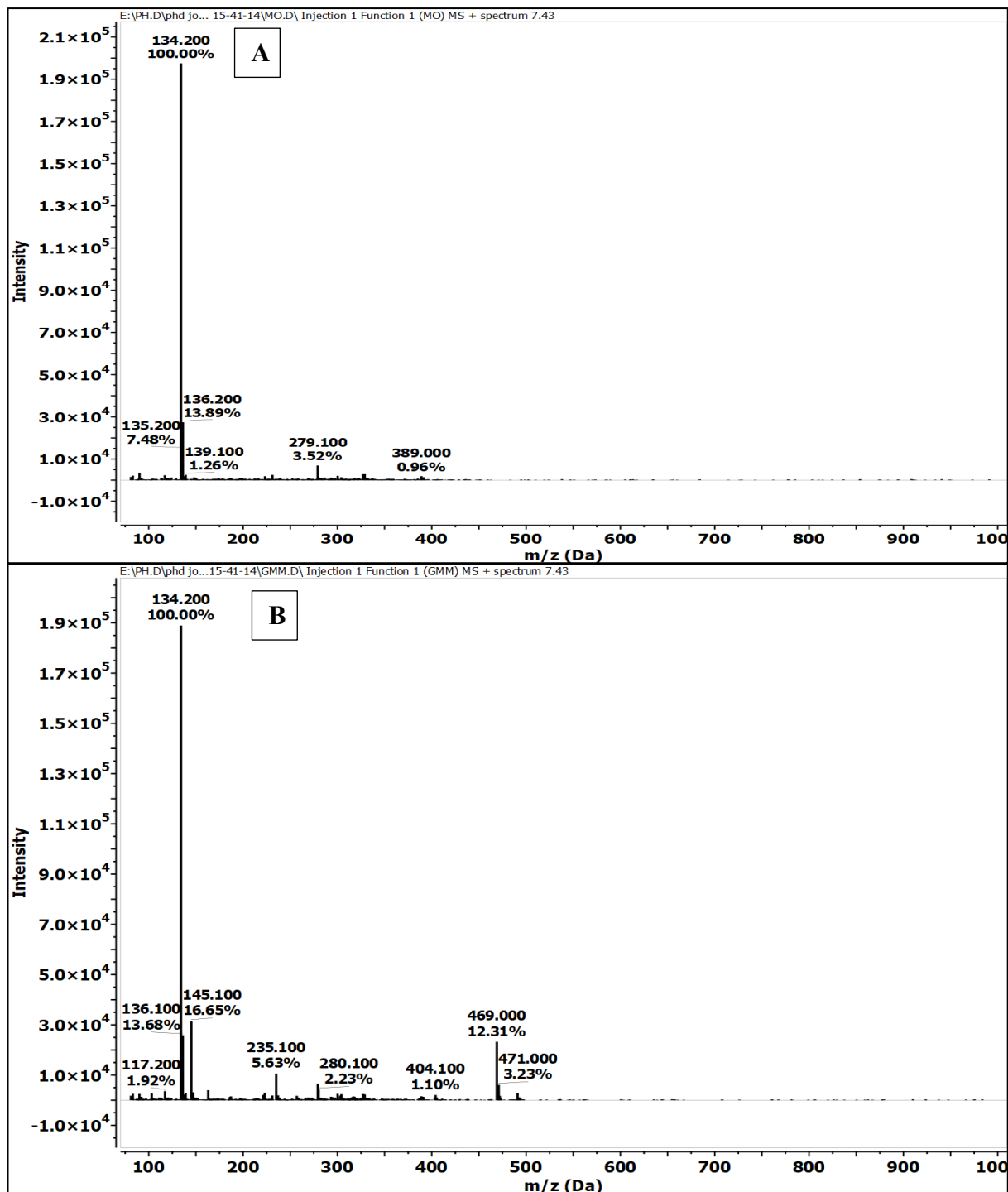
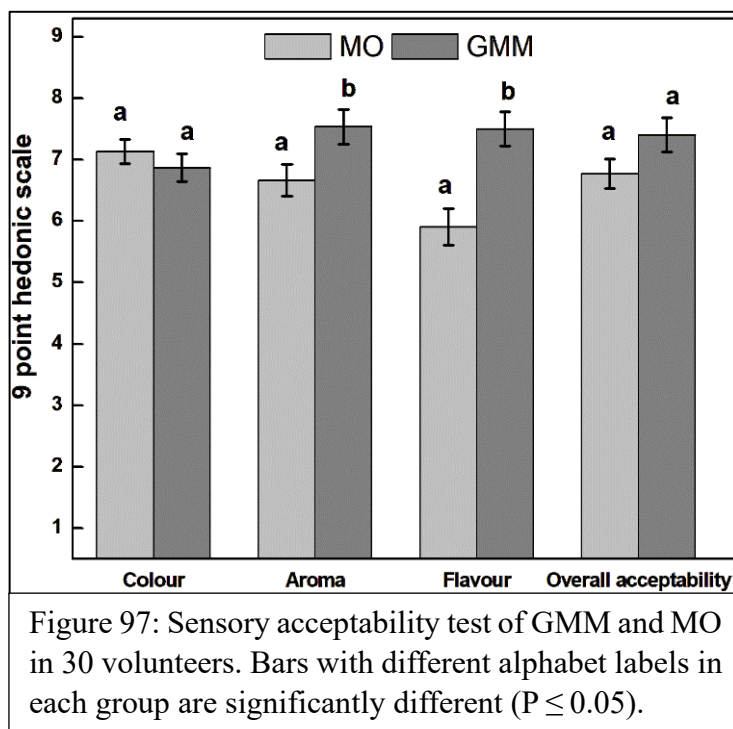


Figure 96: Mass spectrometry plot of (A) GMM and (B) MO after diffusion through the eggshell membrane at retention time 7.43 minutes.

4.4.7. Sensory acceptability test

The sensory acceptability test results show that the volunteers liked the aroma and flavour of the GMM significantly higher than MO at $p < 0.05$. Overall acceptability and colour tests were not significantly different from that of MO (Figure 97).



4.5. Reference

- [1] Jamwal, R., Kumari, S., Balan, B., Kelly, S., Cannavan, A., and Singh, D.K. Rapid and non-destructive approach for the detection of fried mustard oil adulteration in pure mustard oil via ATR-FTIR spectroscopy-chemometrics. *Spectrochimica Acta Part A: Molecular and Biomolecular Spectroscopy*, 244: 118822, 2021.
- [2] Nagarajan, D., and Kumar, T.R. Fourier transform infrared spectroscopy analysis of garlic (*Allium*). *International Journal of Zoology Studies*, 2(6): 11-14, 2017.